THE Marquardt COMPANY VAN NUYS, CALIFORNIA

Report No. TMC 3293-6-3

DRL T-881

Line Item 3

NASA CR-

141780

FINAL REPORT

LINE FLUID ACTUATED VALVE DEVELOPMENT PROGRAM

BY

R. A. LYNCH

Prepared Under Contract NAS 9-13684

By

The Marquardt Company

Van Nuys, California

For

National Aeronautics and Space Administration

Lyndon B. Johnson Space Center

January 1975

TABLE OF CONTENTS

TABLE OF CONTENTS (Cont'd.)

LIST OF FIGURES

LIST OF FIGURES (Cont'd.)

LIST OF FIGURES (Cont'd.)

LIST OF TABLES

THIS PAGE LEFT INTENTIONALLY BLANK

1.0 INTRODUCTION

The program described herein was performed to demonstrate the feasibility of a line fluid actuated valve design for potential application as a propellant control valve on the Space Shuttle. This valve concept offered distinct weight and electrical power advantages over alternate valve concepts. Marquardt initiated design and analysis studies of a unique line fluid actuated valve concept in February, 1973, in anticipation of a strong emphasis on weight contributions of Space Shuttle components. Marquardt management supported the continued design effort as an integral part of the SSRCT preproposal effort and committed funding for the fabrication of the prototype valves to support thruster development. Concurrently, the solicitation for the program described herein was received and responded to. On September 1, 1973, under NASA-JSC Contract NAS9-13684, Marquardt initiated effort on the program described herein, in parallel with the Company funded development activity directed toward producing a minimum weight thruster for the SSRCS. As a result of these concomitant efforts, the objective of this program was, in general, exceeded.

The program reported herein, originated from NASA-JSC under Contract NAS9-13684. The Technical Monitors were Mr. Jack Capps and Mr. James Wiltz of the Auxiliary Propulsion and Pyrotechnics Branch of the JSC. The program was completed under the direction of Mr. Ted Linton, Manager of Space Shuttle Programs. The Project Manager/Principle Investigator was Mr. Bob Lynch. Other Marquardt personnel and their areas of significant contribution to the successful completion of this program are: S. Minton and R. Braendlein, Analysis and Computer Modelling; E. Dugan, Valve Design; J. Tobin, Manufacturing Liaison; and W. Williams, Valve Development Testing.

The design, fabrication, and testing of two prototype units of a line fluid actuated valve concept, described in this report, substantiates the capability of this valve configuration to offer performance characteristics compatible with the SSRCT and yield a significant weight reduction over other valve configurations.

THIS PAGE LEFT INTENTIONALLY BLANK

2.0 SUMMARY

The advent of the Space Shuttle and potential space programs has given rise to the need for larger thrust precision control rockets. Injector valves which meet the flow and response requirements and exhibit long service life, high cycle life, and multiple reuse capability including the ability to survive a wide range of operational environments, are not currently available for this new generation of reaction control rockets.

The Marquardt Company has maintained a continuing effort in the development of precision control valves for aerospace applications. Particular emphasis has been in the area of enhancing service and cycle life capability without compromising operational characteristics. Applications have covered a wide range of both liquid and gaseous propellants and engine thrusts from fractions of a pound to 6000 pounds. A broad spectrum of valve operational concepts and configurations has been analyzed in response to these requirements and many have been demonstrated.

In response to the Space Shuttle requirement for injector valves to control bipropellant flow to the Reaction Control System Engines, a line fluid actuated valve design has been evolved that embodies unique features to enhance life while meeting or exceeding required performance characteristics. Significant weight and power savings over other configurations are realized by this line fluid actuated design. Under NASA-JSC Contract NAS 9-13684, Marquardt has performed a development program to demonstrate the feasibility of this valve configuration.

Marquardt has developed the valve shown in Figure 2-1. Extensive analyses have substantiated the feasibility of this concept and projected performance is within the requirements of Appendix A of the Exhibit "A" Statement of Work of NASA Contract NAS 9-13684. An analog computer model of the proposed configuration was prepared. During the design and analysis phase of the program (Task I), this analog model was employed to substantiate all design parameters before committing the design to test unit fabrication. Two test valves were fabricated during the Task II Hardware Fabrication phase of the program. Valve testing (Task III) was performed primarily in the Marquardt Test Facility in accordance with a NASA-approved Test Plan. The valve's performance, over the range of operating conditions, was documented. One unit was subjected to the specified vibration spectrum and monitored for liquid leakage during exposure. The other unit was vibrated while monitoring low pressure gas leakage. The two test units were then cycle life tested to demonstrate 200,000 cycles of operation, with periodic checks of valve response and leakage throughout the cycling.

LINE FLUID ACTUATED VALVE

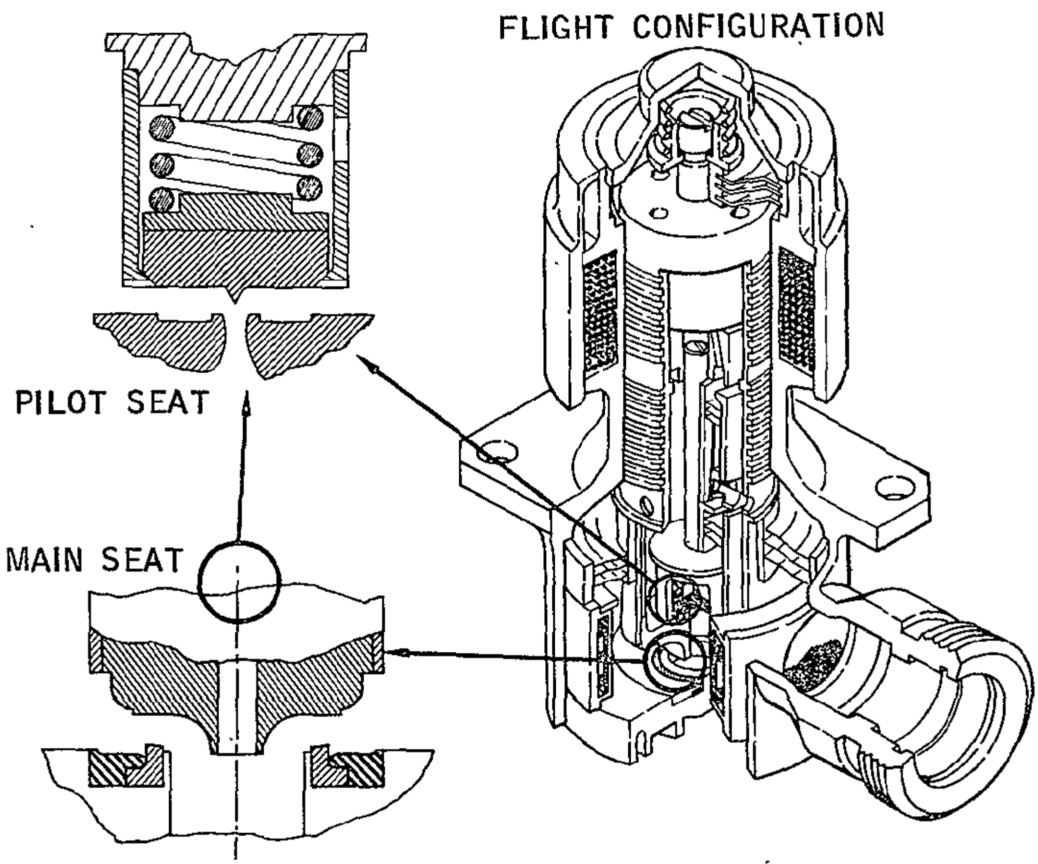

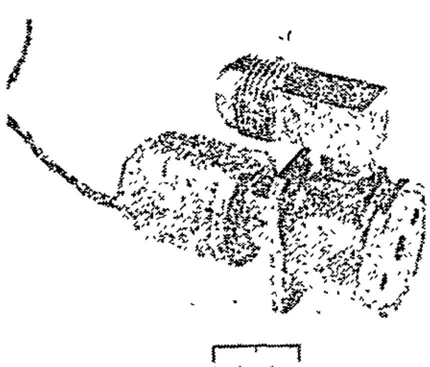

PROTOTYPE CONFIGURATION

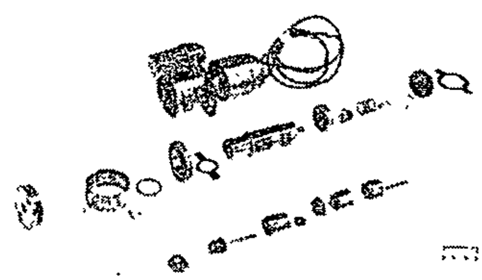

PROTOTYPE CONFIGURATION

Figure 2-1

Upon completion of the test program, a thorough analysis of the test data was made and the results compared with the analog model performance projections. Where deficiencies appeared or where failure to achieve specification performance resulted, design modifications were made. The two test units were disassembled for inspection and examined for wear phenomenon or life limiting characteristics. All design modifications, refurbishment recommendations, and supporting analysis and studies were coordinated with NASA.

Release of approved design modification drawings and refurbishment requirements initiated fabrication of new detail parts for rework of the two test units, as required (Task V). Reassembly of the test units was accomplished in accordance with this plan and the valves acceptance tested to substantiate characteristics of the modified units and delivered to NASA-LBJ Space Center.

The valve is of all corrosion-resistant metallic construction, with the exception of the PTFE poppet closure seals and the solenoid coil. It is designed to have all welded closures at all pressure vessel joints, in the flight configuration, though provisions for mechanical seals to external leakage will be incorporated into development units. The pilot stage armature and poppet are coaxial within the main stage poppet to provide high density packaging. All moving parts in the valve are flexure guided to achieve a design that features no sliding fits. Flat poppet closure interfaces have been incorporated which, when combined with flexure guided elements, effectively eliminate scrubbing action as closure seals engage or disengage, thus enhancing valve cyclic life.

The valve body and detail parts are machined of bar stock. Pressure vessel elements are machined of vacuum arc remelted bar stock to be assured of the highest quality of raw material and finished part. Electron beam welding is used to join ferromagnetic materials to nonmagnetic materials to form the appropriate solenoid magnetic path. After welding, these parts are normalized to desensitize the heat-effected zone and recover maximum resistance to corrosive attack. The body structure uses Inco 718 and 446 Cres ferromagnetic sections. Internal metallic details are made from Inco 718 and 446 Cres ferromagnetic sections as required, with the exception of 302 Cres seat preload springs, and the main stage poppet which is of A-286 hardenable austenitic corrosion resistant alloy. The main stage poppet closure seal and the pilot poppet closure seal are machined of Marquardt processed PTFE bar. Flexure elements are chem-milled from Inco 718 sheet stock to the appropriate pattern.

Flexure guidance of the moving elements of the valve design represents an area of technology in valve design in which Marquardt has made significant contributions. The flexure design to be employed is unique to Marquardt designs and has been employed in a wide range of fluid control components involving far more severe operational requirements than this application. The flexures are spring element

washers, in which a pattern is cut such that the I.D. and O.D. are positively retained and deflection results in bending and torsion of web elements with absolutely no rubbing or sliding. The web pattern is such that high radial stiffness results to assure positive axial alignment and a desired axial spring rate is achieved. A wide range of flexure sizes and patterns have been produced to date and have substantiated the design analysis approach and exhibited cycle life capability well in excess of 10^6 cycles with no change in performance characteristics. The flexure elements are located out of the main flow stream of the valve and are therefore not subject to flow stream impingement phenomenon. The flexure design and their employment in this valve design result in a valve configuration virtually free of self-generated contamination and allows clearances between parts with relative motion that renders the design essentially contamination insensitive in spacecraft applications.

A summary of the projected performance, design goals, and demonstrated performance is presented in Table 2-I.

TABLE 2-I

LINE FLUID ACTUATED SHUTOFF VALVE PERFORMANCE CHARACTERISTICS

PARAMETER	PROJECTED PERFORMANCE	DESIGN GOAL (NASA 9-13684 REQUIREMENTS)	DEMONSTRATED PERFORMANCE
• Operating Fluids	N_2H_4, A-50, MMH, N_2O_4, H_2O, alcohol, freon, solvents, He, N_2	N_2H_4, A-50, MMH, N_2O_4	MMH, N_2O_4, H_2O, He, N_2
• Operating Pressure	350 psig max., 300 psig nom.	350 psig max., 300 psig nom.	0-350 psig
• Proof Pressure	525 psig for 5 minutes	525 psig for 5 minutes	525 psig for 5 minutes
• Burst Pressure	875 psig for 5 minutes	875 psig for 5 minutes	- -
• External Leakage, 0-350 psig	$<1 \times 10^{-6}$ sccs GHe	$<1 \times 10^{-6}$ sccs GHe	No evidence of leakage when immersed in H_2O
• Internal Leakage, 0-350 psig	<50 scch GHe	<50 scch GHe	<50 scch
• Flow Capacity	2.0 lb/sec N_2O_4 @ 300 psig inlet and 30 psid max.	2.0 lb/sec N_2O_4 @ 300 psig inlet and 30 psid max.	2.0 lb/sec N_2O_4 @ 300 psig inlet and 46 psid max.
• Response @ 27 ±1 vdc, 350 psig inlet, 70 °F, Rated Flow	18 ms opening, 15 ms closing	20 ms opening max., 20 ms closing max.	34 ms opening max., 18 ms closing max.
• Operating Temperature	-65 °F to +225 °F (except not with frozen propellants	-65 °F to +225 °F	+40 to +250 °F
• Electrical Power	25 watts @ 30 vdc, 70 °F	Not Applicable	25 watts @ 30 vdc, 70 °F
• Operating Voltage	18 to 32 vdc	18 to 32 vdc	22 to 32 vdc
• Cycle Life	>200,000 cycles, wet and/or dry	>200,000 cycles wet, >5,000 cycles dry	60,000 to 200,000 cycles, wet or dry
• Vibration	Per Figure 4	Per Figure 4	Per Figure 2-1
• Acceleration	±3.5 g	±3.5 g	- -
• Envelope	1.50 in. dia. x 3.80 inches	Not Applicable	1.50 in. dia. x 3.80 inches
• Valve Weight	0.99 lb.	Not Applicable	1.36 lb. (includes 0.21 lb. test inlet fitting)

THIS PAGE LEFT INTENTIONALLY BLANK

3.0 DISCUSSION

3.1 PROGRAM APPROACH

3.1.1 Program Description and Objectives

The objective of this program was the design and demonstration of a lightweight, pulse operated, line fluid actuated valve for potential application to the Space Shuttle RCS. This objective was accomplished by the program described herein. The basic design approach, refined, fabricated and demonstration tested during this effort, is described in Marquardt Proposal No. P4-105, dated 2 July 1973. Extensive design analysis, including analog computer modeling, was completed before fabrication and assembly of two test units. Testing consisted of performance mapping over the anticipated range of operating conditions, vibration testing and life cycle testing. A post test analysis of the test units was performed to assess the impact of the environments on the design. Design modifications were proposed, analyzed and with NASA concurrence, incorporated into the test units as they are refurbished for delivery to NASA for further evaluation. The planned flow of work for this effort is shown in Figure 3-1.

3.1.2 Work Breakdown Structure and Task Descriptions

The work breakdown structure presented is in accordance with the Statement of Work (Exhibit "A") of Contract NAS 9-13684. Each task is made up of subtask elements which define logical work increments which facilitate the timely completion of each task in accordance with the overall program schedule (Figure 3-2) with effective cost control. A contract extension was granted to allow a more extensive test program to be conducted.

3.1.2.1 Task I - Valve Analysis and Design

An intensive design and analysis effort was conducted to expand and refine preliminary analyses of the proposed configuration. Design studies were performed to resolve critical areas and assembly problems. Detail drawings of the final configuration were prepared as the analytical programs confirmed design criteria. This task culminated in a Design Review, at the NASA-LBJ facility, at which time all design data was presented and concurrence in the selected design solicited from the NASA-LBJ Space Center Project Manager. Design analyses included electromagnetic studies of the pilot solenoid, flow analyses, dynamic analyses utilizing the analog computer, stress analyses, materials studies to confirm selections from both the compatibility and fabricability aspects, and definition of optimum assembly techniques.

PROGRAM FLOW DIAGRAM

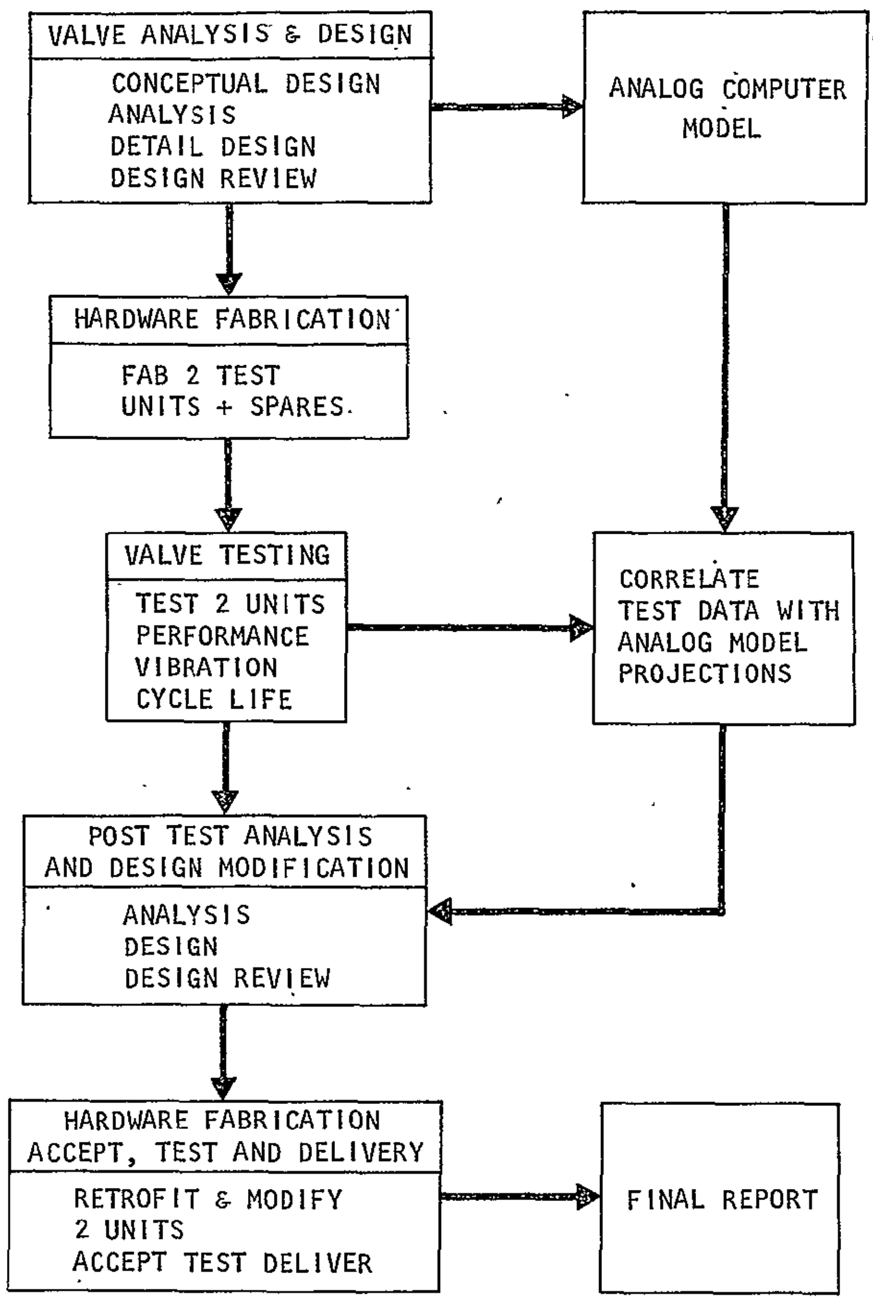

Figure 3-1

PROGRAM SCHEDULE

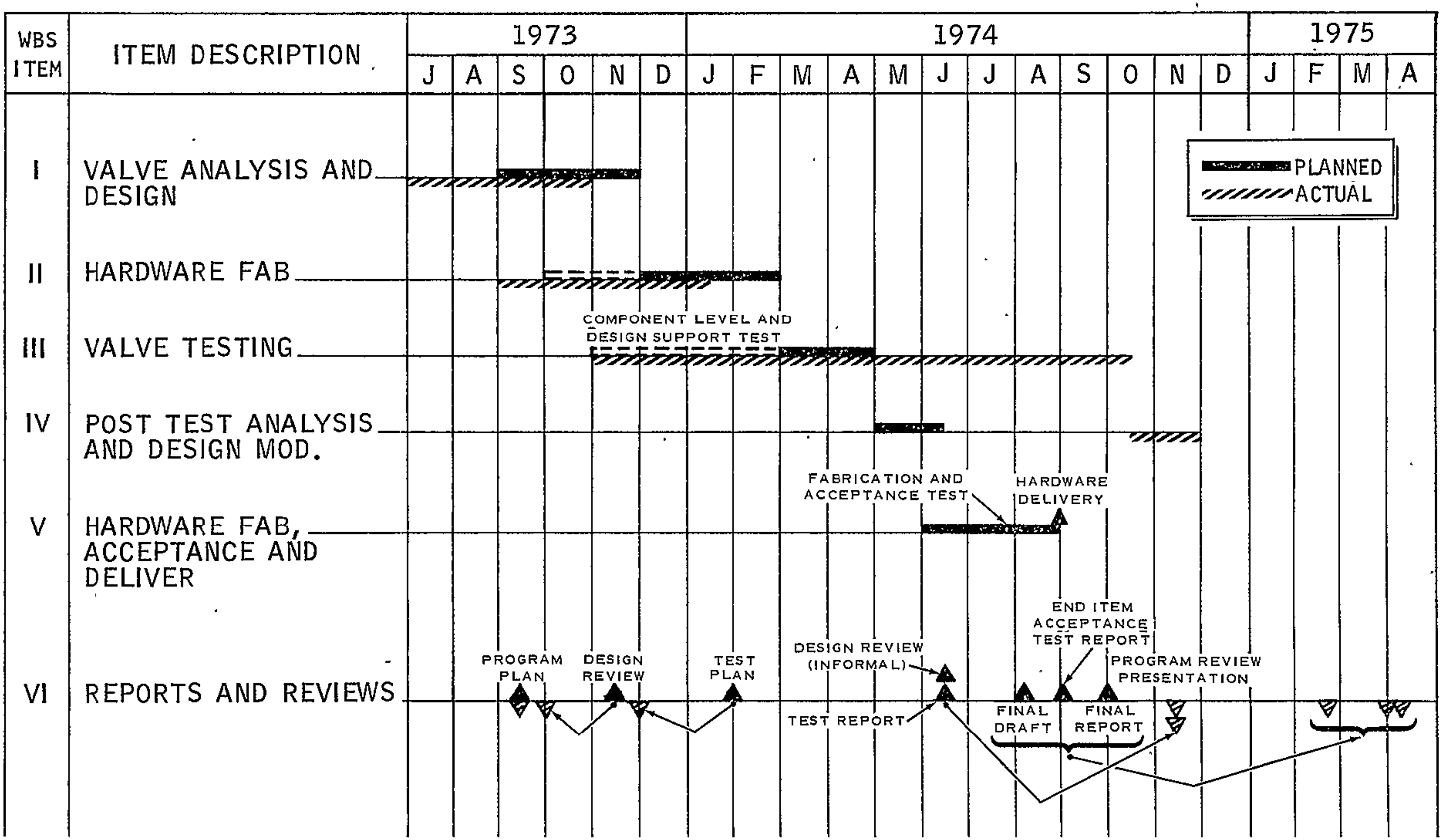

THE Marquardt COMPANY VAN NUYS, CALIFORNIA

TMC 3293-6-3

A75-3-489-12

Figure 3-2

3.1.2.2 Task II - Hardware Fabrication

Upon concurrence in the selected design by NASA-LBJ Space Center, detail drawings were released for fabrication of sufficient detail parts to assemble two complete valves. Additional spares of selected details were also fabricated. Procured items were ordered. Where long lead items may have jeopardized the program schedule, these were identified as early in the program as practical (during Task I effort) and orders placed, on a risk basis, to assure the timely delivery of these items.

As critical elements of the design were identified, during the Task I effort, design element support tests were defined. As an integral part of the Task II effort, fabrication of the test fixtures and test items, necessary to perform these investigatory tests, were fabricated.

All fabrication in support of this program was accomplished with current model shop control practices. Skeletal planning was generated to assure schedule and cost control data feedback for monitoring fabrication status. This planning also provided for the entry of in-process inspection data.

3.1.2.3 Task III - Valve Testing

Two separate test efforts were performed under the Task III work. Concurrent with the Design and Analysis (Task I) specific elements of the design, which require test verification, were identified. These design support tests were performed in accordance with engineering prepared, informal test outlines, as a part of the Task III effort. Data from these tests were immediately fed back to the design and analysis effort to enhance confidence in the design and establish appropriate empirical data for the analytical models.

The second test program of Task III was the valve design verification test program. This effort required the preparation of a Test Plan to establish, in detail, the tests to be performed, data to be acquired, instrumentation requirements, and test hardware utilization. Prior to initiating any testing, this Test Plan was submitted to the NASA Technical Monitor for review and approval. Upon receipt of NASA approval, the two test units were subjected to the test program as defined in the Test Plan. Testing included verification of valve performance over the range of operating conditions of temperature, pressure and voltage, vibration exposure, and cycle life demonstration with interim response and leakage verification checks. All data from these tests were recorded on test data sheets which became an integral part of the respective valve log books.

3.1.2.4 Task IV - Post Test Analysis and Design Modifications

Upon completion of the design verification test program, the test data were compiled and evaluated to correlate actual with predicted performance. In the event that discrepancies existed in this correlation, the reason for these discrepancies was determined, and design modifications required to correct these discrepancies or improve performance defined. The two test units were disassembled and closely inspected for evidence of performance deterioration. If any such deterioration was noted, the particular component was identified and the nature of the deterioration investigated.

3.1.2.5 Task V - Hardware Fabrication, Acceptance Test and Delivery

Following NASA concurrence in the proposed design modifications and/or retrofit and refurbishment resulting from Task IV, the two test units were reworked and refurbished. All work accomplished under this effort was fully documented in the respective valve log books. The reworked/refurbished units were then subjected to the acceptance test portion of the Design Verification Test Plan. These test data are compiled in the valve log books and also as an end item test report. The valves shall then be cleaned, packaged, and delivered to NASA-LBJ Space Center.

3.1.2.6 Task VI - Reports and Reviews

Under the direction of the Project Manager and utilizing the Marquardt Configuration Management System, all data acquired and generated during the performance of this program were identified. In accordance with the overall program schedule, specific reports and plans were prepared for timely transmittal to NASA. The data management system provided for periodic updating or revisions, as required, to documents submitted to NASA, with appropriate identification coding to reflect the currentness of the document.

3.2 DESIGN CRITERIA

The design requirements, imposed by the contract statement of work are summarized in Table 3-I. These requirements define a valve suitable for possible use on the Space Shuttle RCS. The criteria apply to a line fluid actuated valve design (pilot operated).

In view of Marquardt's active participation in the Space Shuttle and ultimate selection as the contractor for the Reaction Control Thrusters, additional criteria were self-imposed to assure substantial valve design margins for this particular application. These additional criteria and the rationale are as follows:

TABLE 3-I

VALVE DESIGN CRITERIA

Parameter		Criteria
Fluid Compatible for 10 years with		N_2H_4, A-50, MMH, N_2O_4
Pressure:	Operating	300 psig nominal, 350 psig maximum
	Proof	525 psig for 5 minutes
	Burst	875 psig for 5 minutes
Leakage:	External	1 x 10^{-6} SCCS He maximum, 0-350 psig
	Internal	50 SCCH He maximum, 300 psig
Flow Capacity		2.0 pps N_2O_4 at 300 psig and 30 psid maximum
Response:	Open and/or Close	0.020 second maximum at 27 vdc, 300-350 psig, -65 to +225°F
Operating Temperature		-65 to +225°F
Electrical Power		2 amps maximum @ 32 vdc, 70°F
Minimum Operating Voltage @ 300 psi inlet pressure		18 vdc @ +70°F; 20 vdc @ +150°F
Maximum Operating Voltage		32 vdc
Cycle Life		200,000 wet cycles; 5,000 dry cycles
Sliding Parts/Seals		Design with minimum
Vibration (Random)		90-170 H_z @ +12 dB/Octave 170-375 H_z @ 1.65 g's/H_z 375-2000 H_z @ -6 dB/Octave 1 minute/axis
Acceleration		3.5 g's for 1 minute/axis
Dribble Volume		Minimize
Inlet Fitting		AN Male
Outlet Fitting		AN or Flange Type

TABLE 3-I (continued)

VALVE DESIGN CRITERIA

Parameter	Criteria
Weight	Minimize
Electrical Connection	30 ± 0.5 in. of shielded lead wire
Surface Coatings	None on normally wetted surfaces
Lubrication	None required
Dielectric Strength	No failure at 500 vac. rms, 60 H_z for 1 minute
Insulation Resistance	>100 megohms @ 500 vdc

Criteria	Rationale
Proof pressure of 1000 psi	Assume safe containment of ignition overpressures
Burst pressure of 5000 psi	Preclude catastrophic failure in event of an injector manifold explosion
Electrical power of <1 amp at 32 vdc, 70°F	Minimize vehicle power and power supply weight
Sliding parts/seals - none allowed	Minimize self-generated contamination
Provide integral 74 micron abs. filter	Preclude ingestion of large particles which could cause catastrophic leakage

3.3 VALVE ANALYSIS AND DESIGN (TASK I)

3.3.1 Principles of Operation and Description

The establishment for a sound technology base, substantiated by comprehensive analysis, is a vital prerequisite to committing to prototype fabrication, an advanced, design line fluid actuated valve for the Space Shuttle Program. Marquardt's initial effort (Task I), under NASA-JSC Contract NAS 9-13684, was the performance of extensive analysis and design studies, using computer modeling, to establish and substantiate design criteria for the proposed configuration. The line fluid pressure actuated valve, shown in Figure 3-3 and defined by Marquardt's Drawing X29550, establishes the baseline valve design.

The valve is of all corrosion-resistant metallic construction, with the exception of the PTFE poppet closure seals and the solenoid coil. It is designed to have all welded closures at all pressure vessel joints, in the flight configuration, though provisions for mechanical seals to external leakage will be incorporated into development units. The pilot stage armature and poppet are coaxial within the main stage poppet to provide high density packaging. All moving parts in the valve are flexure guided to achieve a design that features no sliding fits. Flat poppet closure interfaces have been incorporated which, when combined with flexure guided elements, effectively eliminate scrubbing action as closure seals engage or disengage, thus enhancing valve cyclic life.

LINE FLUID ACTUATED VALVE

FLIGHT CONFIGURATION

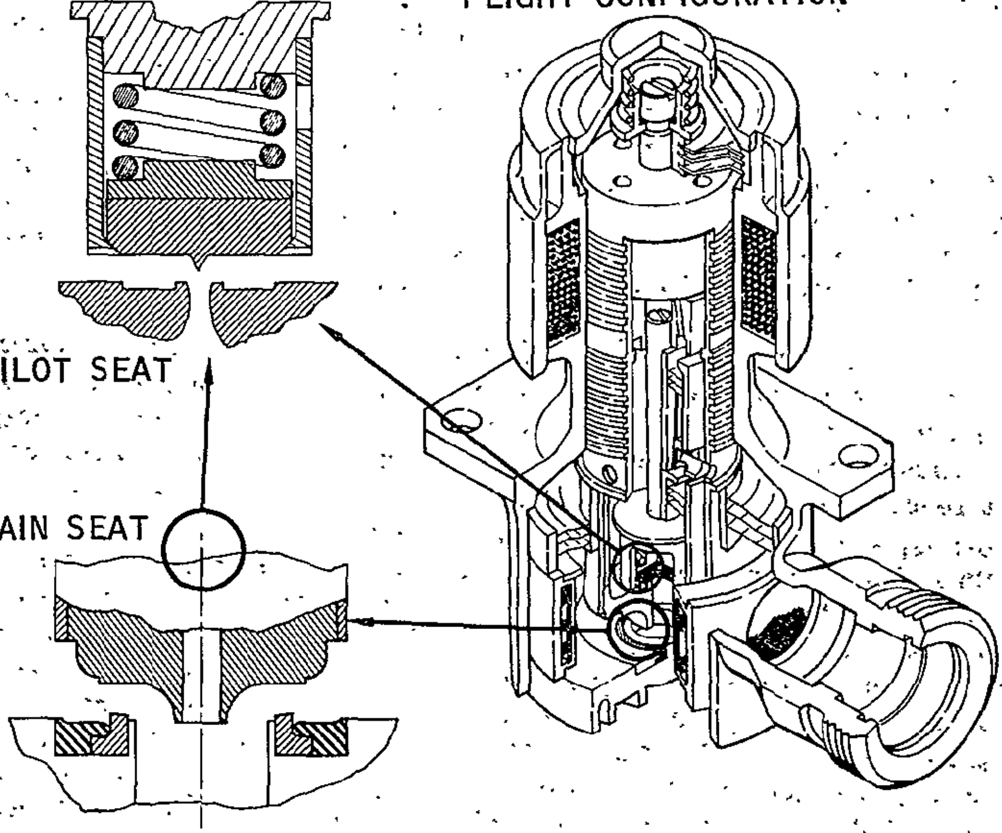

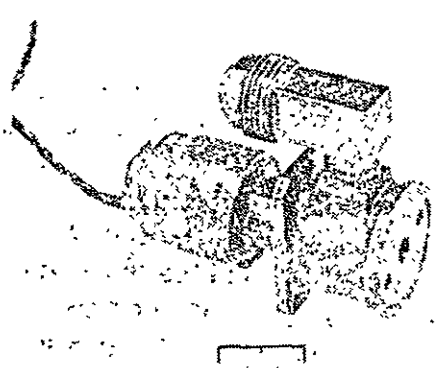

PROTOTYPE CONFIGURATION

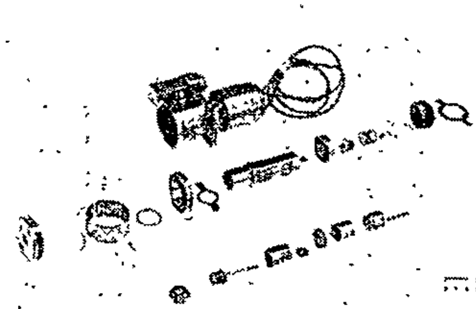

PROTOTYPE CONFIGURATION

Figure 3-3

With reference to Figure 3-4, which is a schematic representation of the design, operation of the valve is described as follows:

With the solenoid coil de-energized, the main coil spring and the pilot armature flexures provide preloads which hold the respective poppets in the closed (as shown) position. Fluid entering the valve's inlet at inlet pressure P_1 flows through the passages in the main stage poppet and the pilot poppet until all volumes upstream of the respective main and pilot stage seats are at the inlet pressure ($P_1 = P_2$). Under these conditions, with P_3 at zero, both poppets are pressure loaded closed as well as preloaded closed by the flexures and spring. These loads are more than sufficient to create leak-tight sealing, at each seat, under all operating conditions.

With the application of a "command open" electrical signal to the valve coil, a flux is generated in the solenoid circuit (ϕ) which creates tractive forces at the armature gap (g_p). At the design pull-in current, this tractive force is sufficient to overcome preload and pressure forces acting on the pilot armature-poppet assembly, and this assembly moves upward, reducing the "air" gap (g_p). As the pilot armature-poppet moves upward, flow is initiated through the pilot stage seat (Q_{2-3}). The pilot armature-poppet continues moving upward through its stroke (S_p) at which point the poppet strikes the annular ring which contains bleed ports. By design, the poppet obstructs flow from the bleed passages between the interior and exterior of the main stage poppet (Q_{1-2} reduces to zero). With flow through the pilot seat (Q_{2-3}) pressure (P_2) within the main stage poppet and in the cavities above the main stage poppet labyrinth seal, decays. As P_2 decays, pressure forces are generated which move the main stage poppet upward through its stroke (S_m). By design, the labyrinth seal leakage flow ($Q_{L\ 1-2}$) and the pilot stage flow (Q_{2-3}) are equal when the valve is in the full-open position and result in a P_2 pressure level such that a net opening pressure force is exerted on the main stage poppet (the pilot poppet is maintained open by the command signal in the coil).

With termination of the "command open" electrical signal to the valve's coil, the flux field (ϕ) collapses and the tractive forces at the "air gap" (g_p) diminish until the flexure preload forces and flow forces cause the pilot armature-poppet to move downward, closing the pilot stage seat and preventing flow across it ($Q_{2-3} = 0$). This action also opens the bleed ports to initiate flow through the bleed ports (Q_{1-2}). The bleed port flow Q_{1-2} and the labyrinth seal flow ($Q_{L\ 1-2}$) cause P_2 to increase, approaching P_1. This reduction in pressure differential across the main stage (P_1-P_2) causes opening pressure forces to decrease and ultimately become closing pressure forces. These pressure forces, acting with the coil spring preload forces, cause the main stage poppet to translate downward until closure of the main stage seat is achieved.

A73-6-489-8 C

LINE FLUID PRESSURE ACTUATED SHUT-OFF VALVE SCHEMATIC

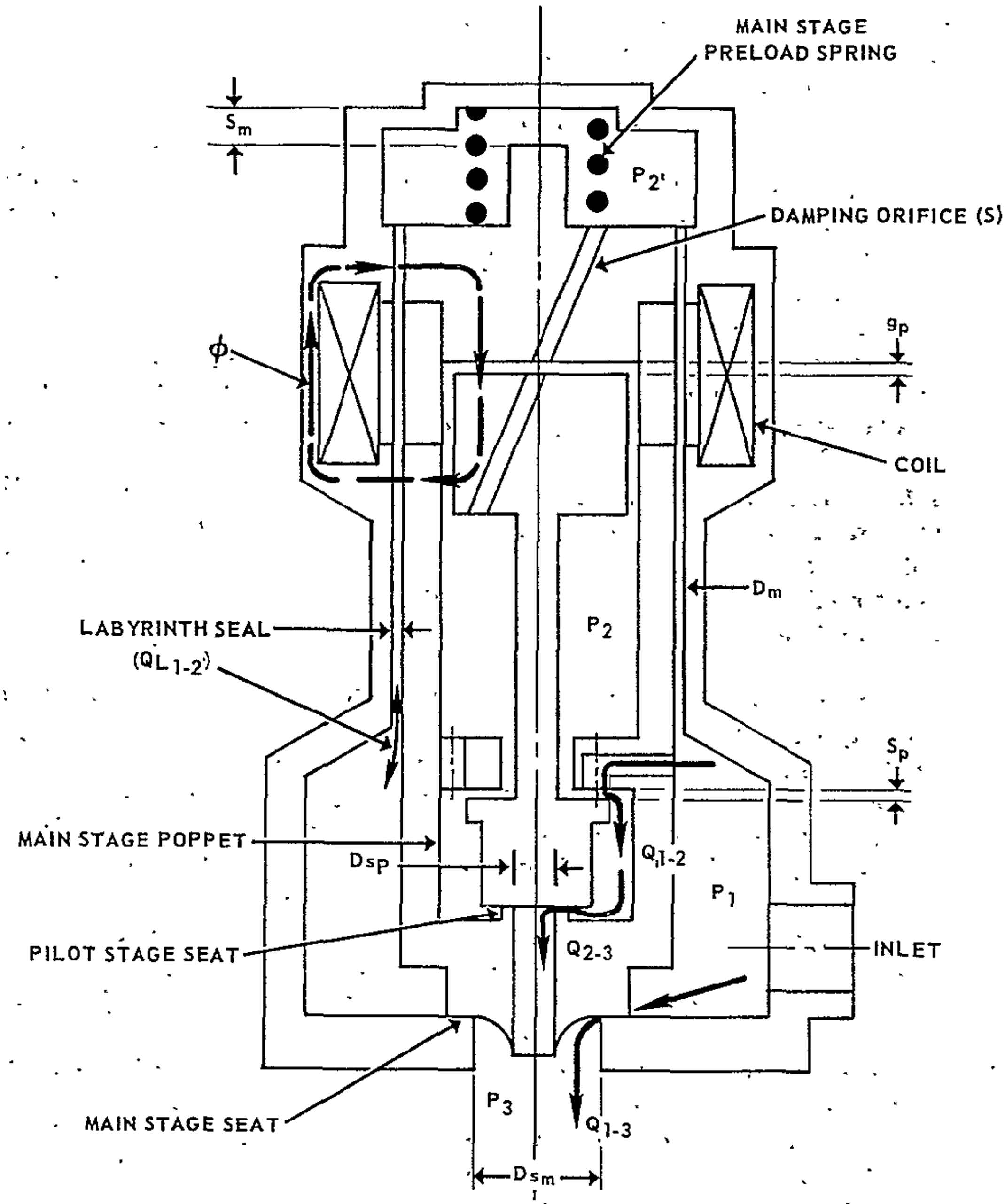

Figure 3-4

The valve body and detail parts are machined of bar stock. Pressure vessel elements are machined of vacuum arc remelted bar stock to be assured of the highest quality of raw material and finished part. Electron beam welding is used to join ferromagnetic materials to nonmagnetic materials to form the appropriate solenoid magnetic path. After welding, these parts are normalized to desensitize the heat-affected zone and recover maximum resistance to corrosive attack. The body structure uses Inconel 718 with 446 Cres ferromagnetic sections. Internal metallic details are made from Inconel 718 and 446 Cres ferromagnetic sections as required, with the exception of 302 Cres coil springs and the main stage poppet which is of A286 hardenable austenitic corrosion resistant alloy. The main stage poppet closure seal and the pilot poppet closure seal are machined of Marquardt processed PTFE bar. Flexure elements are chem-milled from Inconel 718 sheet stock to the appropriate pattern. Where mechanical joints are used to retain assemblies, electron beam "spiking" of the joint is employed to positively lock elements in position.

Packaging of the pilot stage coaxial and within the main stage poppet enhances packaging density and allows the pilot flow to enter the main stage flow port with minimum dribble volume. This packaging concept also allows for assembly and complete checkout of the pilot stage as an independent and separate unit from the main stage.

Two types of poppet closure seals are incorporated in the design, each being the optimum for their respective functions. The pilot stage employs a spring-loaded seal within the poppet. This seal closes against a raised, controlled width land seat to form a leak-tight seal. The interface concept limits, dimensionally, the compression of the seal material by providing a positive metal-to-metal stop and limits the seal material stress by properly sizing the seal preload of the coil spring. The pressure differential across the seal, in the closed position, provides additional sealing impetus. The coil spring also allows for thermal growth and contraction without changing the design sealing plane, allows for seal float so that it can adjust to minute misalignments (out of parallelism) of the mating planes, and essentially isolates the seal material from the impact loads of closure. This design concept has been fully developed and verified by relatively small diameter valve seats for seat cycle life in excess of 10^6 cycles, operating temperature ranges of over 500°F, and operating pressures up to 3000 psi. Analysis and test data for a similar valve seat application wherein this design concept was incorporated may be found in Reference 4 (Section 6 of this document).

The main stage poppet closure seal size does not make it amenable to the above-described design concept. The selected approach employs a captive PTFE ring in the valve seat which interfaces with the main stage poppet on

closure. This design concept is based upon the highly successful Marquardt R4D valve seat design in that the retention technology is common, using the concept of the controlled compression teflon primary seal and a metal-to-metal stop secondary seal immediately downstream of the soft seal. Fabrication and machining techniques developed during the Apollo R4D Valve Program will be employed to produce this valve seat. The teflon ring is machined to a form which assures positive mechanical retention and is held in place by a metallic retainer ring which is pressed into place and electron beam welded for positive retention. Dimensions are selected such that the retainer ring maintains an axial squeeze on the teflon throughout the operating temperature, yet does not give rise to extrusion or recession of the seal material. The inner retention lip, machined into the seat structural element, prevents overstress of the teflon upon closure by positively stopping the poppet after a controlled compression of the teflon by the poppet. This downstream positive stop concept also allows upstream pressure, acting on the teflon, to provide additional impetus to sealing by forcing the teflon toward the "zero gap" metal-to-metal interface. The teflon seal land width, contour and protrusion above the inner retention lip are selected to assure elastic-range seal interface stresses, over the range of operating temperatures and pressures, that will result in a "zero-liquid-leakage" seal. The flexure guided poppet and flat seal interface design combine to form a seal design that eliminates scrubbing or scuffing during mating and demating of the interface, thus greatly enhancing cycle life capability.

Flexure guidance of the moving elements of the valve design represents an area of technology in valve design in which Marquardt has made significant contributions. The flexure design to be employed is unique to Marquardt's designs and has been employed in a wide range of fluid control components involving far more severe operational requirements than this application. The flexures are spring element washers, in which a pattern is cut such that the I.D. and O.D. are positively retained and deflection results in bending and torsion of web elements with absolutely no rubbing or sliding. The web pattern is such that high radial stiffness results to assure positive axial alignment and a desired axial spring rate is achieved. A wide range of flexure sizes and patterns have been produced to date and have substantiated the design analysis approach and exhibited cycle life capability well in excess of 10^6 cycles with no change in performance characteristics. The flexure elements are located out of the main flow stream of the valve and are therefore not subject to flow stream impingement phenomenon. The flexure design and its employment in this valve design result in a valve configuration virtually free of self-generated contamination and allows clearances between parts with relative motion that render the design essentially contamination insensitive in spacecraft applications.

The maintenance of clearance with essentially sealing capability at the main stage poppet labyrinth seal presents a design challenge. Preliminary design studies assumed an effective clearance (radial) at this location of 0.001 inch, and turbulent flow when pressure differentials were present across this area. Since this magnitude of actual clearance is not practical due to tolerance effects, temperature effects and assembly difficulties, a labyrinth seal or series of grooves in the main stage poppet O.D. in this area will be employed. By creating a series of orifices in this area, minimizing the land width of each and providing adequate groove width to eliminate entry velocity effects, the actual radial clearance in this area can be increased to the order of 0.010 inch while maintaining a path with a resistance to flow equivalent to 0.001 clearance or less. By localized flow analysis, the ratios of radial clearance to groove depth and land width to groove width and land profile are designed to create a turbulent flow regime and a low flow coefficient. As an integral part of the design and analysis program, a design support test effort was performed to substantiate the analysis and confirm the selected design configuration. This technique of achieving a "seal" while maintaining tolerable clearances between moving elements has been used extensively in servomechanism controllers and valves.

On the basis of the analyses and design studies performed, projected performance and characteristics of the valve are listed in Table 3-II.

3.3.2 Static Analysis - Main Stage

3.3.2.1 Flow Requirement

To meet the specification requirement of 30 psi maximum valve pressure drop at a flow rate of 2.0 pps of N_2O_4, adequate flow area must be maintained in the valve open condition. Equating valve flow to equivalent orifice flow, the minimum flow area at the valve seat can be defined by:

TABLE 3-II

LINE FLUID ACTUATED SHUTOFF VALVE

PROJECTED PERFORMANCE CHARACTERISTICS

Parameter	Characteristics
Operating Fluids	N_2H_4, A-50, MMH, N_2O_4, H_2O, alcohol, freon solvents, He, N_2
Operating Pressure	350 psig max; 300 psig nominal
Proof Pressure	525 psig min for 5 minutes
Burst Pressure	875 psig min for 5 minutes
External Leakage - 0-350 psig	$<1 \times 10^{-6}$ SCCS GHe
Internal Leakage - 0-350 psig	<50 SCCH GHe
Flow Capacity	2.0 lb/sec N_2O_4 @ 300 psig inlet and 30 psid max
Response @ $27^{\pm 1}$ vdc, 350 psig inlet, 70°F, rated flow	18 ms opening 15 ms closing
Operating Temperature	-65°F to +225°F (except not with frozen propellants)
Electrical Power	25 watts @ 30 vdc, 70°F
Operating Voltage	18 to 32 vdc
Cycle Life	>200,000 cycles, wet and/or dry
Vibration	per Figure 3-5
Acceleration	±3.5 g
Envelope	1.50 dia x 3.8 inches
Valve Weight	0.99 lb

SHUTTLE RANDOM VIBRATION SPECTRUM

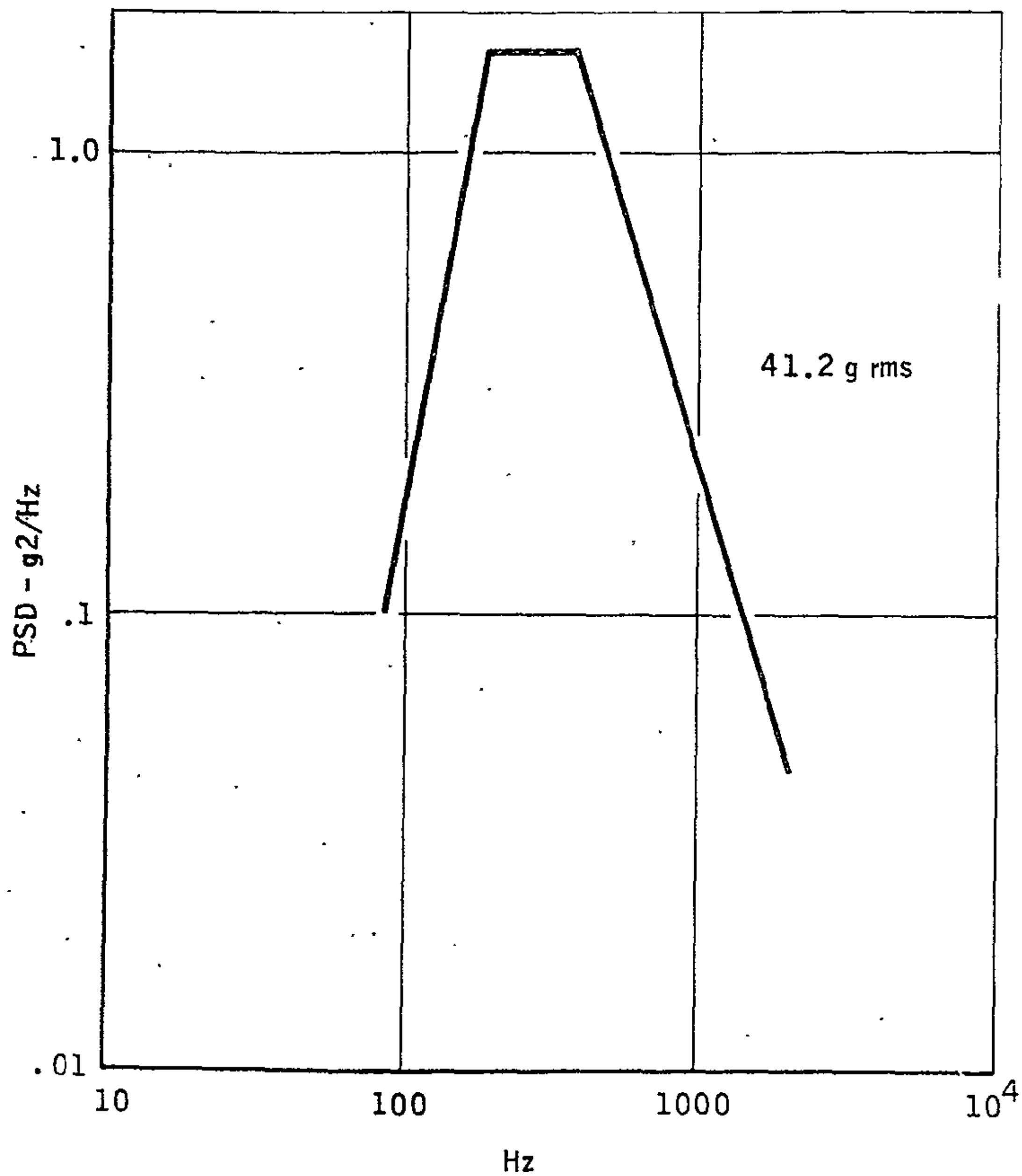

Figure 3-5

ORIGINAL PAGE IS
OF POOR QUALITY

$$A_t = \frac{W}{K_1 C_d \sqrt{\frac{P}{spg}}}$$

Where: A_t = flow area - in^2

W = required flow rate - $\frac{lb}{sec}$

C_d = orifice coefficient - (dimensionless)

ΔP = pressure drop - psi

spg = specific gravity, relative to water, of flowing fluid - (dimensionless)

K_1 = Constant - $\frac{in^3\ sec}{(lb)^{1/2}}$

For a flat poppet seat configuration, the flow area can be defined by:

$$A_t = \pi D_s S$$

Where: D_s = seat diameter - in.

s = poppet stroke - in.

For an assumed orifice flow coefficient of 0.65, the relationship of seat diameter and poppet stroke are plotted in Figure 3-6.

On the basis of parametric studies, utilizing the analog computer model described in Section 3.3.3, a seat diameter of 0.40 inch and a seat preload of 3.0 lbs was selected for the main valve seat. Since the design is a pressure unbalanced poppet, seat loading will be proportional to valve pressure differential. This relationship is plotted in Figure 3-7, where the seat loading is expressed in pounds per circumferential inch of seal surface.

MAIN SEAT DIAMETER VS. STROKE

For 30 psid @ 2.0 pps N_2O_4

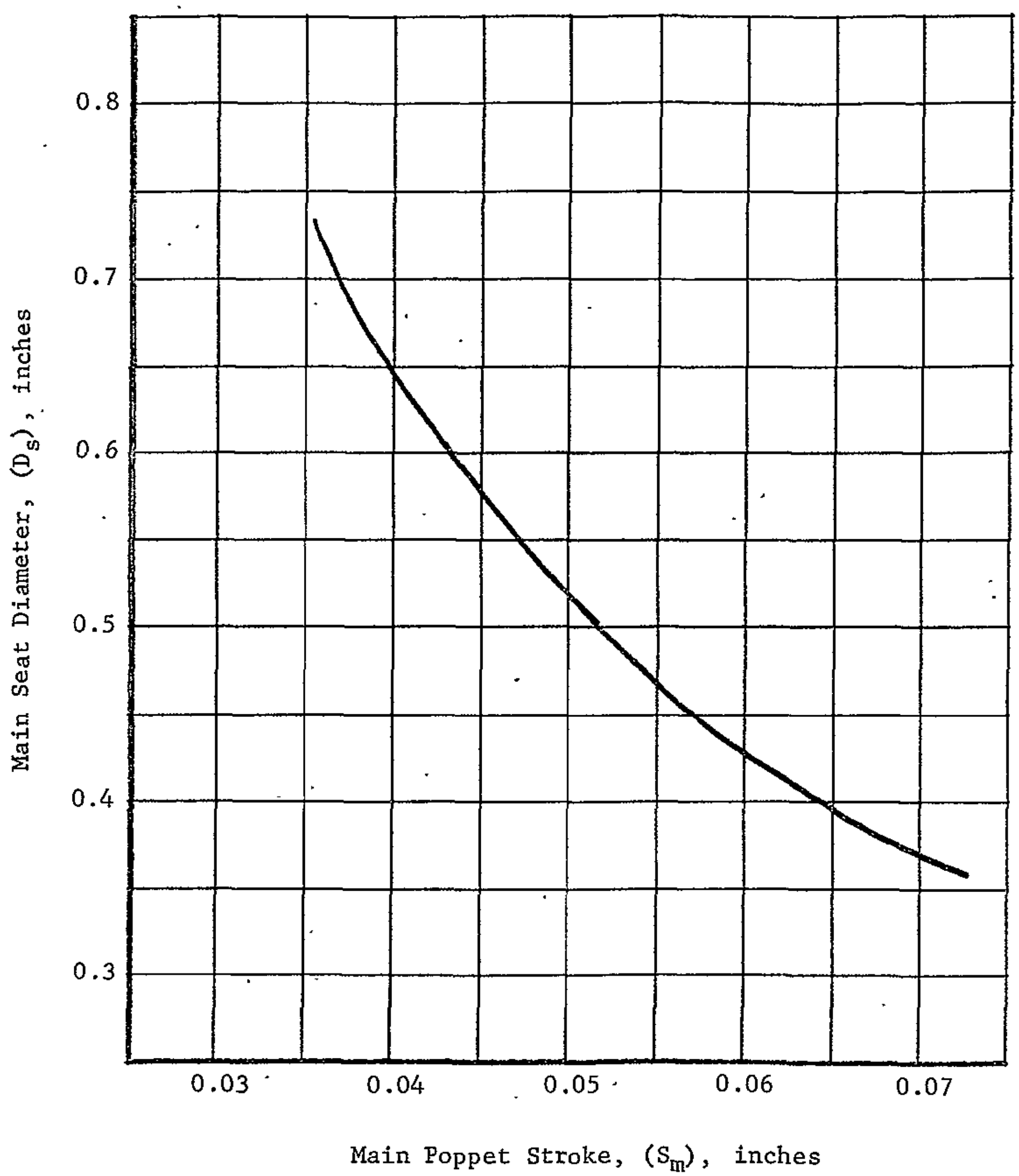

Figure 3-6

MAIN SEAT CLOSED ΔP VS. SEAT LOAD RATE

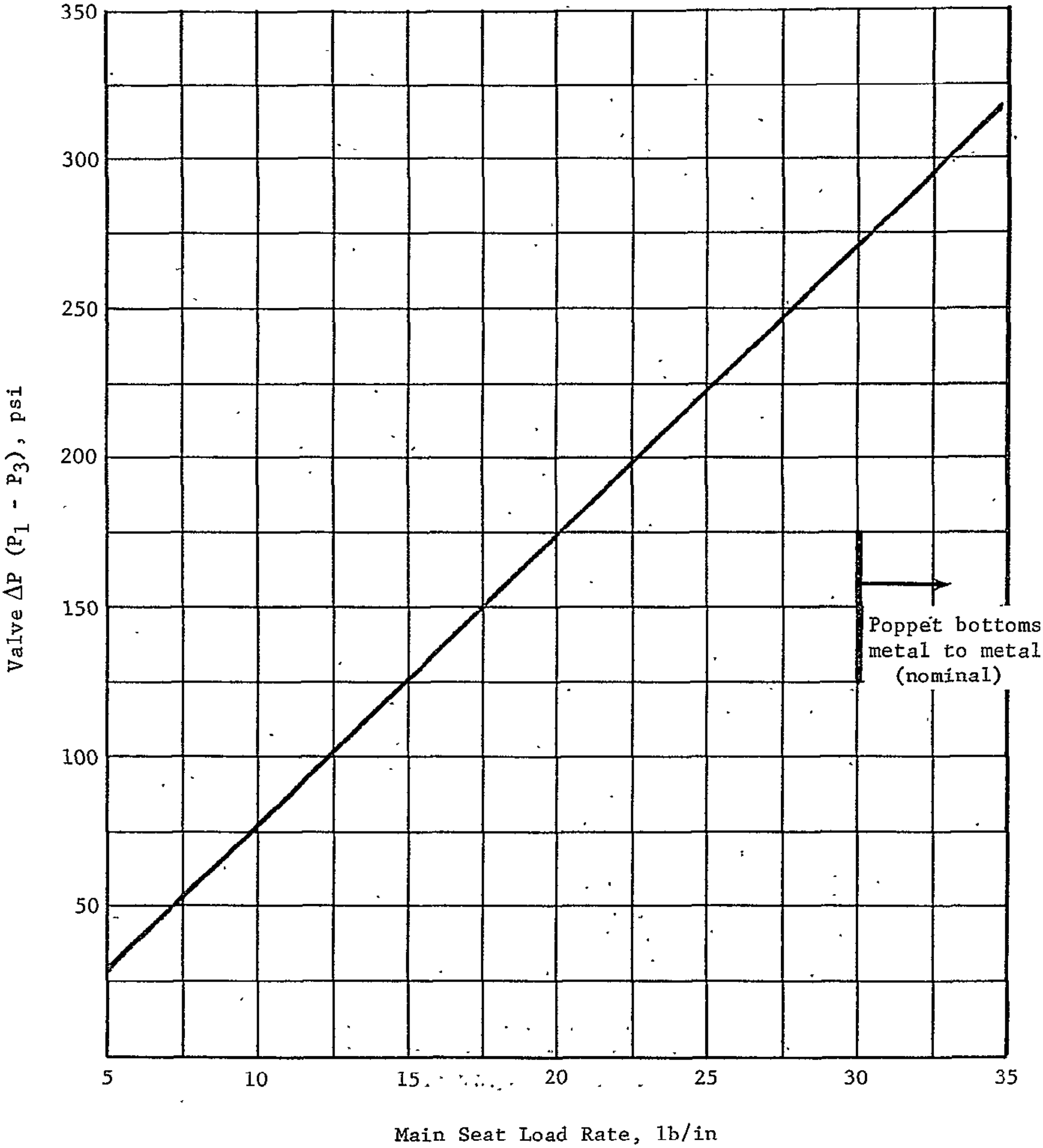

Figure 3-7

With reference to the operational schematic Figure 3-4, the generalized force balance equation for the main valve can be written as:

$$F = -F_{pre} - KS_m + \frac{\pi}{4} D_m (P_1 - P^1_2) - \frac{\pi}{4} D_s (P_1 - P_3)$$

Where: F = net force on poppet (+ opening - closing - lb)

F_{pre} = seat preload - lb = 3.0 lb

K = spring rate - lb/in. = 30 lb/in.

S_m = poppet stroke (from closed position) - in.

D_m = diameter of piston - in. = 0.75 in.

D_s = diameter of seat - in. = 0.4 in.

P_1 = inlet pressure - psi

P^1_2 = pressure in pilot cavity - psi

P_3 = outlet pressure - psi

For the valve closed condition (S_m = 0) and setting F equal to zero, the relationship between valve pressure differential ($P_1 - P_3$) and the differential across the main piston ($P_1 - P^1_2$) can be derived. This defines the threshold of valve cracking, since an increase in ($P_1 - P_2$) or a decrease in ($P_1 - P_3$) will result in a positive (opening) net force on the poppet. This relationship is shown in the upper curve of Figure 3-8. Capability to achieve the required piston differential pressure to effect valve cracking is a function of the labyrinth seat clearance and length and the pilot valve flow diameter of 0.1 inch (Ref. Figure 3-17) and employing the leakage model of Section 3.3.2.2, the main piston pressure differential can be correlated to the labyrinth seal clearance and length. This correlation is plotted in the lower curves of Figure 3-7.

When the valve is fully open, pressure differentials must exist to generate sufficient force to overcome mechanical forces. Setting the net poppet force equal to zero in the force balance equation, and with the stroke at 0.065, the relationship between valve pressure differential ($P_1 - P_3$) and main piston

pressure differential ($P_1 - P_2$) is determined. This characteristic is shown in the upper plot of Figure 3-8. Using the labyrinth leakage model and assuming a pilot valve flow diameter of 0.10 inch, main piston differential can be expressed as labyrinth clearance and labyrinth leak path length as shown in the lower plot of Figure 3-9.

From the curves of Figures 3-8 and 3-9, and with a labyrinth seal length of 1.5 inches, it is apparent that a labyrinth seal radial clearance of no greater than 0.014 inch will assure valve cracking at valve differentials up to 400 psi. However, a stable full open position is very dependent upon valve differential pressure and labyrinth clearance. At a differential of 30 psi labyrinth radial clearance must be less than 0.012 inch. It is also evident that a valve differential of at least 12 psi is required to maintain the poppet in the full open position even if labyrinth seal clearance is reduced to 0.000 inch. To assure large margins at all anticipated operating conditions and to minimize sensitivity of the valve to tolerance and eccentricity effects in the labyrinth seal area, a nominal radial clearance of the labyrinth seal of 0.0025 to 0.0040 inch is selected. During development testing, increasing of this clearance to reduce particulate sensitivity will be vigorously pursued.

3.3.2.2 Labyrinth Seal Analysis and Development

The establishment of a "seal" at the main piston O.D. without any sliding or rubbing action is the crux of the long life valve design. Conceptual analysis assumed that an 0.001 inch radial clearance, with either turbulent or laminar flow, was the maximum allowable clearance to assure proper performance. Since this magnitude of clearance is impractical to assure no sliding or rubbing throughout valve stroking, even using flexure guided elements, the analysis and development of a labyrinth seal and its leakage flow modeling were pursued. By introducing a series of lands and grooves perpendicular to the flow path, turbulent flow would be induced and flow would be less dependent upon the radial clearance at the lands. Each land would act as a sharp edged orifice and the cumulative effect of all lands would be a very low orifice coefficient, thereby offering high resistance to flow. Reference data were primarily concerned with labyrinth seals employed in compressible fluid flow, rotating seals as in turbines and the "Visco seal" where a liquid-gas interface seal is achieved. It, therefore, became apparent that a simplified, analytical solution to the labyrinth seal leakage flow, as used in this application, was not readily available. A generalized model was developed which assumed that fully developed turbulent flow is not realized between the lands, since insufficient length is available to dissipate the velocity and fully developed laminar flow is not realized at the lands due to insufficient land length to realize a true laminar velocity profile.

VALVE ΔP (P_1 - P_3) VS. LABYRINTH RADIAL CLEARANCE AND PRESSURE DIFFERENTIAL (P_1 - P_2) TO EFFECT VALVE CRACKING

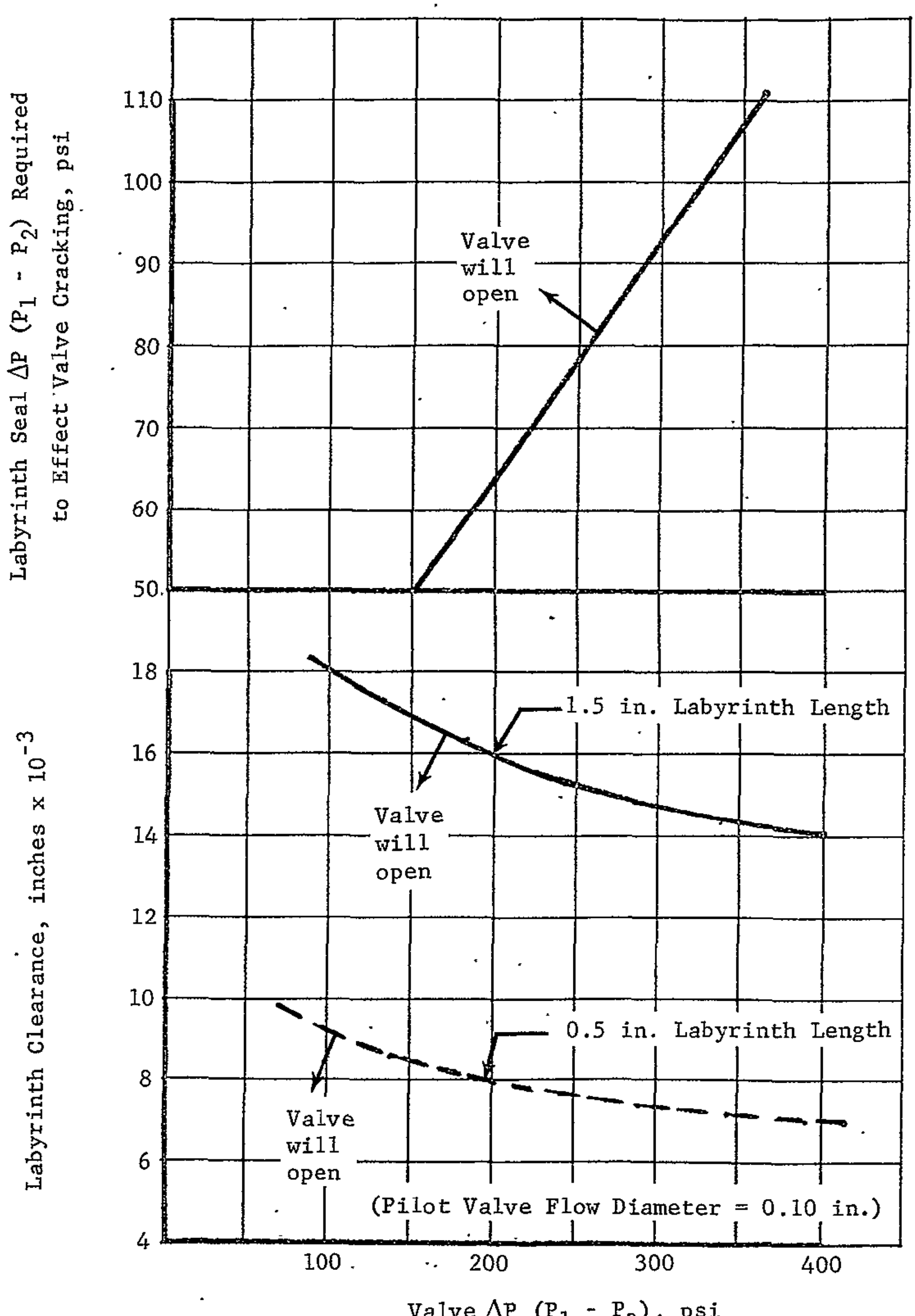

Figure 3-8

VALVE ΔP $(P_1 - P_3)$ VS. LABYRINTH RADIAL CLEARANCE AND PRESSURE DIFFERENTIAL $(P_1 - P_2)$ TO EFFECT VALVE FULL OPEN CONDITION

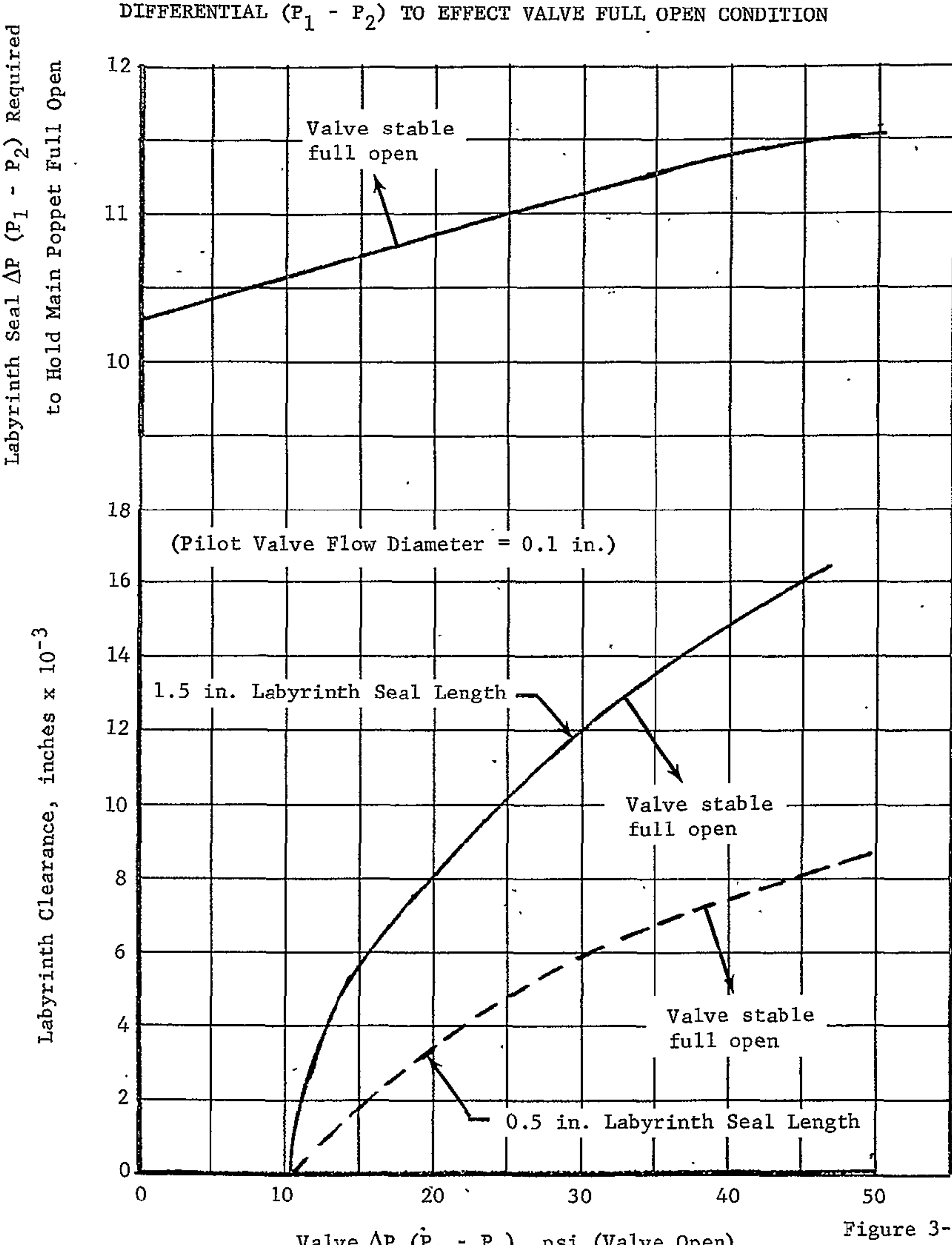

Figure 3-9

Concurrently, test hardware was fabricated and water flow tests conducted to establish leakage flow characteristics as a function of pressure differential, labyrinth seal length, labyrinth geometry, and radial clearance. Test data were correlated with the leakage model to determine appropriate constants.

For the labyrinth geometry selected for this application and applying appropriate conservative constants, developed from test data correlation, the leakage flow model takes the form:

$$Q_2 = \frac{4.527 \times 10^5 D_m \ell \mu}{\rho b} \left[\sqrt{1 + \frac{15.353 \times 10^{-5} \rho b^4 \Delta P}{\ell^2 \mu^2 n}} - 1 \right]$$

Where: Q_2 = leakage flow rate - in. ^{3}/sec.

D_m = annular passage mean diameter - in.

ℓ = length of labyrinth land - in.

μ = fluid viscosity - $\frac{\text{lb-sec}}{\text{ft}^2}$

ρ = fluid density - lb/ft^3

b = radial clearance at land - in.

ΔP = pressure differential - lb/in.^{2}

n = number of lands

A portion of the seal leakage test data is shown in Figure 3-10 for a seal length of 0.5 inch. In Figure 3-11, the test data and leakage model predictions are shown for several radial clearances and labyrinth geometries.

As is evident from the labyrinth leakage model wherein both laminar and turbulent flow regimes exist, flow rate is dependent upon fluid density and viscosity. The pilot flow area, which constitutes the remaining portion of the pressure divider element that affects valve operation, is experiencing turbulent flow only and the flow rate is therefore dependent upon fluid density only. For the range of operating fluids and operating temperatures, variations in the respective flows can be anticipated. For the primary usage fluids (MMH and N_2O_4) and employing the leakage model and turbulent flow equations, the

PISTON SEAL LABYRINTH DEVELOPMENT TEST RESULTS

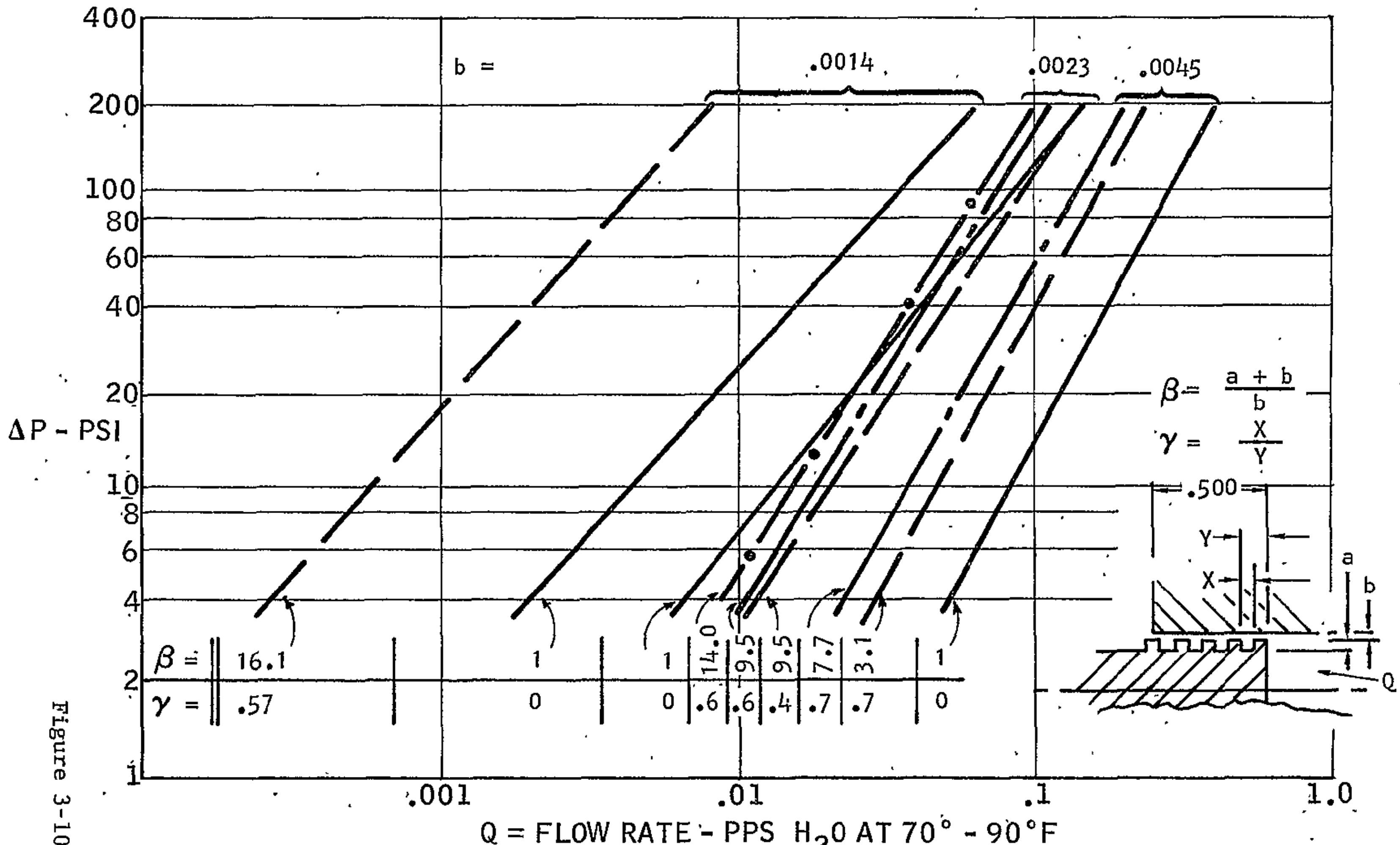

Figure 3-10

LABYRINTH SEAL LEAKAGE MODEL CORRELATION WITH TEST DATA

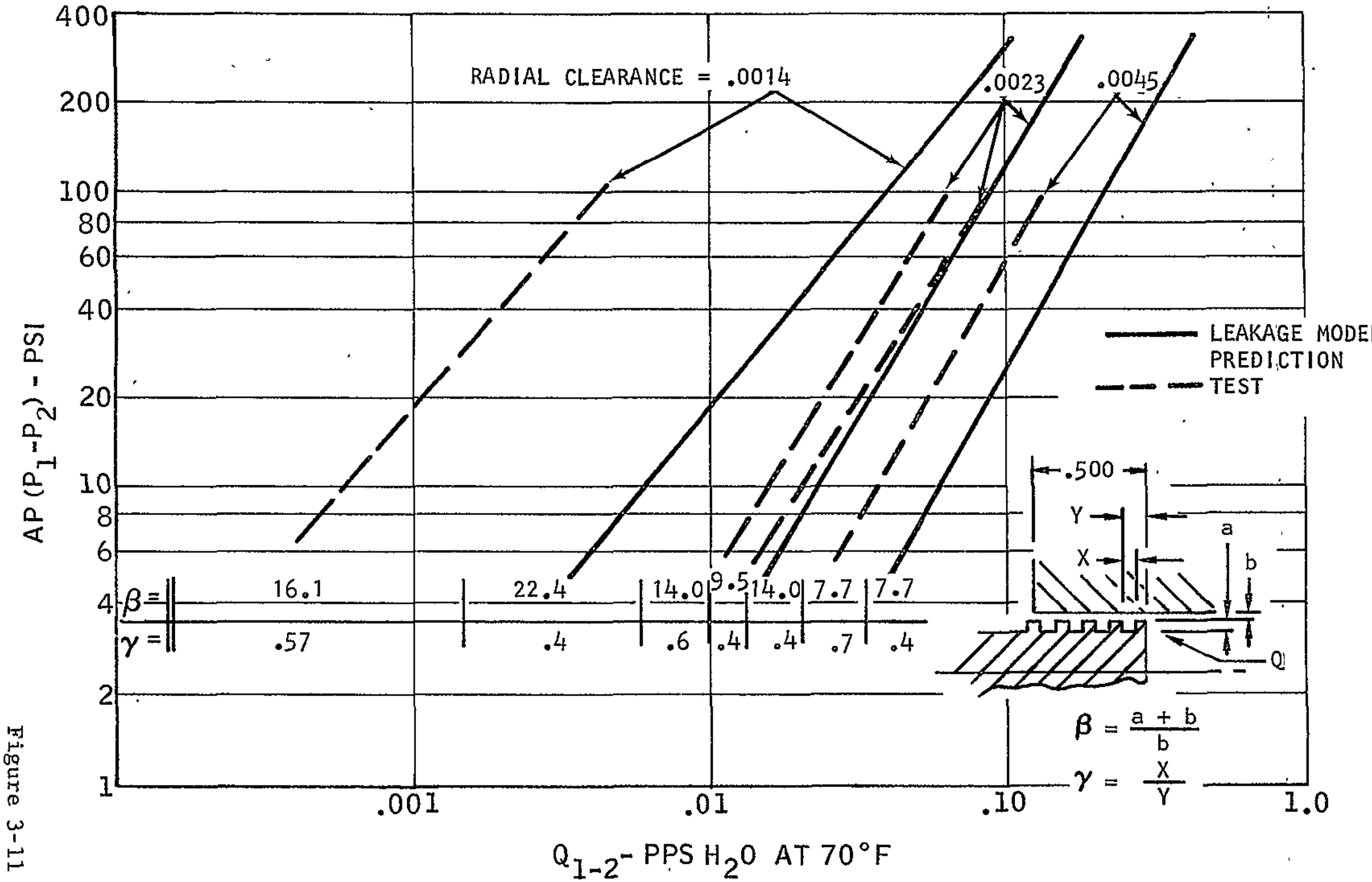

Figure 3-11

THE Marquardt COMPANY VAN NUYS, CALIFORNIA

A75-2-711-12

variations in volumetric flow as a function of temperature, for the labyrinth seal and the pilot flow diameter, can be determined. The dependence of the labyrinth seal flow on viscosity is also a function of pressure differential since the laminar portion of the flow will decrease as the flow velocity increases. The temperature effects on fluid viscosity and fluid density are shown in Figure 3-12, wherein the variation in labyrinth flow is shown for pressure differentials from 10 to 100 psi (greater variations occur at the lower pressure differentials). The corresponding variations in pilot valve flow, with temperature tend to offset labyrinth flow variations, thus minimizing variations in performance due to temperature.

3.3.2.3 Main Poppet Preload

A main poppet preload of 3.0 pounds (valve closed) was determined from conceptual design analog model iterations. These iterations confirmed the desirability of minimizing the mechanical spring rate of the main poppet to enhance valve full open stability. Subsequent analyses utilized the 3.0 pounds preload and employed a spring rate of 30 pounds/inch, resulting in acceptable performance characteristics. To achieve these values, the flexure guidance elements and a coil spring are employed. The net effective load vs. stroke characteristic of these elements is shown in Figure 3-13. The nonlinear spring characteristic is attributable to the flexure guidance element design. To enhance life margins of the flexures, the main poppet stroke of 0.065 would require a large span element $\frac{OD-ID}{2}$, thus greatly enlarging the overall valve diameter and significantly increasing valve weight. Thus, by employing the flexures in a configuration wherein they deflect one-half the stroke from the null position (flat state), their span may be reduced and cycle life enhanced. Using the coil spring as the force element, the seat preload of 3.0 pounds is achieved by installing the spring with a load of 3.0 pounds, plus the load necessary to deflect the flexures main poppet stroke/2 inches from the null position. The overall effect is to create two distinct spring rates, but with a net overall spring rate of less than 30 lb/inches. Several advantages are realized by this approach, in addition to minimized valve weight and enhanced flexure cycle life:

- The main poppet spring mass system exhibits two distinct natural frequencies which will dampen excitation.
- The soft initial spring rate aids in accelerating the piston during opening.
- The high final spring rate aids acceleration of the piston in closing.

PILOT VALVE AND LABYRINTH SEAL FLOW vs TEMPERATURE

LABYRINTH SEAL FLOW RATIO SHOWN FOR 10 TO 100 PSID

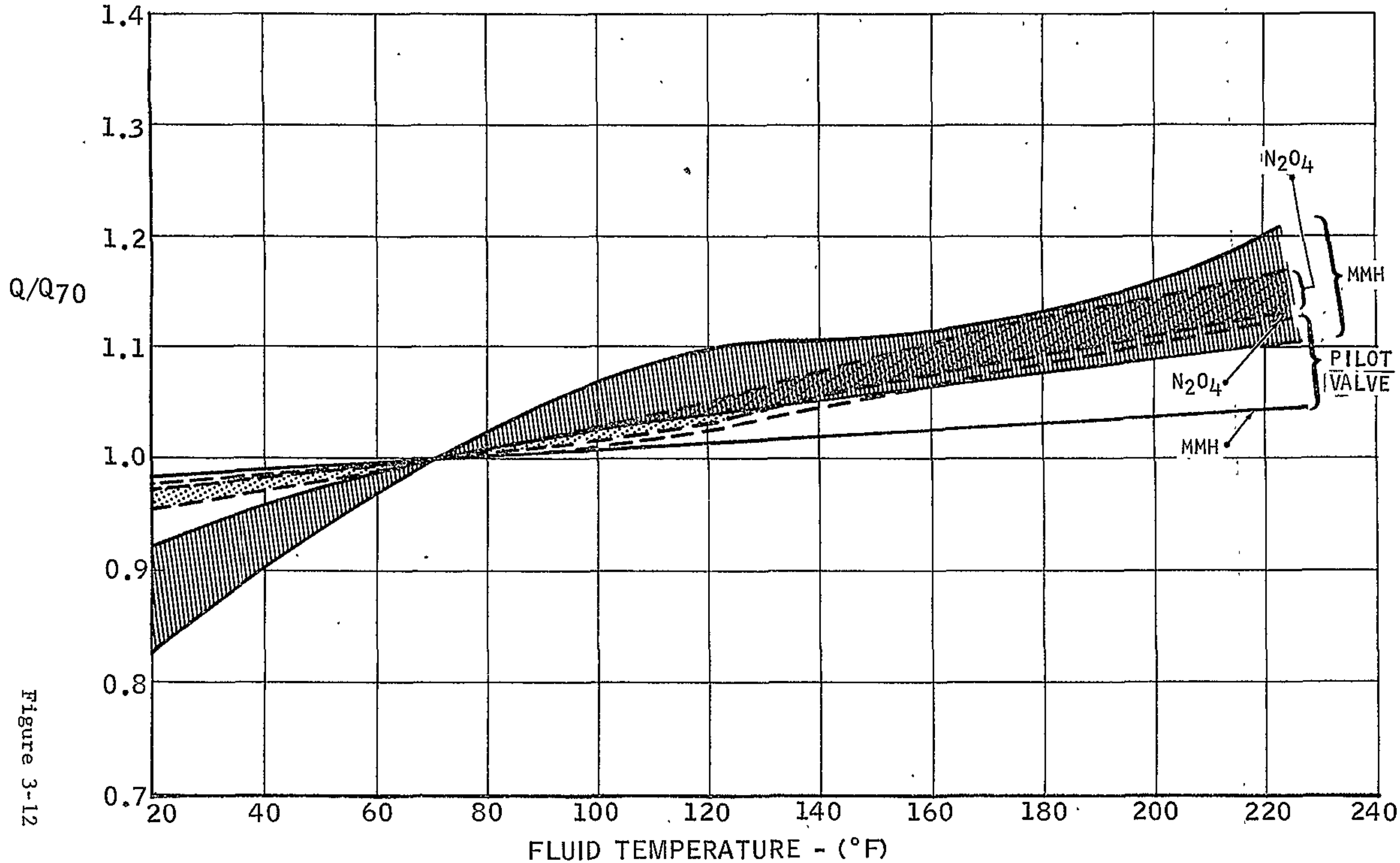

THE Marquardt COMPANY VAN NUYS, CALIFORNIA

TMC 3293-6-3

A75-1-711-5

Figure 3-12

MAIN POPPET MECHANICAL LOAD VS. STROKE

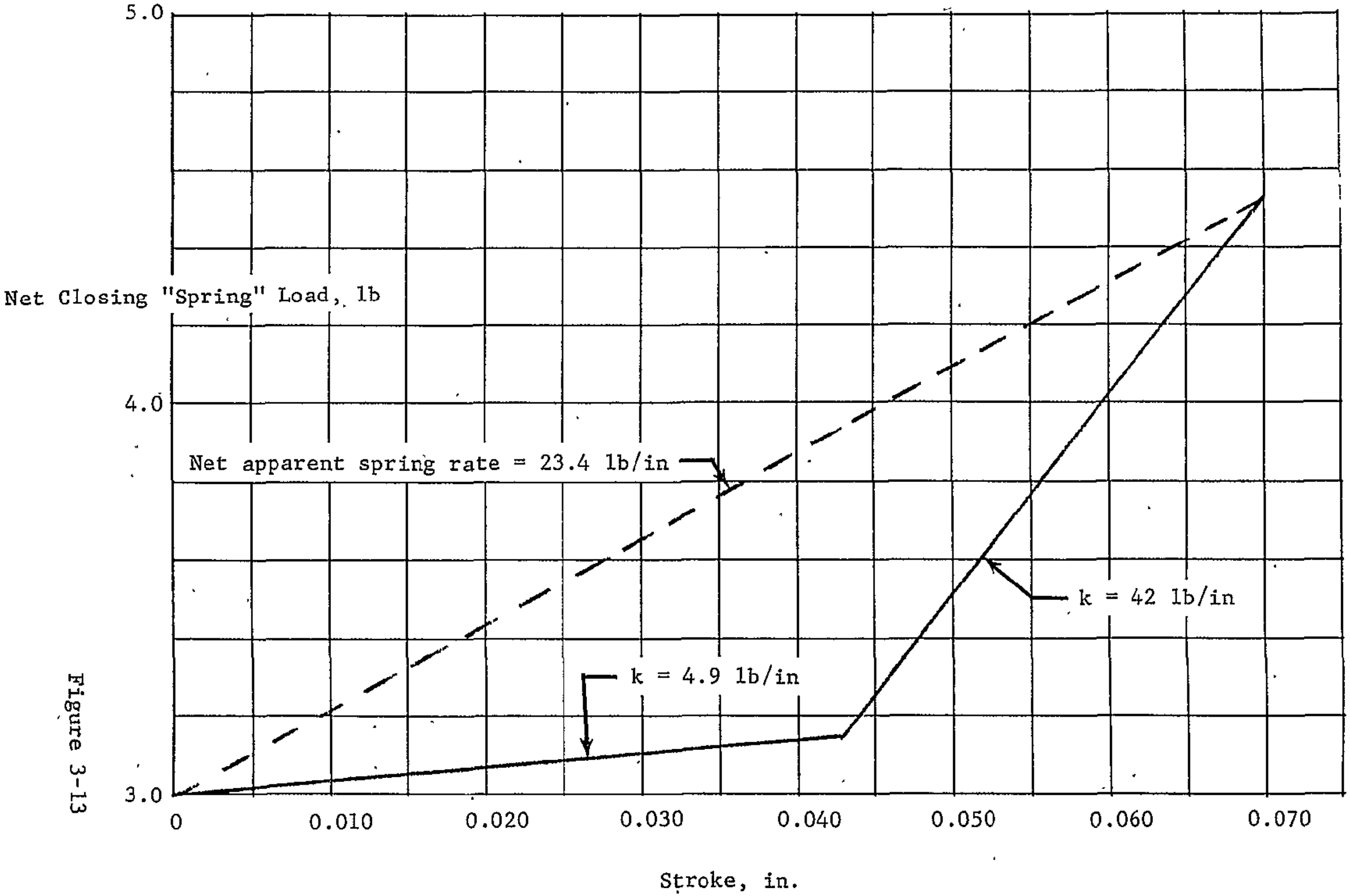

Figure 3-13

3.3.3 Dynamic Analysis - Main Stage

Dynamic analysis of the design represents the most crucial area of the design effort, since operational characteristics are confirmed. The design is a complex hydraulic and mechanical network. Simultaneous solution of all flow and force balances of the design during valve operation is essential to assure a stable design. Analog computer modeling is the optimum technique to synthesize the design and perform a complete evaluation analysis.

An elementary analog model of the valve concept was constructed and iterated during the preliminary design effort, to establish the feasibility of the design and determine nominal design criteria. With the development of the leakage model and its confirmation by test, and the design and analysis studies of other critical elements, the analog model was refined. Provisions were added to accommodate the various damping factors, the nonlinear main poppet spring rate, the labyrinth leakage flow model, the damping chamber volume effects and refinement of downstream volume characteristics. The block diagram of the analog model is shown in Figure 3-14.

Using Marquardt's Beckman Ease Model 1100 analog computer, approximately 100 iterations of the model were performed to evaluate operational and design variables. A typical output data trace for the nominal valve design at nominal operating conditions is shown in Figure 3-15. Analog iterations were performed over the range of labyrinth seal design parameters, such as seal length and radial clearance, to assess tolerance impact on valve performance. Response characteristics, as a function of these parameters, is plotted in Figure 3-16. On the basis of these results, a labyrinth seal length of 1.5 inches was selected. Labyrinth seal radial clearance for the prototype units was selected at 0.0025 to 0.0040 inch. Since sensitivity to tolerance effects is minimized, this range represents a practical tolerance, the clearance is compatible with the integral 75 μ filter and overall system contamination level, with respect to insensitivity to particulates, and subsequent modifications to investigate larger clearances later in development are most economical.

For the selected labyrinth seal clearance, valve response sensitivity to pilot flow diameter or flow capacity was evaluated. Figure 3-17 plots the response of the main poppet as a function of pilot flow diameter for labyrinth seal lengths of 0.5 and 1.5 inches. The relative insensitivity, to pilot flow diameter, of the 1.5 inch long seal length confirms its selection for the prototype valve. Since pilot valve diameter refers only to flow area from the pilot chamber into the outlet volume, closing response will be insensitive to this flow for all intensive purposes.

SYSTEM BLOCK DIAGRAM

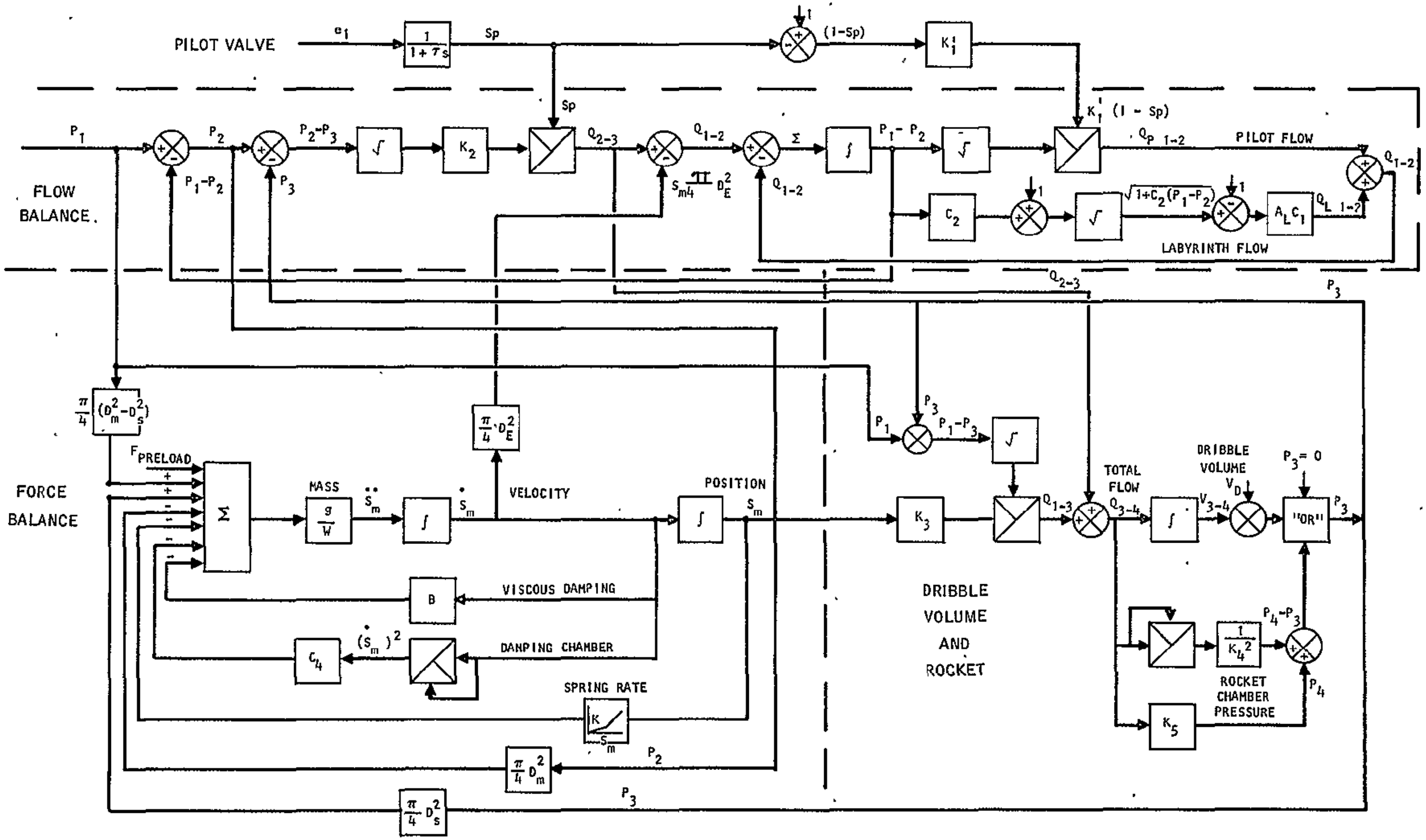

Figure 3-14

THE Marquardt COMPANY VAN NUYS, CALIFORNIA
TMC 3293-6-3
A75-2-711-10

ANALOG MODEL OUTPUT TRACE

- NOMINAL DESIGN
- NOMINAL CONDITIONS
- RUN NUMBER 43

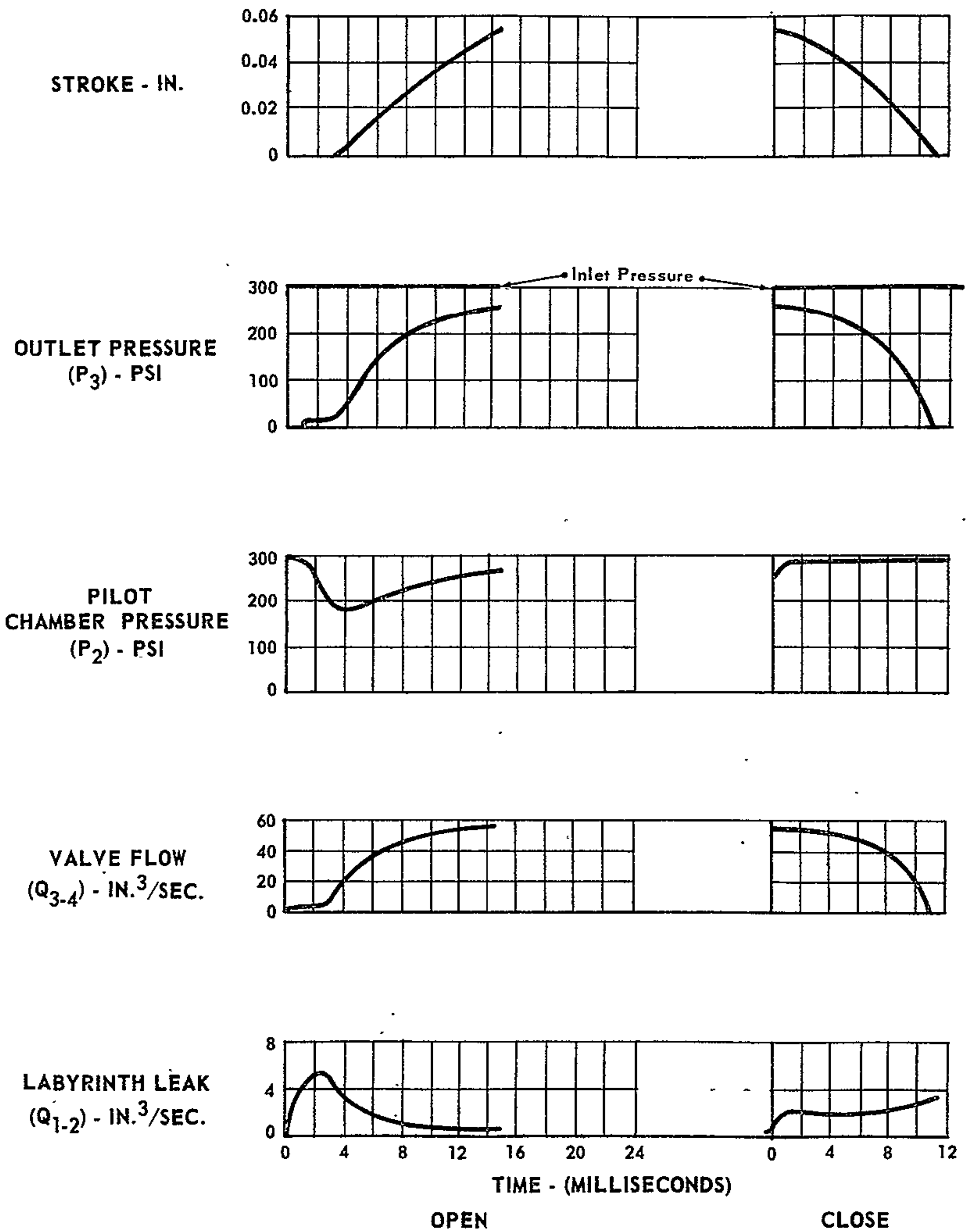

Figure 3-15

VALVE RESPONSE VS. LABYRINTH RADIAL CLEARANCE

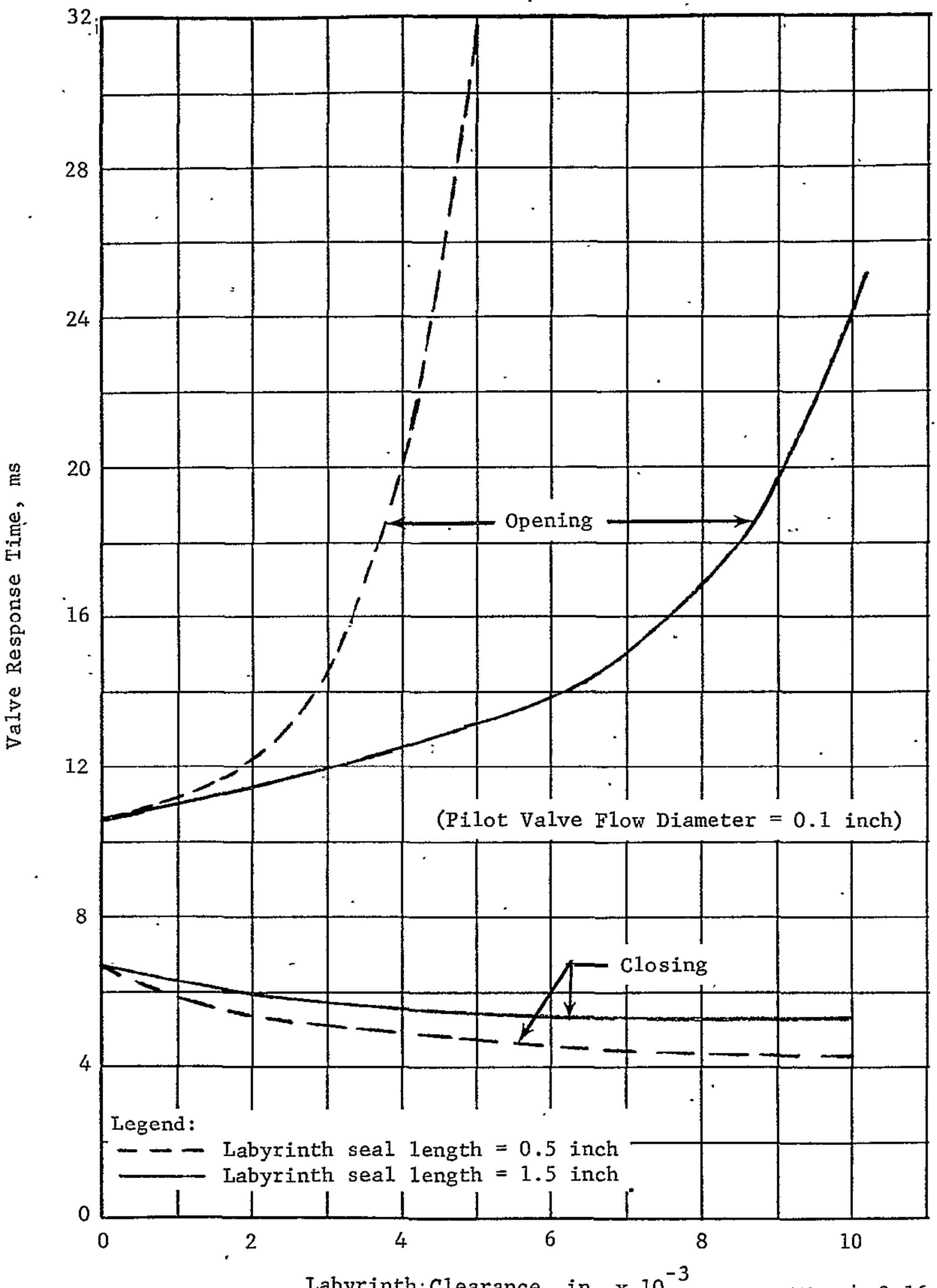

Figure 3-16

VALVE RESPONSE VS. PILOT VALVE FLOW DIAMETER

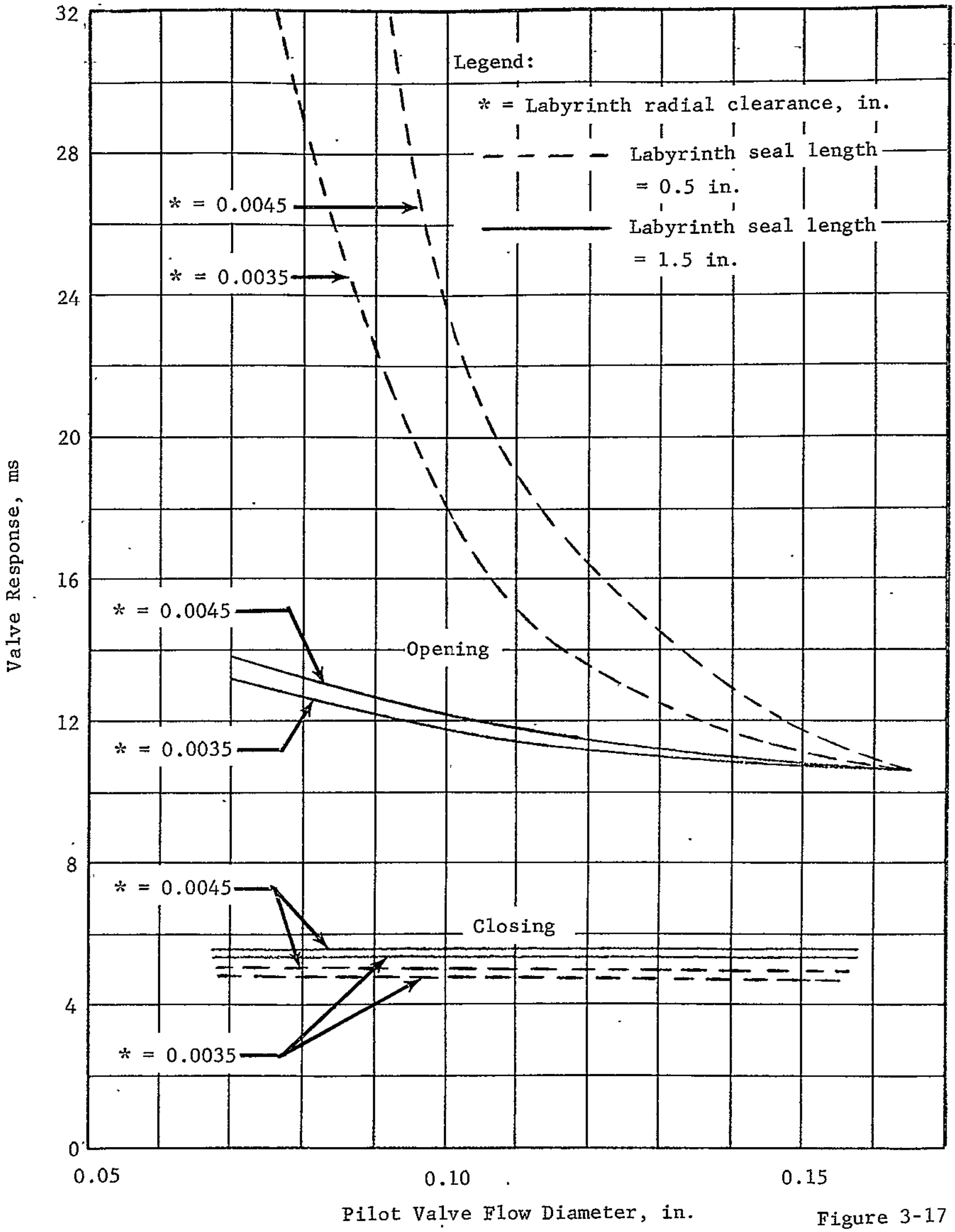

Figure 3-17

The predominant damping element of the design is the orifice between the damping chamber and the interior of the main piston/pilot chamber. The hydraulic porting design of the valve is such that this orifice is most effective during the closing mode, since the volume displaced by the main piston stroke must be filled with fluid media and the primary source of this fluid enters the pilot chamber through the pilot upper orifices and flows through the damping orifice into the damping chamber. Figure 3-18 illustrates the influence of damping orifice diameter on response. For reasons of limiting closing impact forces, which are discussed later in this report, a high damping factor (0.060 in diameter orifice) was selected for the prototype design.

(Note: Closing response characteristics in Figures 3-16 and 3-17 are based upon a 0.147 inch damping orifice).

From both the static analysis and analog model iterations, it is apparent that the valves' performance characteristics are responsive to the inlet pressure. To resolve the magnitude of this sensitivity, two phenomena were investigated:

- Valve response as a function of inlet pressure level.
- Dynamic reactions to pressure perturbations superimposed on inlet pressure during opening and closing.

Inlet pressure sensitivity is shown in Figure 3-19 for the nominal design. Response times will increase with decreasing inlet pressure level, as expected; however, the characteristic remains relatively flat throughout the anticipated usage pressure range (200 to 350 psi) and inlet pressure does not amplify sensitivity to other parameters.

For a bipropellant engine application, disparities in inlet pressures of the respective propellants result in valve response mismatch. Mismatch, as a function of these pressure differentials, is shown in Figure 3-20.

The nature of most system pressure perturbations can be characterized by a rapidly damped sinusoidal oscillation. The analog computer model was iterated while superimposing a sinusoidal inlet pressure oscillation of 50 psi amplitude on the nominal inlet pressure. Frequency of the oscillations was varied, using the function generator, until the output signals reflected a significant impact on valve performance characteristics. Figure 3-21 illustrates the analog output trace for a 60-cycle $\pm$ 50 psi inlet pressure oscillation. Phasing of the valve opening command relative to the pressure oscillation was varied to achieve maximum effect on valve performance. It is

VALVE RESPONSE VS. LABYRINTH RADIAL CLEARANCE

AT VARIOUS DAMPING ORIFICE DIAMETERS

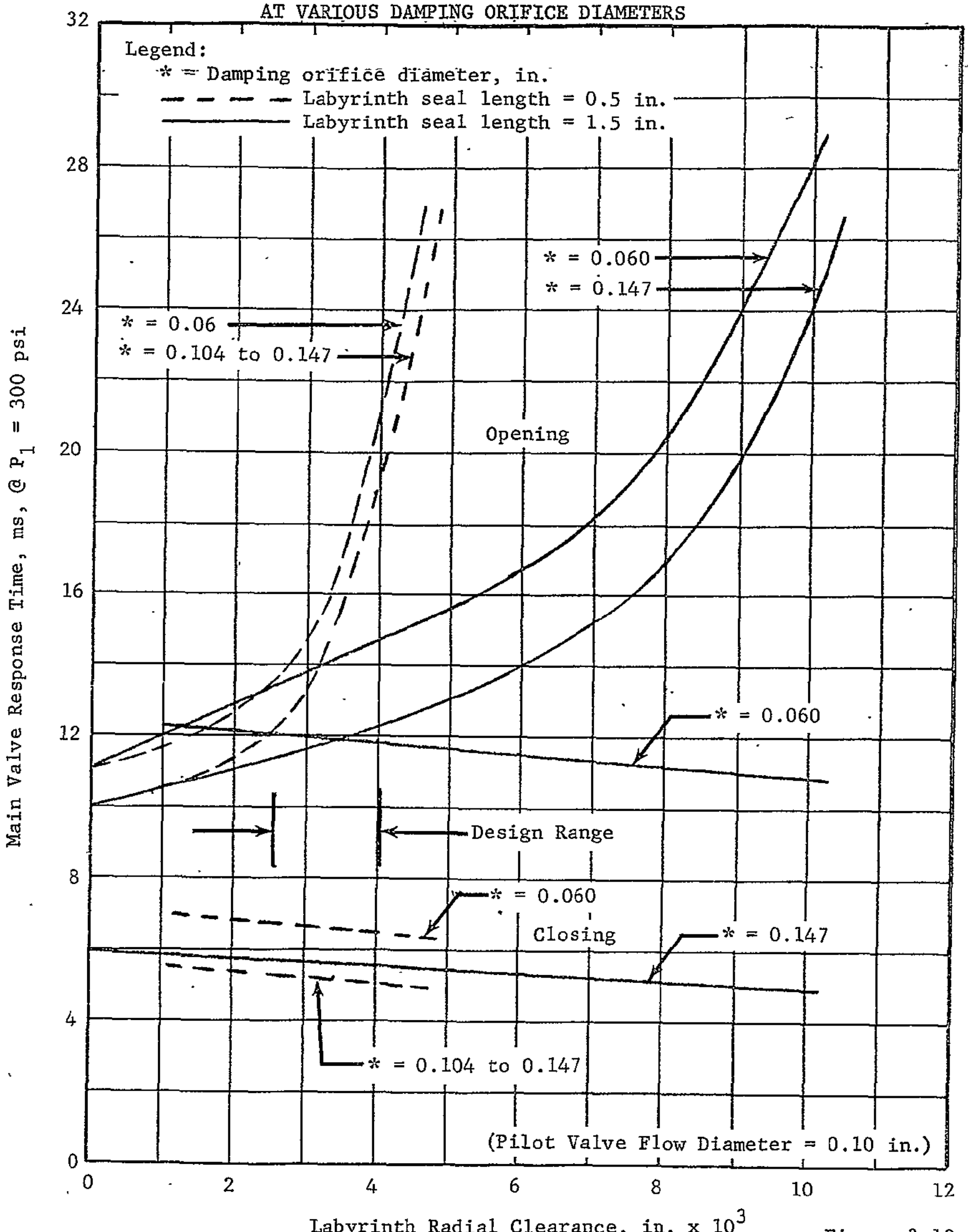

Figure 3-18

MAIN VALVE RESPONSE VS. SUPPLY PRESSURE

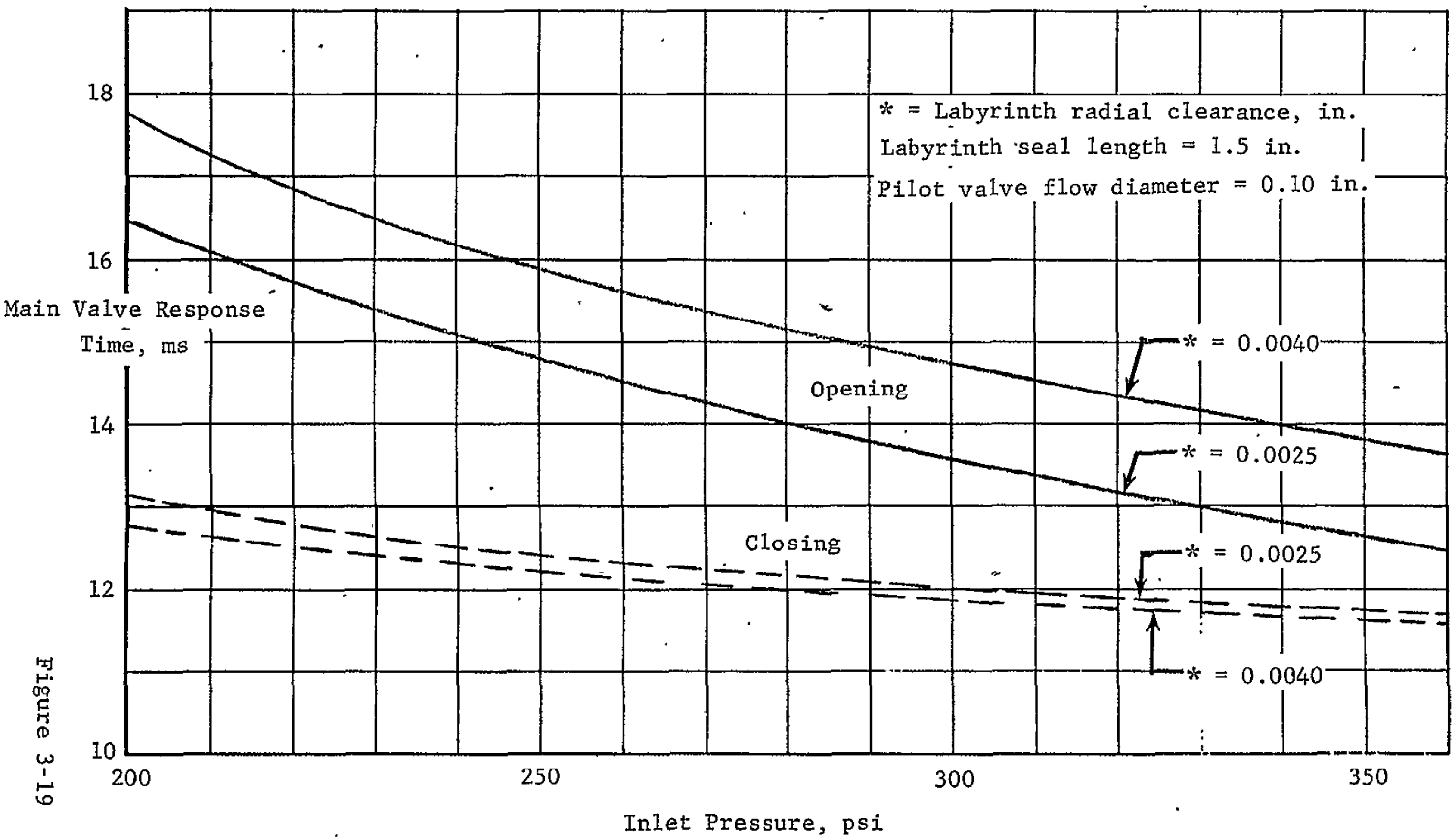

Figure 3-19

EFFECT OF INLET PRESSURE DIFFERENTIAL
ON PAIRED VALVE OPENING RESPONSE

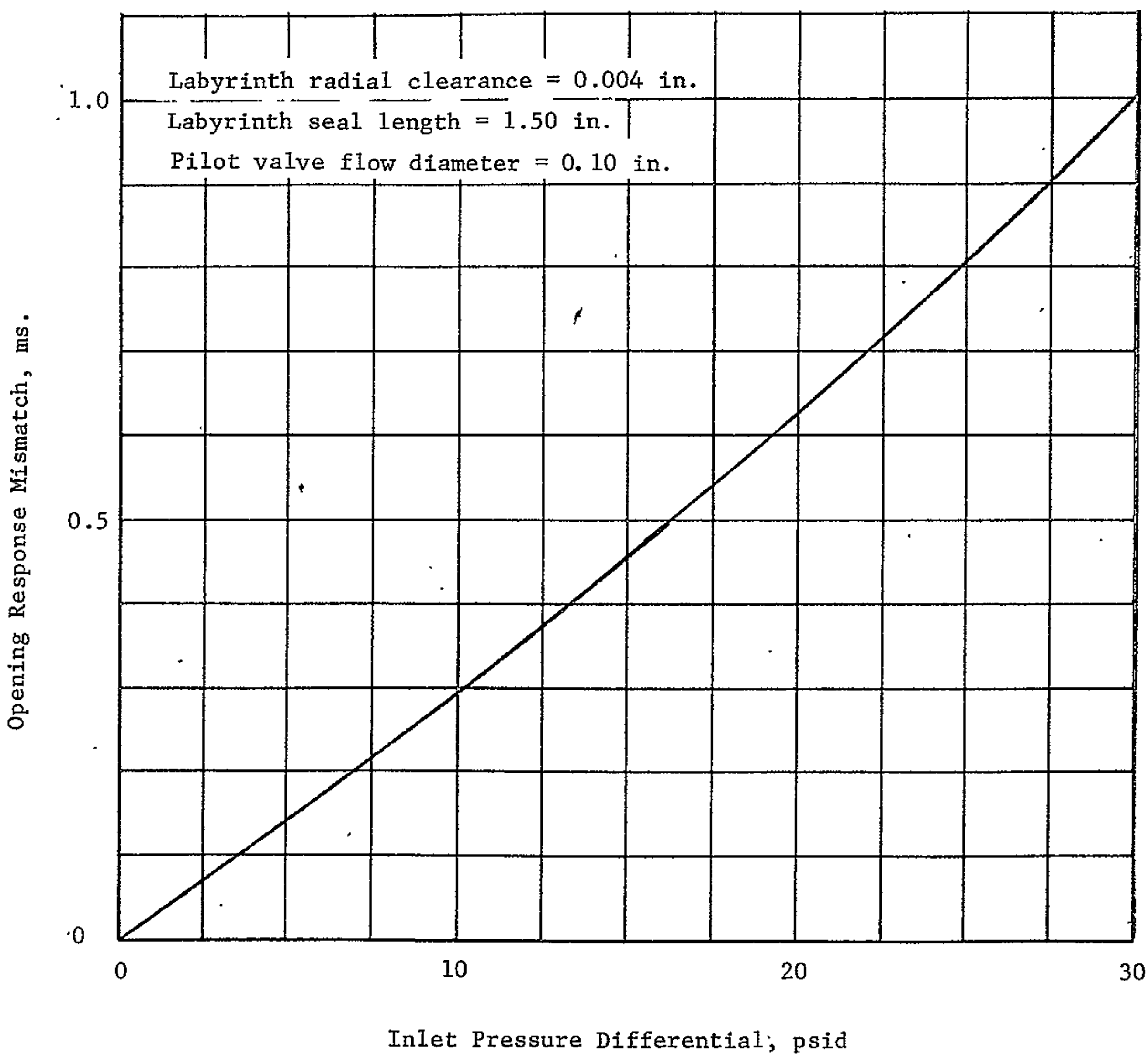

Figure 3-20

ANALOG MODEL OUTPUT TRACE

- NOMINAL DESIGN
- NOMINAL CONDITIONS WITH ± 50 PSI 60 Hz SINUSOIDAL INLET PRESSURE OSCILLATIONS
- RUN NUMBER 38

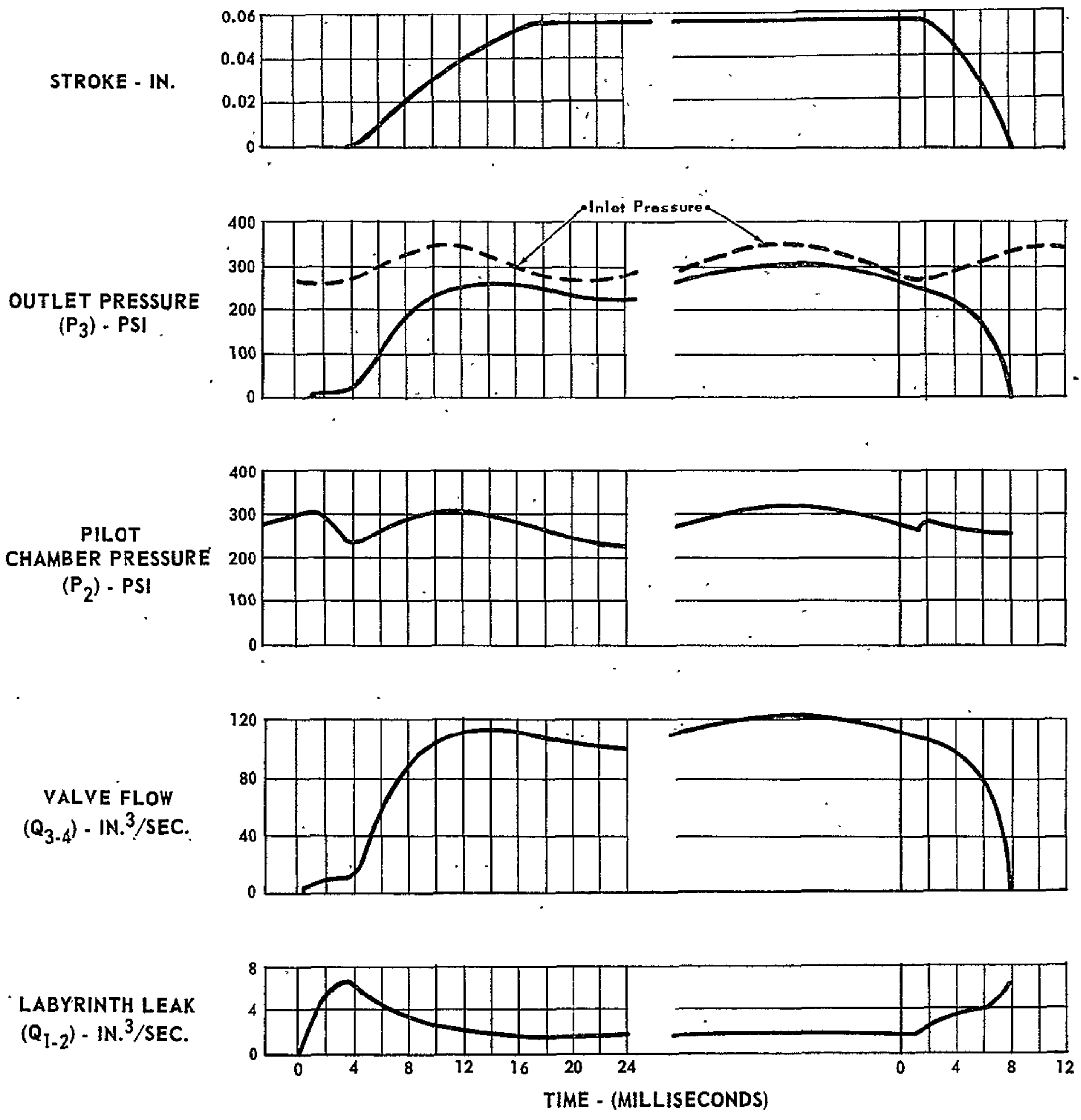

Figure 3-21

evident from the poppet stroke trace (upper trace) that stable valve operation occurs although the stroke time is prolonged primarily due to the selected phasing, which resulted in the inlet pressure decreasing, or being at a value less than nominal inlet pressure during valve opening and closing transients.

Confirmation of stable valve performance under the most adverse inlet pressure conditions was achieved by iterating the analog model with a square wave $\pm$ 200 psi inlet pressure perturbation superimposed on the nominal inlet pressure. Phasing and frequency of the pressure perturbations was iterated for maximum impact on valve performance. This impact is shown in the output traces of Figure 3-22. Despite the severity of the operating conditions, stable and continuous stroking of the valve resulted in both the opening and closing mode. Transmission of the pressure perturbations throughout the valve is apparent from the analog traces, yet valve operation remained stable during transients and in static conditions.

From the analog output traces of poppet stroke during closing, wide variations in poppet terminal velocity occur, dependent upon damping orifice size. Investigations into terminal velocity magnitude and the subsequent impact loads and stresses on the seat were performed to assure proper damping that would maximize seat cycle life. Figure 3-23 presents poppet velocity traces for the two extremes of damping orifice diameter. Figure 3-24 presents the relationship between poppet terminal velocity and seat impact load and stress.

To maximize seat life, damping to limit terminal velocity to 15 inch/seconds was selected. A single damping orifice of 0.060 inch diameter will limit nominal terminal velocity to 10 inch/seconds, which will ensure a relatively soft closure of the poppet onto the main seat.

3.3.4 Valve Sensitivity to Design and Fabrication Variables

The cumulative effect of all design and fabrication variables can be expressed as a function of labyrinth radial clearance. The impact on performance can then be readily assessed by reference to Figure 3-18. Using the leakage model, and simplifying, the expression for radial clearance becomes:

ANALOG MODEL OUTPUT TRACE

- NOMINAL DESIGN
- NOMINAL CONDITIONS WITH ± 200 PSI SQUARE WAVE OSCILLATION OF INLET PRESSURE
- RUN NUMBER 40

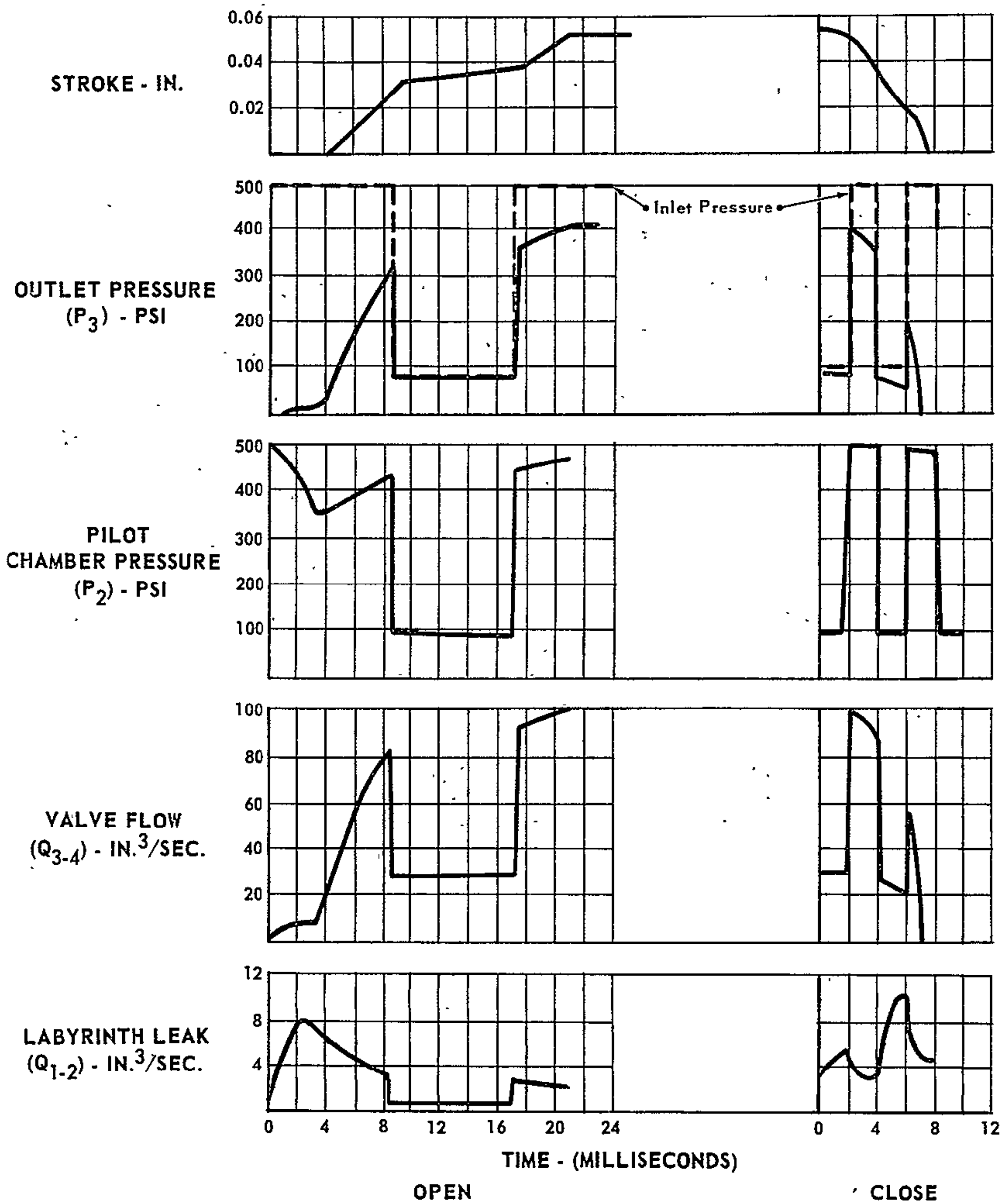

Figure 3-22

ANALOG MODEL TRACE - MAIN POPPET VELOCITY

- NOMINAL DESIGN - RUN NUMBER 43
- WITH REDUCED DAMPING - RUN NUMBER 39

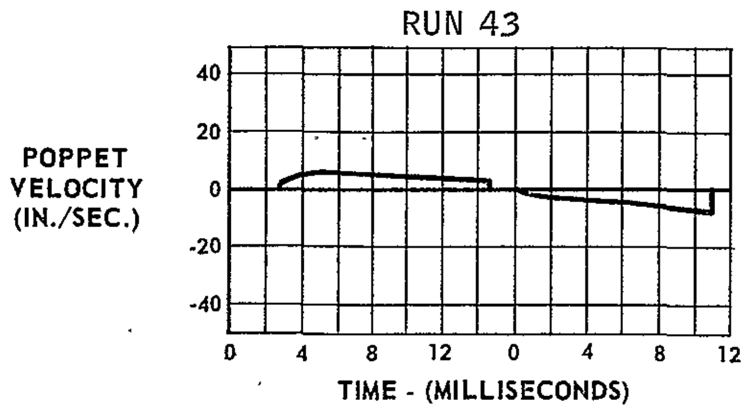

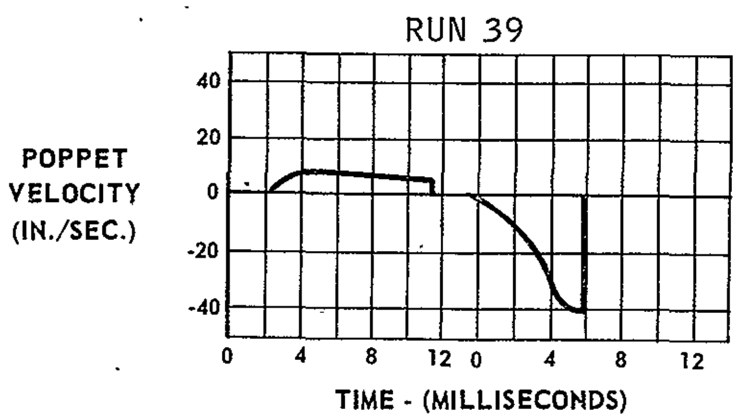

Figure 3-23

VALVE CLOSING TERMINAL VELOCITY VS.
SEAT IMPACT LOAD AND STRESS

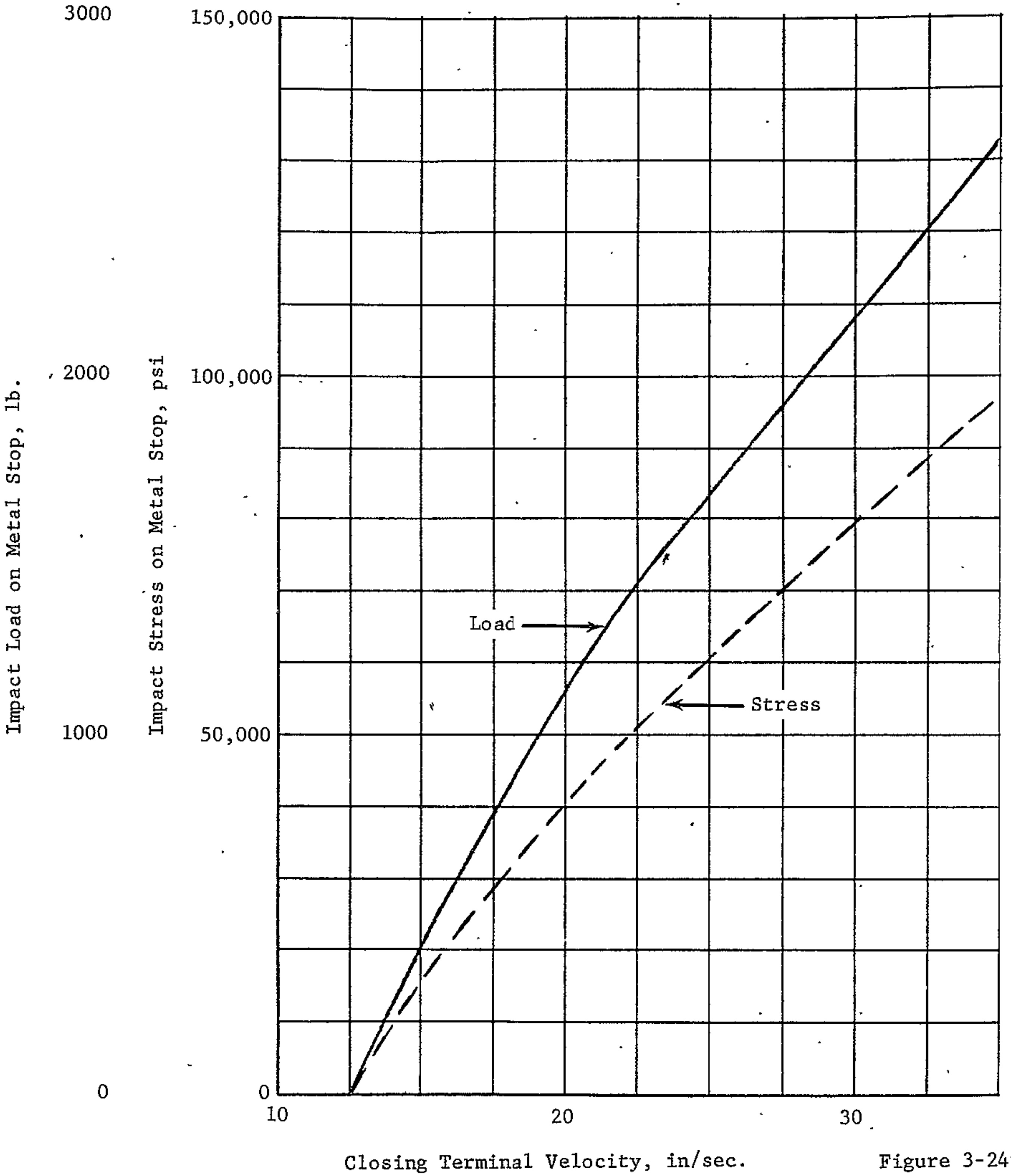

Figure 3-24

$$b = \frac{S_p D_p C_{D\,2-3}}{D_m \sqrt{F_o}} \sqrt{\cfrac{1 - \cfrac{\cfrac{F_o + \frac{\pi}{4} D_s}{P_1 - P_3}}{\pi/4\, D_m}}{\cfrac{\cfrac{F_o}{P_1 - P_3} + \frac{\pi}{4} D_s}{\frac{\pi}{4} D_m}}}$$

Where subscript p refers to the pilot section and m refers to the main piston, F relates to the labyrinth geometry form factor. Differentiating each variable with respect to itself, the sensitivity relationship takes the form:

$$\frac{db}{b} = \frac{dS_p}{S_p} + \frac{dD_p}{D_p} + \frac{dD_m}{D_m} + \frac{dC_{D\,2-3}}{C_D} - \frac{1}{\alpha}\frac{dF}{F}$$

Dimensional variables S_p, D_p and D_m will be obtained from detail drawings and sensitivity estimated from the root sum-square of the total, yielding:

$$\frac{db}{b} \text{ Dimensional} = \pm\ 2.5\%$$

Systematic variable impact was estimated on the basis of test data for similar type flow paths such that:

$$\frac{db}{b} \text{ Systematic} = \pm\ 22.6\%$$

Net sensitivity, expressed as labyrinth radial clearance thus becomes:

$$db = b\left[(\pm\ 0.025) + (\pm\ 0.226)\right] = \pm\ 0.001 \text{ inch}$$

With reference to Figure 3-18, this represents minor variations in valve response, the primary performance characteristic influenced by these variables.

3.3.5 Pilot Valve Design Analysis

Analog analyses resulted in the selection of a pilot stage flow area of 0.00595 in^2. On the basis of the seat diameter vs. net seat load of Figure 3-25, a nominal seat diameter of 0.10 inch was selected. A parametric analysis of the electromagnetic actuator for the pilot stage was performed using a TMC-developed APL computer program. The resultant data are plotted in Figure 3-26, wherein electrical power and weight are traded off against seat diameter and operating flux density of the actuator ferromagnetic material. On the basis of this analysis, a prudent selection, providing margin and growth potential, an 8 kilogauss operating flux density was made. This yields an electrical power requirement of 25 watts at 30 vdc and 70°F. The analysis program provides for a pull-in voltage of no more than 15 vdc at 250°F under worst case pressure conditions. Provisions were made for the additional parasitic gap resulting from the coaxial packaging concept.

3.3.6 Main Seat Design

Sealing of the main poppet, with the valve de-energized, is achieved by a captive TFE seal ring, positively retained in the seat assembly and integral with the valve outlet. A machined annular ring of Marquardt-molded virgin TFE is installed into the seat. A retainer ring of Inconel 718 is then pressed into the seat to retain the TFE by controlled radial and axial compression. The retainer ring is EB welded to the seat to form a single structural element. The TFE seal form and dimensions are selected on the basis of the required sealing diameter, extremes of thermal and pressure environment, and to assure a long-life resilient seal at the interface with the poppet. A final machine cut of the TFE seal is made after assembly into the seat to establish the protrusion of the TFE above the metal plane which will positively limit poppet motion. This protrusion or "proud," together with the selected TFE form dimensions and installation compressions, assures elastic deformation throughout its life.

A summary of the seal dimensions, installation strains at various temperatures and operational stress levels is presented in Figure 3-27. The design approach employs the technology utilized in the Marquardt R4D propellant valves. Flexure guidance of the piston assures the absence of life compromising scrubbing during mating and demating of the sealing interfaces. The differential angle between the seal and the mating poppet surface (6°) gives rise to a pressure energizing effect on the TFE, forcing the teflon toward the zero clearance interface at the downstream metal-to-metal stop interface.

PILOT VALVE SEAT DIAMETER VS. FORCE AND
STROKE FOR 0.00595 IN^2 FLOW AREA

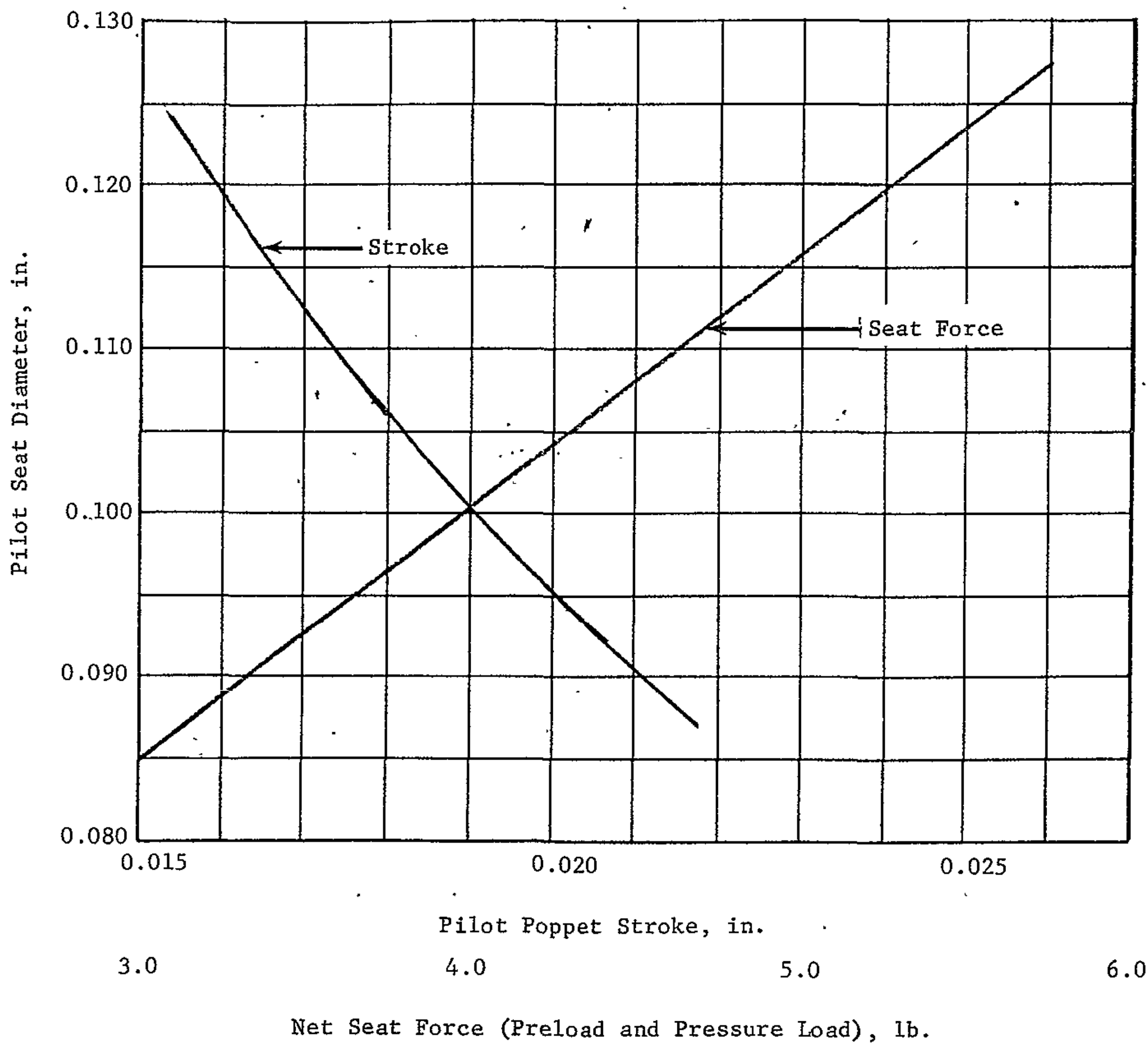

Figure 3-25

PILOT VALVE ACTUATOR WEIGHT VS. POWER

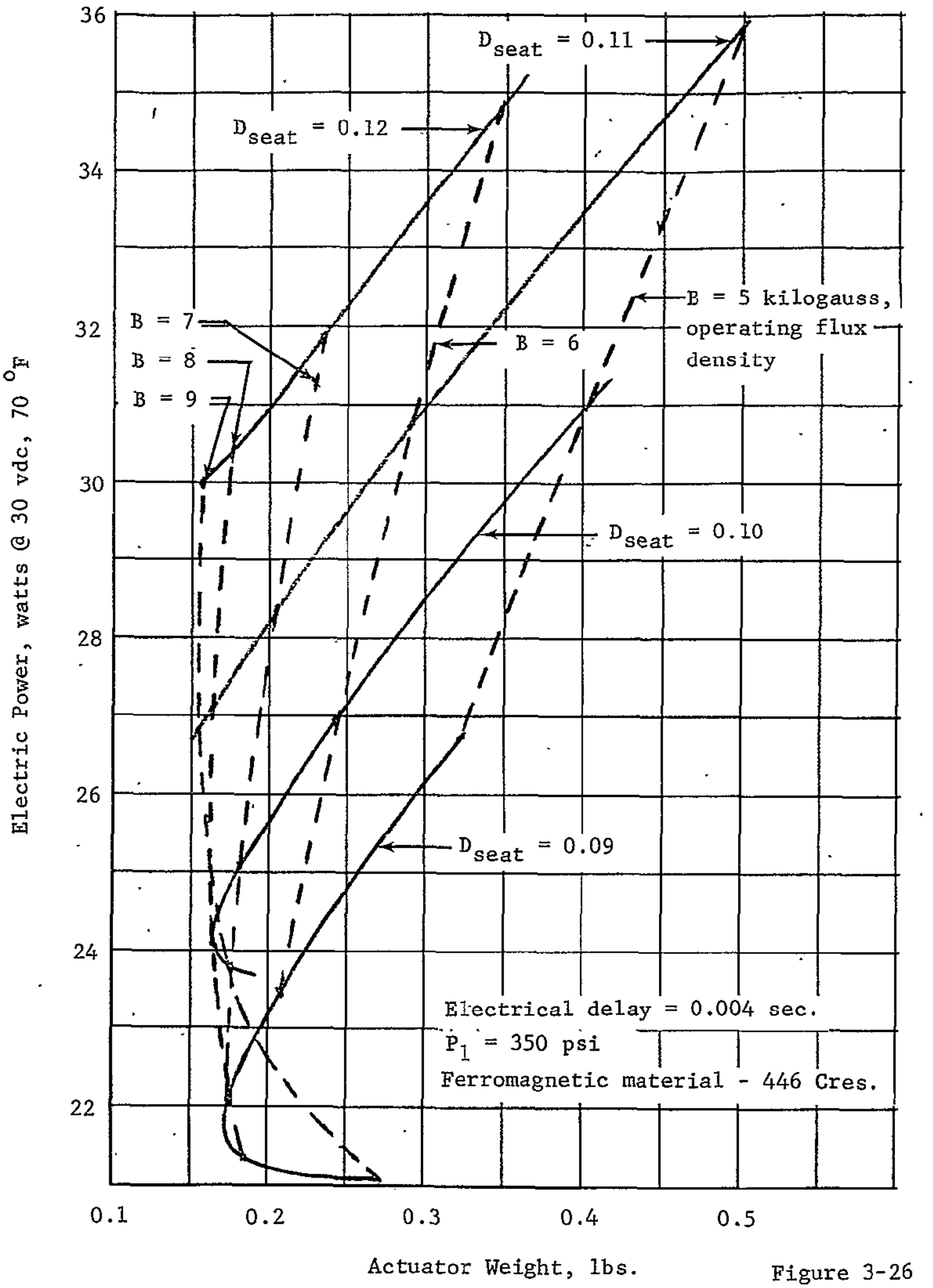

Figure 3-26

MAIN SEAT DESIGN

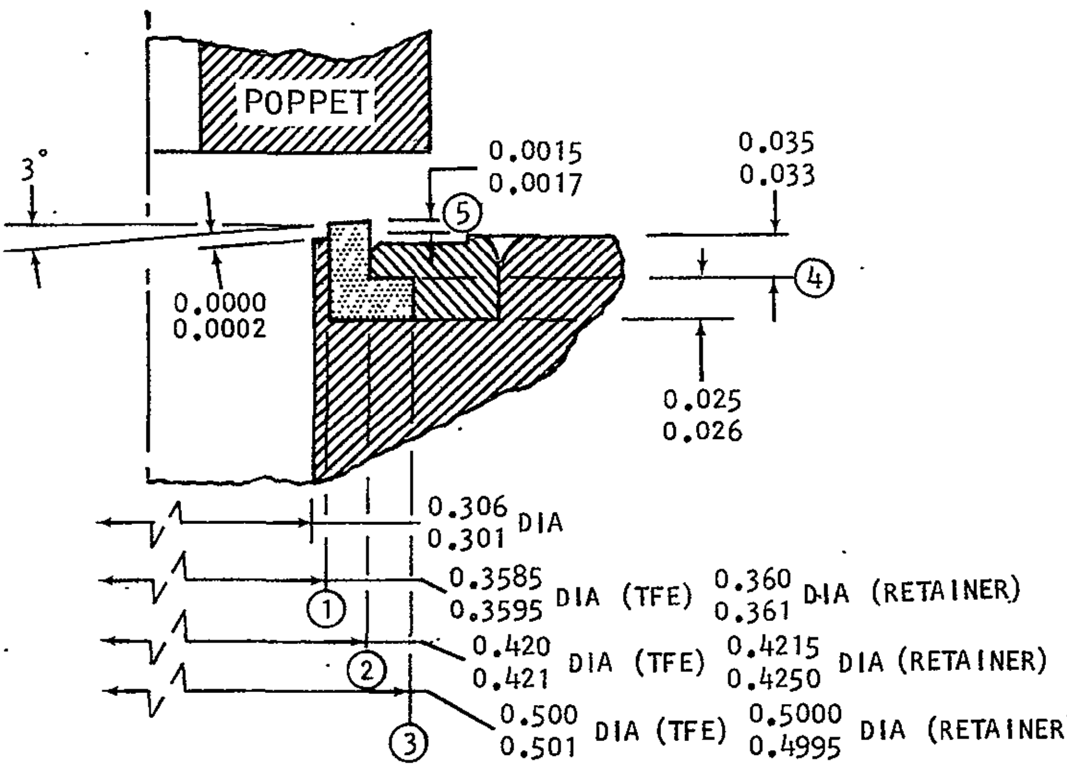

LOCATION	+CLEARANCE -SQUEEZE 70°F	VOLUMETRIC COMPRESSION	VOLUMETRIC EXPANSION @ 250°F	VOLUMETRIC CONTRACTION @ -40°F
1	- 0.0005 0.0025 DIA.	1.2 to 5.5 %	4.05 to 4.15 %	2.38 to 2.50 %
2	+ 0.0005 0.0025 DIA.			
3	- 0.0000 0.0015 DIA.			
4	- 0.0010 0.0025			
	MEAN VALVE CLOSED SQUEEZE - 70°F	250°F	-40°F	COMPRESSIVE STRESS FOR FULL SQUEEZE
5	0.00075 0.00085	0.00084 0.00094	0.00070 0.00079	850 to 1080 PSI

Figure 3-27

The seat design offers a high tolerance for particulate contamination by virtue of the primary TFE seal which has capability to ingest particulates, trapped during closure, without jeopardizing sealing capability. A low probability of particulate encounter at the downstream metal-to-metal secondary seat exists, since the land width is minimized and the poppet closure action creates a seal at the TFE interface before metal-to-metal contact is achieved, acting to filter the flow media as the poppet closes.

3.3.7 Pilot Valve Seat Design

The relatively small size of the pilot flow diameter (0.100 inch) allows the use of a simple and proven floating seal design Marquardt has employed on similar size valves. The sealing element of TFE is carried in the poppet and is spring loaded to limit stresses, isolate impact loads, and compensate for minute out of parallelism at mating. The teflon seal interfaces with an annular land machined into the integral outlet seat. Land dimensions and seal retention are such that a controlled compression of the TFE occurs on mating. The seal preload spring assures adequate interface stresses to attain a seal, and pressure unbalance forces give added sealing stress margins. The seal preload spring isolates the seal from the balance of the poppet mass, thereby eliminating impact problems. Thermal excursions do not have any effect on the sealing plane as the seal material is allowed to grow and retract relative to this plane.

Marquardt has employed this seat/poppet seal design in several small propellant valves which have demonstrated cycle life in excess of 10^6 cycles over temperature ranges of -150 to +400°F, with gaseous leakages of less than one SCCH.

A section view and key dimensional summary of the selected design is shown in Figure 3-28.

The large volume of TFE, relative to the sealing contact area, enhances the particulate injestion capacity of the seal design. The narrow sealing land of the seat minimizes the probability of encounter with particulates upon closure, thus rendering this closure insensitive to contamination.

3.3.8 Materials Selection

A simple materials system, commensurate with the required functions, was selected for the prototype design. As shown in Figure 3-29, the basic structural material is Inconel 718. Ferromagnetic sections required to complete the appropriate magnetic circuit are of Type 446 corrosion; resistant steel.

PILOT VALVE SEAT DESIGN

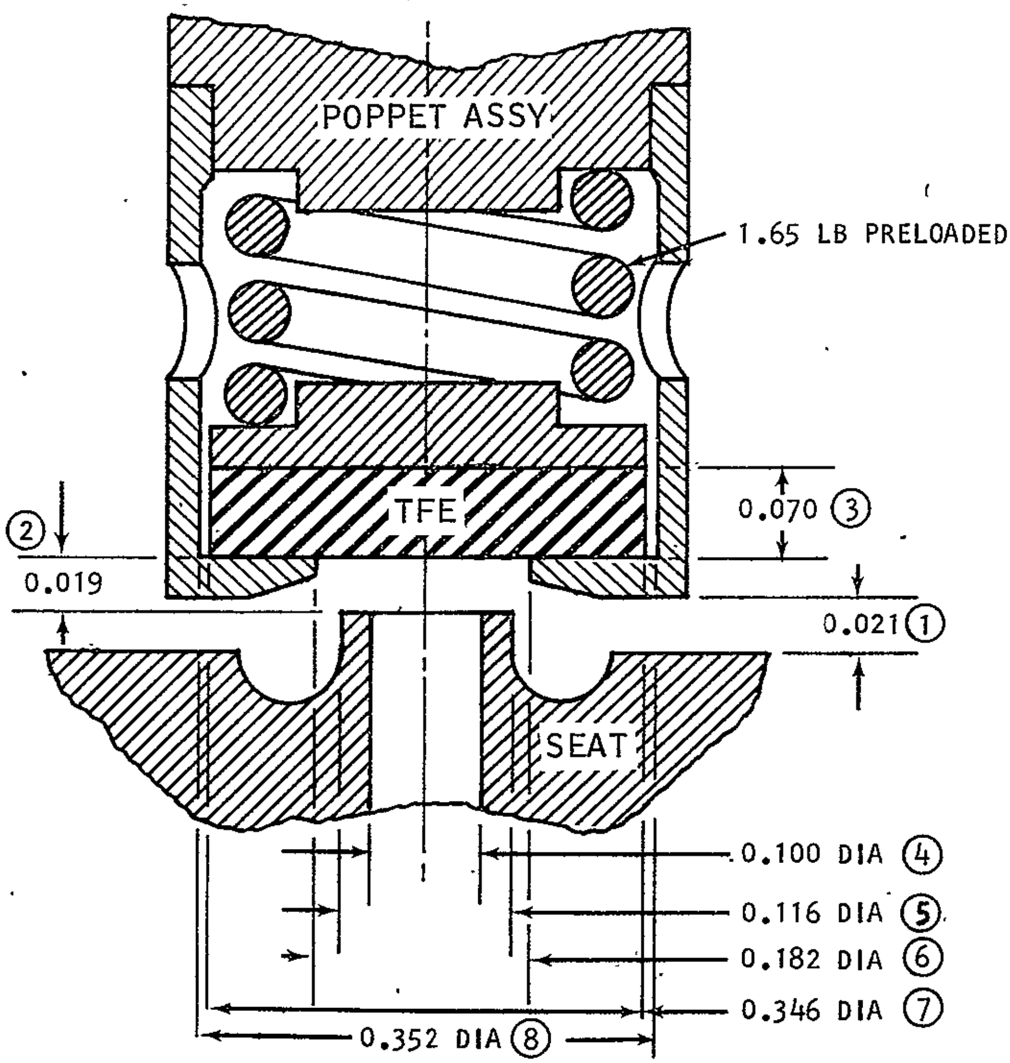

DIMENSION NOS.	@ +250° F	@-65° F	@70° F
① - ②	0.0015 0.0025	0.0015 0.0025	0.0015 0.0025
⑧ - ⑦	0.0054 0.0027	0.0055 0.0135	0.0020 0.0100
③	0.0669 0.0750	0.0653 0.0733	0.0660 0.0740

Figure 3-28

LINE FLUID ACTUATED VALVE MATERIALS SELECTION

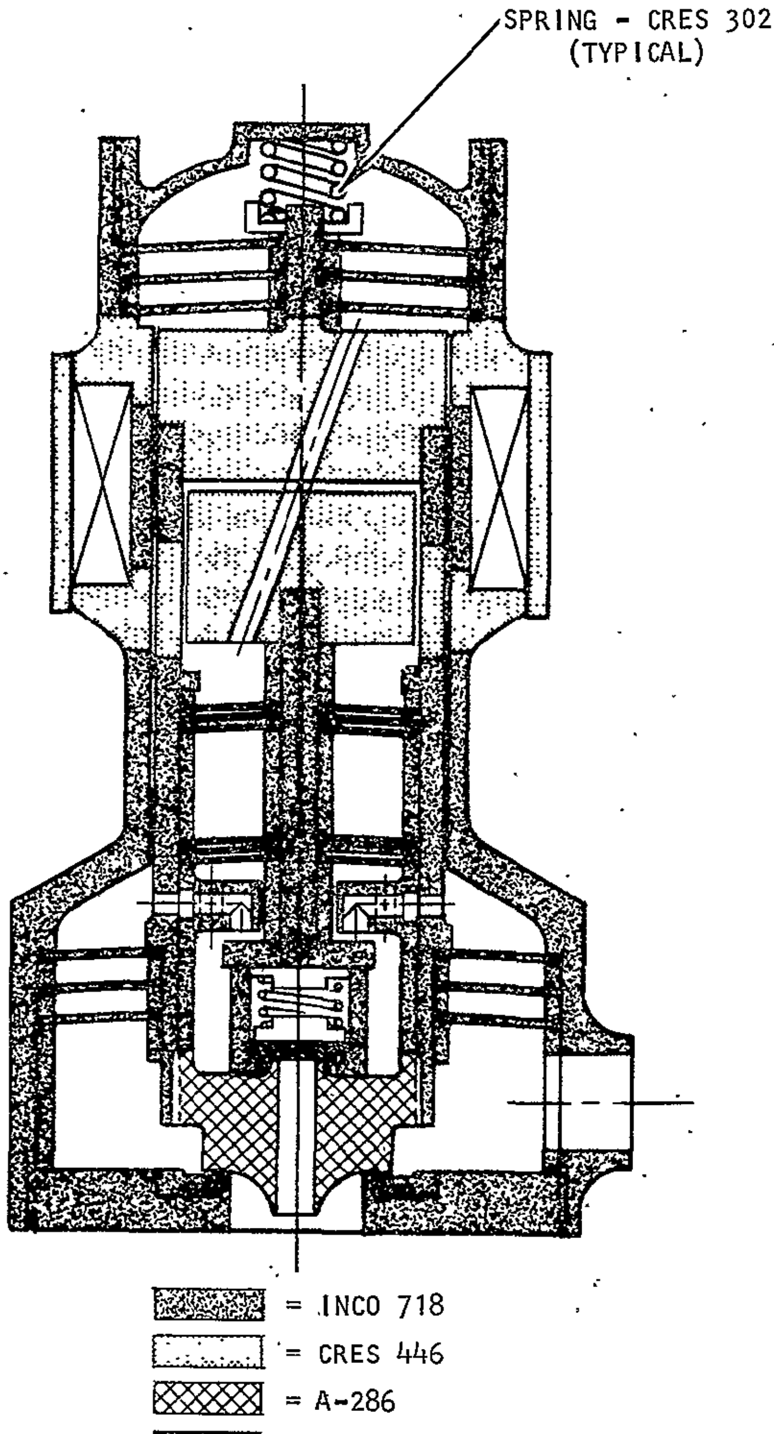

Figure 3-29

All structural welding is accomplished by the electron beam process, with post-weld heat treating to normalize the weld joint and achieve maximum toughness of the Inconel 718. All internal details are of Inconel 718, with the exception of the A286 main poppet, which was selected for its hardness, the TFE seals, and the Type 302 Cres coil springs which can ultimately be fabricated of Inconel 718. All materials have documented long-term compatibility with all usage fluids.

The structural capability of the pressure vessel is 10,000 psi, selected to assure integrity in the event of any unforeseeable rocket engine explosion. This structural capability is achieved at negligible weight penalty.

3.3.9 Valve Checkout

The normal usage fluids of the valve are earth storable propellants. However, it is anticipated that checkout of the valve would be desirable using referee fluids or even gaseous media. Since the design is sensitive to fluid properties, operational capabilities were evaluated for several usage fluids. A summary of performance parameters that can be verified while using several candidate fluids is presented in Figure 3-30. Complete verification of the valve, including response of both pilot and main stages, can be accomplished using either gaseous or liquid test media.

3.3.10 System Priming

Since the design utilizes fluid flow and the resultant pressure drops to create valve operating forces, rather than relying solely on an external power source, an inadvertent operation of the valve during the priming of a system in which the valve is located, is of concern. A comprehensive analysis to determine the magnitude was considered impractical since testing of the prototype would resolve any concern. However, on a worst case basis, wherein respective volumes of the valve, separated by orifices, are assumed to fill and rise to the supply pressure sequentially, such that the full supply pressure exists across the orifices during filling, does indicate that inadvertent operation of the main poppet will result if the differential pressure across the labyrinth seal and upper pilot orifices exceed 6 psi and fluid is flowing through these passages. Based on the volume to be filled, at a pressure differential of 300 psi, the main poppet would cycle from closed to open to closed during the 8 millisecond period it would take to fill the volume within the main piston and damping chamber.

Figure 3-31 summarizes several potential system priming procedures and possible effects on the valve. During prototype testing, a comprehensive evaluation of priming phenomenon will be conducted.

VALVE CHECKOUT

Test Fluid	Test Condition	Performance Parameter
Liquid - Water Alcohol Propellant	50 - 400 psi 2.0 pps N_2O_4 equiv.	Main seat liquid leakage Pilot seat liquid leakage Opening response Closing response Operating current Pressure drop
Gas - GN_2 He Air	0 - 525 psi	Main seat leakage Pilot seat leakage Operating current
	0 - 50 psi	Main poppet function
	0 - 100 psi step input to valve inlet with solenoid coil energized	Main poppet function
Gas - GN_2	125 - 350 psi flowing	Valve function Leakage Operating current Response (by correlation)

Figure 3-30

SYSTEM PRIMING

I. GROUND PROPELLANT PRIMING

1. Evacuate system.
2. Fill under 6 psid maximum propellant pressure.
3. Raise to pad pressure.
4. Raise to operational pressure.

II. IN FLIGHT PRIMING

A. Isolation valve to thruster valve dry and at launch ambient pressure.

1. Open isolation valves at full system operational pressure.
2. Fire clearing burst of thruster to exhaust gas bubble.

B. Isolation valve to thruster valve dry and at launch ambient pressure.

1. Open thruster valve to evacuate lines.
2. Close thruster valve.
3. Open oxidizer isolation valve.
4. After 5 seconds, open fuel isolation valve.
5. After 5 seconds, system is operational.

C. (Same as B above, except open isolation valves simultaneously - thruster(s) may "burp").

D. (Same as C above, except propellant supply incorporates flow limiter to limit pressure ramp during filling of valve - no thruster burp.)

Figure 3-31

3.3.11 Valve Purging

Capability to render the valve safe for any servicing or maintenance operations in its immediate vicinity requires that the valve be purgeable such that, as a maximum, only trace quantities of propellants remain in the valve. This can be accomplished by either displacing the propellant with a pressurized inert gas, or vacuum removal of the liquid by opening the valve to a space environment, or applying a vacuum at some convenient location on the system.

The random orientation of the valve or exposure to a zero g environment, generally makes positive pressure inert gas displacement purging unreliable. Therefore, emphasis was placed on evaluating vacuum purging capability.

For simulation purposes, a Marquardt R4D valve was filled with liquid MMH, pressurized to 250 psig, and held for 24 hours. A vacuum was then applied to the valve inlet while monitoring pressure. Figure 3-32 presents the time-pressure history of this test. Valve weight was measured and compared with dry valve weight, measured before introducing the MMH. Valve disassembly and examination also confirmed no visible residue of liquid propellant.

The results of this demonstration test are applicable to the line fluid actuated valve, since the test unit, though not of the same configuration, possesses clearances and potential propellant traps similar to that of the proposed valve.

3.4 HARDWARE FABRICATION (TASK II)

Fabrication of the prototype valves and associated tooling and fixturing were accomplished using the Marquardt model shop and selected outside machine shops. No unique or persistent machining problems were encountered other than the anticipated difficulties of machining Inconel 718. All welded joint EB weld schedules were developed on sample pieces prior to performing the weld operations on the prototype unit details.

Some difficulties were encountered in brazing the flexure elements into the cartridge configuration. Subsequent to brazing, the cartridges are machined to final overall dimensions for proper fit and assembly stack-up. During this machining, several poor quality braze joints were disclosed. Though sufficient numbers of each flexure cartridge were obtained to meet the prototype valve requirements, a manufacturing study was initiated to eliminate this type of

FUEL PURGE TESTS

R-4D Valve, P/N T12384, S/N 008

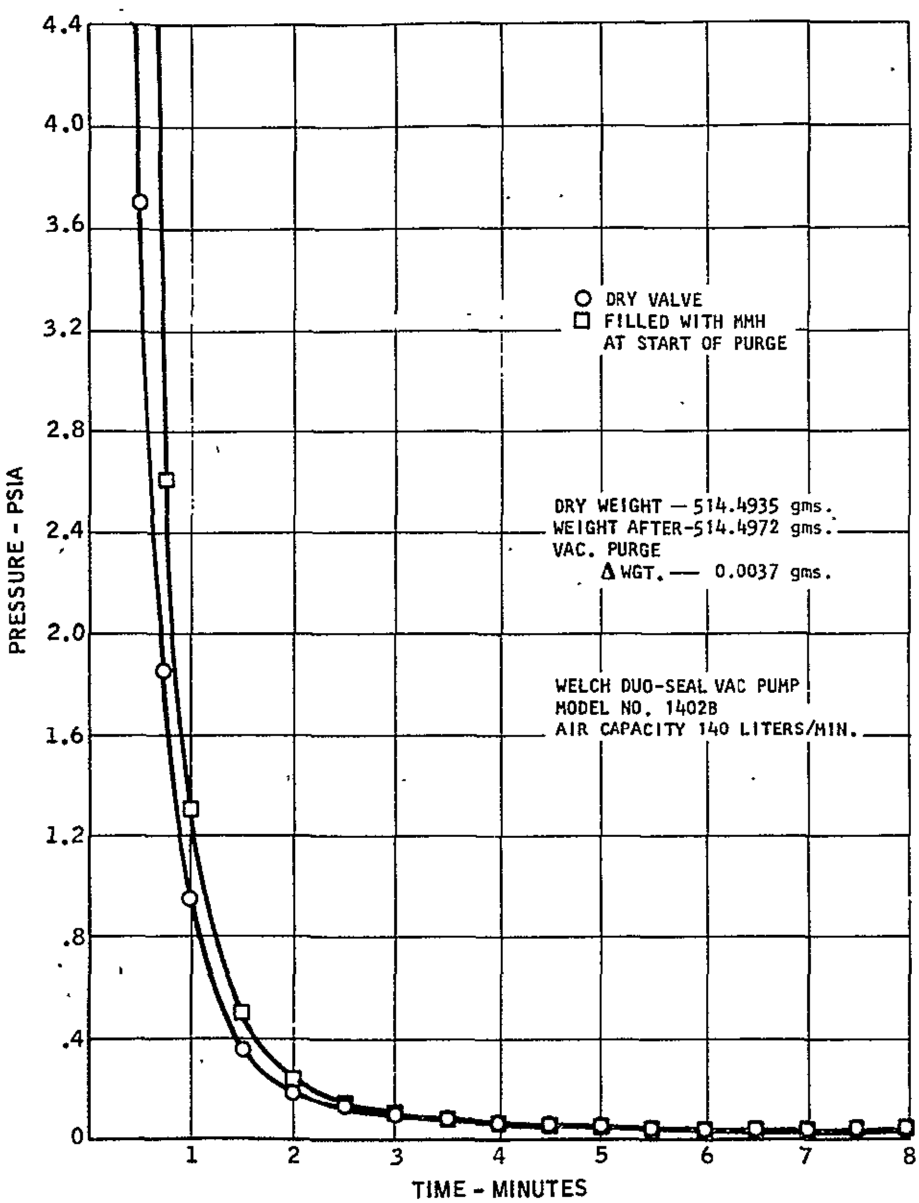

Figure 3-32

problem. As well as investigating the braze joint design, this study encompassed joint preparation and detail parts cleaning, braze furnace quality, braze cycle, braze alloy composition and form, and raw material composition and quality studies. Several joint design configurations were evaluated, along with improvements in other facets of the procedure and as of this writing, nearly 100% yield of brazed flexure cartridges can be confidently projected with the processes and controls currently being used.

As detail parts and subelements were completed and inspected, solvent and ultrasonic cleaning were employed to remove foreign contaminants and manufacturing residues. Build-up of subassemblies and the final assembly was performed in a controlled area to maintain assembly cleanliness. When removal from the controlled area was required for a specific operation such as EB welding, ultrasonic detergent cleaning and rinsing were performed immediately upon the item(s) as they were returned to the controlled area.

Figure 3-33 presents a flow diagram for the fabrication and build-up of the prototype valve. No unusual problems were encountered during the fabrication process, except as noted above.

3.5 VALVE TESTING (TASK III)

The following paragraphs present, in chronological order, the results of the testing performed on two prototype P/N X29550 line fluid actuated valves. In parallel with this testing, the Marquardt Company was conducting thruster testing on a bipropellant rocket engine intended for the SSRCT, which incorporated two valves of the same configuration. The results of the thruster testing are not delineated herein but are significant in that exposure to usage propellants and operational environments were demonstrated.

The test units described herein are identified as S/N 002 and S/N 004 of P/N X29550 and were identical in configuration, except for specific assembly clearances as noted herein.

For purposes of standardizing nomenclature relative to valve design details and features, refer to Figure 3-4.

3.5.1 Initial Valve Assembly and Checkout

After cleaning detail parts, build-up of the two prototype valves was accomplished in the Controlled Area of Bldg. 32. Various preloads, spring rates and key functional dimensions were measured at this time and are documented in Table 3-III, along with the electrical characteristics of the valve coils.

VALVE FABRICATION FLOW DIAGRAM

X29550 VALVE BUILD-UP

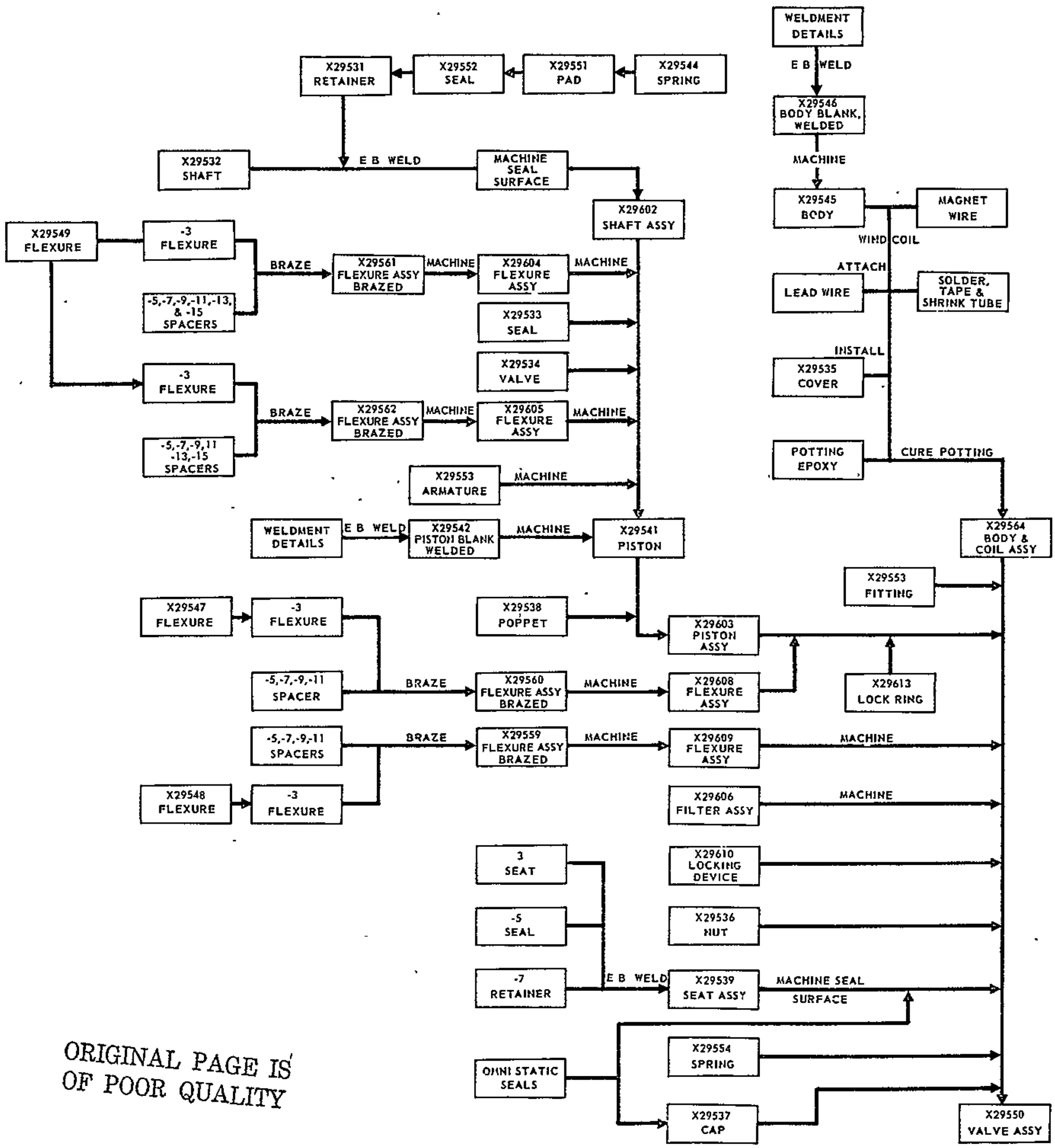

ORIGINAL PAGE IS OF POOR QUALITY

Figure 3-33

TABLE 3-III

VALVE ASSEMBLY CHARACTERISTICS SUMMARY

	COIL RESISTANCE AT 68°F	INSULATION RESISTANCE AT 500 VDC	DIELECTRIC STRENGTH	MAIN POPPET PRELOAD	MAIN POPPET STROKE	PILOT POPPET PRELOAD	PILOT POPPET STROKE	PILOT ARMATURE GAP-VALVE OPEN	MAIN POPPET SPRING RATE	PILOT POPPET SPRING RATE
S/N 002	37.14 OHMS	3×10^5 MEG.	0.1 MA AT 450 VAC < 0.5 MA AT > 450 VDC	2.9 LB.	0.068	0.085 LB.	0.019	0.0068	38.2 LB./IN.	144.7 LB./IN.
S/N 004	36.91 OHMS	10^6 MEG.	0.12 MA AT 600 VDC	3.1 LB.	0.061	1.1 LB.	0.021		32.8 LB./IN.	142.8 LB./IN.
DESIGN GOAL	35.4 OHMS		< 0.5 MA AT 600 VDC	3.0 LB.	0.060 0.065	1.6 LB.	0.020 0.025	0.002	30 LB./IN. (EFFECTIVE)	250 LB./IN.

Leakage checks indicated marginal sealing of the main seat due to the accumulation of tolerances of alignment and squareness, and available TFE "proud." Replacement seats were fabricated increasing the slope angle of the TFE, thus doubling the "proud." On reassembly, positive sealing resulted.

Water flow characteristic tests indicated that the main poppet was modulating at low pressures. As was hypothesized during the design effort, flow stagnation was occurring, as a result of the radial flow across the main seat, at the pilot outlet, reducing the apparent pilot stage pressure drop. A plug nozzle "diverter" was installed on the flat poppet face to effect the turning of the radial flow into the outlet passage, and a linear flow characteristic resulted at valve pressure drops of greater than 20 psi. The rounding of sharp corners in the seating area of the main poppet effected reduction in valve pressure drop and subsequently the outlet diameter was increased from 0.301/0.306 in. diameter to 0.326/0.328 in. diameter with a further pressure drop reduction. Flow characteristic evolution is shown in Figure 3-34.

Response tests were commenced with current traces and pressure traces (upstream or downstream) recorded simultaneously. This testing indicated relatively slow main poppet transit times and also left some question as to main poppet position relative to the current trace characteristics, as pressure traces were inconclusive. A special cap and nut were fabricated allowing an LVDT* to be attached to the main poppet, permitting positive indication of position. To improve main poppet travel time, additional bleed holes were drilled to reduce damping and the pilot seat effective diameter was increased 20% to reduce pressure drop at that orifice to effect greater labyrinth seal pressure drop. The addition of one damping hole (two total) resulted in response improvement. Two additional holes were added (four total) and satisfactory transit times resulted. The progression of valve response and number of damping holes is shown in Figure 3-35.

Composite traces of valve current, voltage and LVDT output permitted assessment of poppet position during transit and correlation with valve coil "signatures." Figure 3-36 presents a typical composite and indicates that current and voltage traces provide indicators to assess valve response characteristics. The LVDT output trace confirms the nearly linear, main poppet transit characteristic as projected by the analog computer model. Terminal velocities also appear well within the range of analytical predictions.

Before commencing the formal test program, an informal cycle life test at ambient temperature was performed. Initial tests resulted in premature

* Linear Variable Displacement Transducer

VALVE FLOW CHARACTERISTIC REFINEMENT

S/N 001 Valve

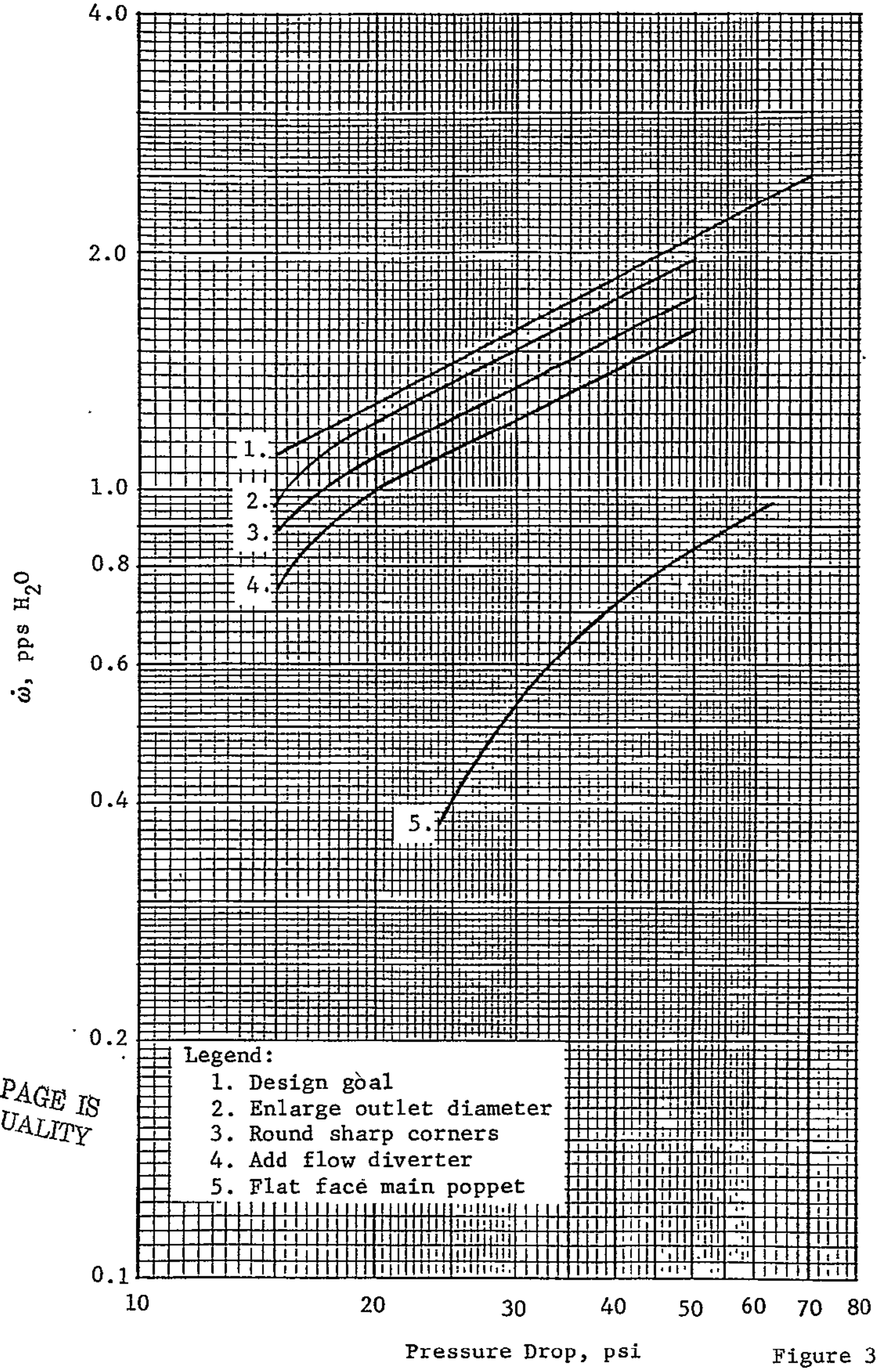

Figure 3-34

VALVE RESPONSE VS. DAMPING

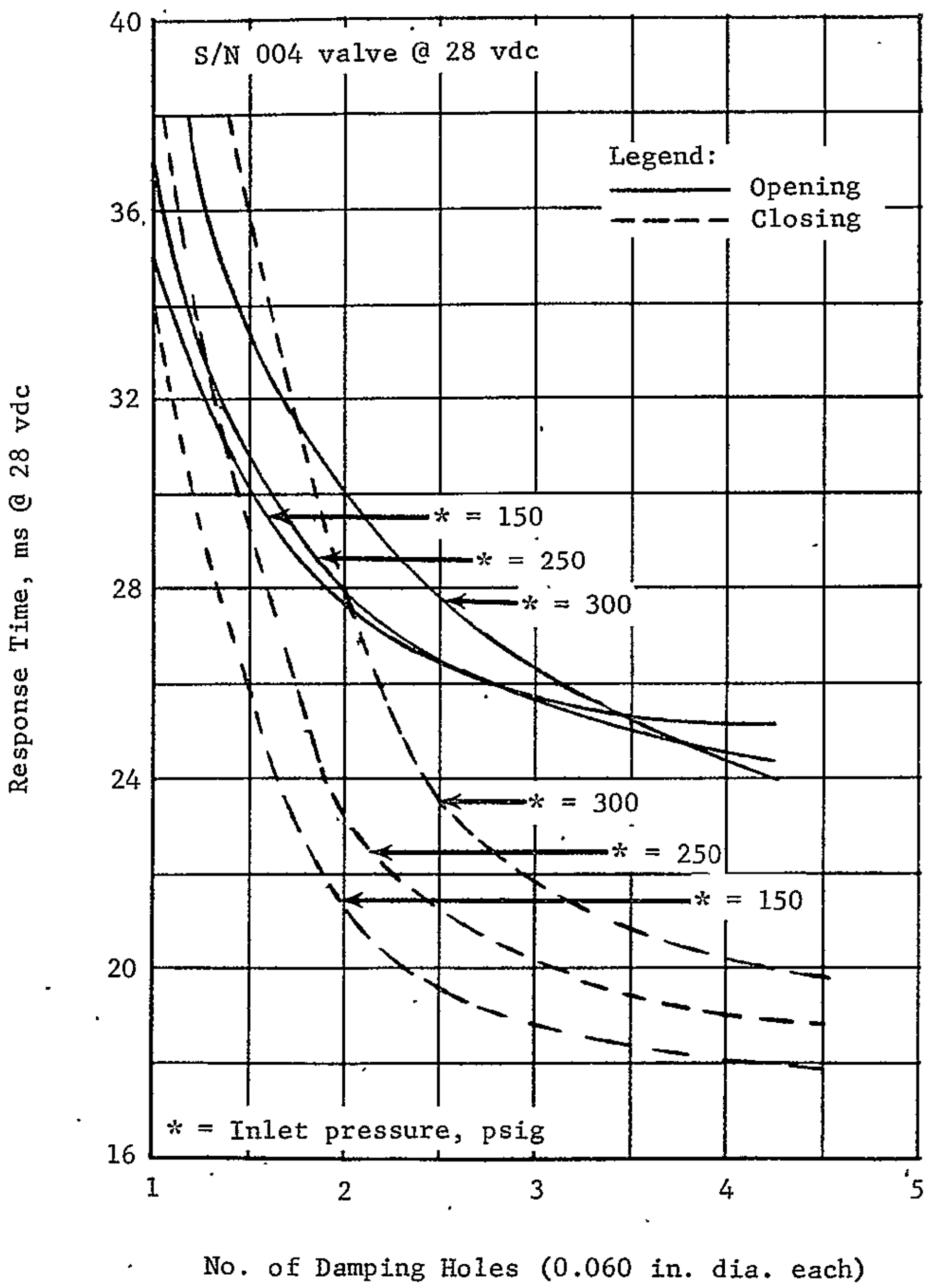

Figure 3-35

COMPOSITE RESPONSE TRACE

S/N 004 Valve @ 28 vdc, 300 psi

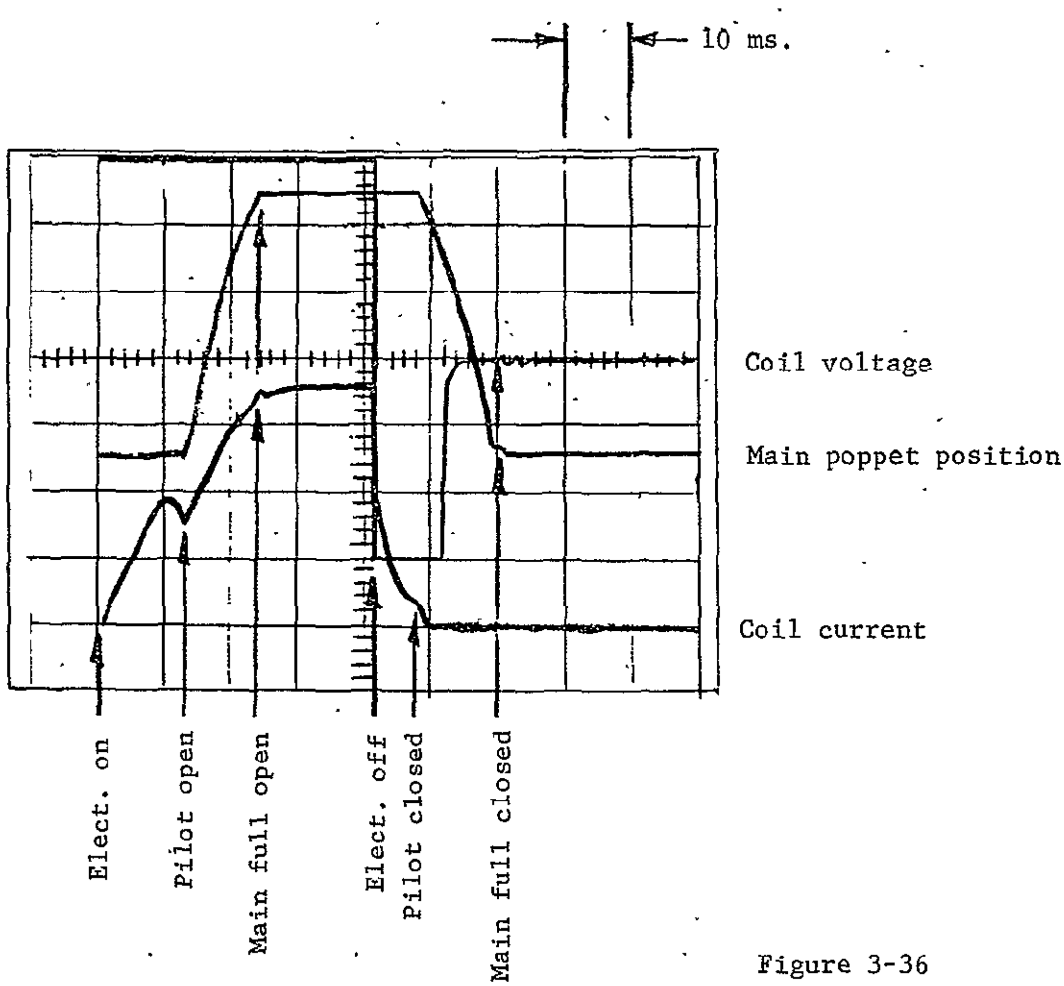

Figure 3-36

failure of the pilot seal after 20,000 and 50,000 cycles for the two test units. The nature of the failure was an errosion of the teflon, downstream of the sealing interface with the seat land, that propagated upstream, undermining the TFE at the sealing interface. A total of six alternate designs of pilot seat were tested over the next few weeks which contributed to an understanding of the phenomenon that caused the initial failures and evolved a design that demonstrated a life of 200,000 cycles. This evolution is summarized in Figure 3-37.

This preliminary test effort resulted in the above-described design refinements and modifications. The resultant valve demonstrated sufficient capability to be confidently committed to the planned test program. Figure 3-38 summarizes the design refinements implemented during this portion of the test program.

3.5.2 Development Testing

The two prototype valves were refurbished to incorporate the design refinements described in Section 3.5.1. Marquardt Test Plan (MTP) No. 0218 had been drafted and approved by NASA-JSC to define the requirements of the testing to be performed on the two valves.

All testing, except vibration, was performed in the Controlled Area of Bldg. 32 of the Marquardt test facility. All performance testing was accomplished at a single test set-up to limit test to test variables. As shown in Table 3-IV, the S/N 002 valve exhibited a longer pilot stage magnetic air gap (pilot poppet stroke + pilot armature air gap), and pilot response time was anticipated to be slightly slower than that of the S/N 004 valve. Also, the longer main poppet stroke of the S/N 002 valve would result in a lower pressure drop characteristic and a slightly longer main poppet transit time. These off-design-goal dimensions were purposely not corrected in order to evaluate their impact on performance and indicate valve manufacturing tolerance sensitivity.

3.5.2.1 Valve Acceptance Test

Each test valve was subjected to a series of tests to establish baseline performance characteristics against which subsequent performance parameters could be measured to assess the impact of the various exposure test conditions, and usage history. This effort also documents the prototype valves characteristics relative to the design goals and analytical predictions. The results of this testing are summarized in Table 3-IV and Figure 3-39.

PILOT SEAT DESIGN AND VERIFICATION SUMMARY

CONFIG.	SECTION VIEW	TEST	RESULTS	REMARKS
I	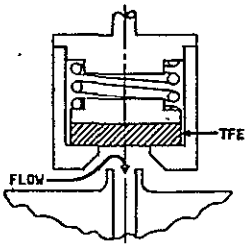	CYCLE AT; 250 PSI INLET PRESSURE ~30 PSID 70°F, 28 VDC 40 MS ON, 40 MS OFF	LEAKAGE AFTER 25,000 CYCLES, TFE ERODED AT INTERFACE WITH METAL DEFLECTOR	DISCONTINUITY AT INTERFACE OF DIVERTER TO SEAL INITIATES TURBULENCE
II	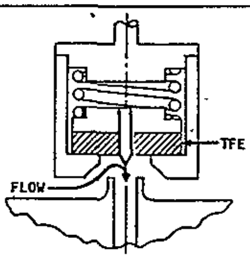	CYCLE AT; 250 PSI INLET PRESSURE ~30 PSID 70°F, 28 VDC 40 MS ON, 40 MS OFF	LEAKAGE AFTER 83,000 CYCLES TFE ERODED AT I.D. OF SEAL LAND	LOWER SEATING BEARING STRESS REDUCES DEFORMATION OF TFE. SMOOTHER FLOW CONTOURS
III	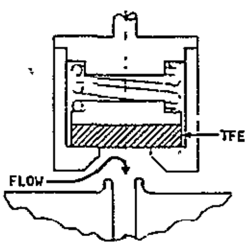	CYCLE AT; 250 PSI INLET PRESSURE ~30 PSID 70°F, 28 VDC 40MS ON, 40MS OFF	LEAKAGE AFTER 20,000 TO 50,000 CYCLES. TFE ERODED ALONG PERIMETER OF INTERFACE WITH SEAL LAND, INITIATING AT I.D.	ANNULUS AT I.D. OF SEAT LAND IS METERING AREA
IV	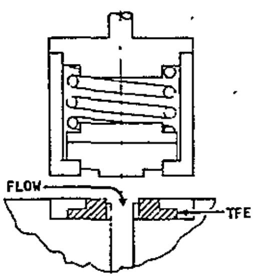	CYCLE AT, 250 PSI INLET PRESSURE ~30 PSID 70°F, 28 VDC 40MS ON, 40MS OFF	LEAKAGE AFTER 115,000 CYCLES. EROSION OF TFE INITIATING AT I.D. OF SEAL	METERING DIAMETER IS 0.005 INCH DOWNSTREAM OF I.D. OF TFE SEAL
V	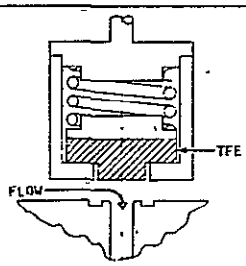	CYCLE AT; 250 PSI INLET PRESSURE ~30 PSID 70°F, 28 VDC 40MS ON, 40 MS OFF	LEAKAGE AFTER 100,000 TO 200,000 CYCLES. SOME TFE EROSION STILL EVIDENT.	WIDENED SEAT LAND AND RADIUSED CORNER AT I.D. METERING MUST BE FARTHER DOWNSTREAM OF SEAL TO ELIMINATE EROSION POTENTIAL
VI	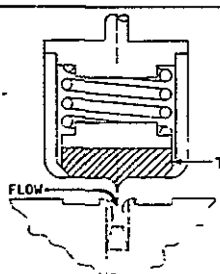	CYCLE AT; 250 PSI INLET PRESSURE ~30 PSID 70°F, 28 VDC 40 MS ON, 40 MS OFF	NO LEAKAGE TO 190,000 CYCLES. SLIGHT LIQUID LEAK AFTER 200,000 + CYCLES. LOCALIZED DAMAGE TO SEAL. NO EVIDENCE OF EROSION OR INCIPIENT EROSION. LOCALIZED DAMAGE CORRESPONDS TO LOCAL DISCONTINUITY AT NOZZLE INSERT INTO SEAT.	SELECTED DESIGN - MACHINE LAND AND NOZZLE INTEGRAL TO PRECLUDE DISCONTINUITIES.

Figure 3-37

VALVE DESIGN CHANGES IMPLEMENTED

ORIGIN OF CHANGE	RATIONALE FOR CHANGE	CHANGE WAS	CHANGE IS	EFFECT OF CHANGE
1. HIGH VALVE ΔP REQUIRED FOR VALVE FULL STROKING	FLOW STAGNATION AT MAIN SEAT CAUSED HIGH PILOT BACK PRESSURE (THIS CHANGE ANTICIPATED DURING VALVE DESIGN)	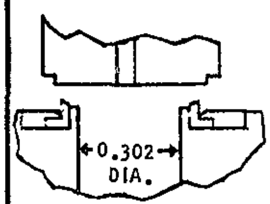	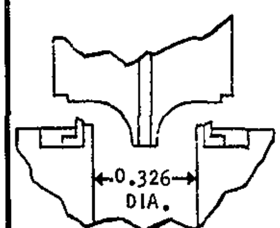	A) STABLE VALVE OPERATION TO <15 PSID B) VALVE FLOW AT 30 PSID INCREASED FROM 0.55 PPS TO 1.42 PPS
2. SLOW OPENING AND CLOSING RESPONSE	EXCESSIVE DAMPING INCREASE NUMBER OF DAMPING HOLES	1 (0.060 DIA.)	4 (0.060 DIA.)	IMPROVED RESPONSE WAS / IS OPEN = 37MS / 24.5MS CLOSE = 39MS / 19 MS
3. PILOT SEAL ERROSION	FLOW COUNTOUR CONDUCIVE TO ERROSION DUE TO STREAM IMPINGMENT; IMPROVE FLOW COEFFICIENT AND SHROUD SEAL TO PRECLUDE DIRECT IMPINGEMENT; WIDEN SEALING LAND TO REDUCE LOCAL BEARING STRESSES	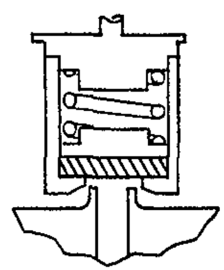	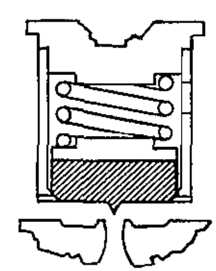	CYCLE LIFE INCREASED FROM 30 TO 50K CYCLES TO >200,000 CYCLES

Figure 3-38

A74-3-587-31A

TABLE 3-IV

ACCEPTANCE TEST SUMMARY
(Ref. MTP 0218, Appendix A)

Test	Test Conditions	Test Valve S/N	Test Results	Remarks
Coil Resistance	Correct Measured R to 68°F	002	37.14 ohms	
		004	36.99 ohms	
Insulation Resistance	Coil to Case @ 500 vdc for 60 Seconds	002	300,000 megohms	
		004	10^6 megohms	
Dielectric Strength	Coil to Case @ 600 vac rms for 60 Seconds	002	.1 ma @ 450 vac	Intermittant leak of >.5 ma above 450 vac.
		004	.12 ma	
Proof Pressure	525 psig He for 5 Minutes	002	No evidence of leakage	Valve immersed in water.
		004	"	
Seat Leakage	Helium @ 20 psig	002	800 scch	
	300 psig		33 scch	
	20 psig	004	0.5 scch	
	300 psig		0.0 scch	
Operating Current	@ 300 psig Inlet Pull-In	002	.408 amp	
	Drop-Out		.147 amp	
	Pull-In	004	.372 amp	
	Drop-Out		.142 amp	
Pressure Drop	← SEE FIGURE 3-7 →			
Response Pilot Only	@ 300 psig Inlet, 28 vdc, 30 psid	002	Open-14.5 ms, Close-7.5 ms	
		004	Open-11.0 ms, Close-8.0 ms	
Response Main + Pilot	@ 300 psig Inlet, 28 vdc, 30 psid	002	Open-32.0 ms, Close-16.0 ms	
		004	Open-26.5 ms, Close-16.0 ms	

VALVE FLOW CHARACTERISTICS

Acceptance Test 4/29/74

S/Ns 002 & 004

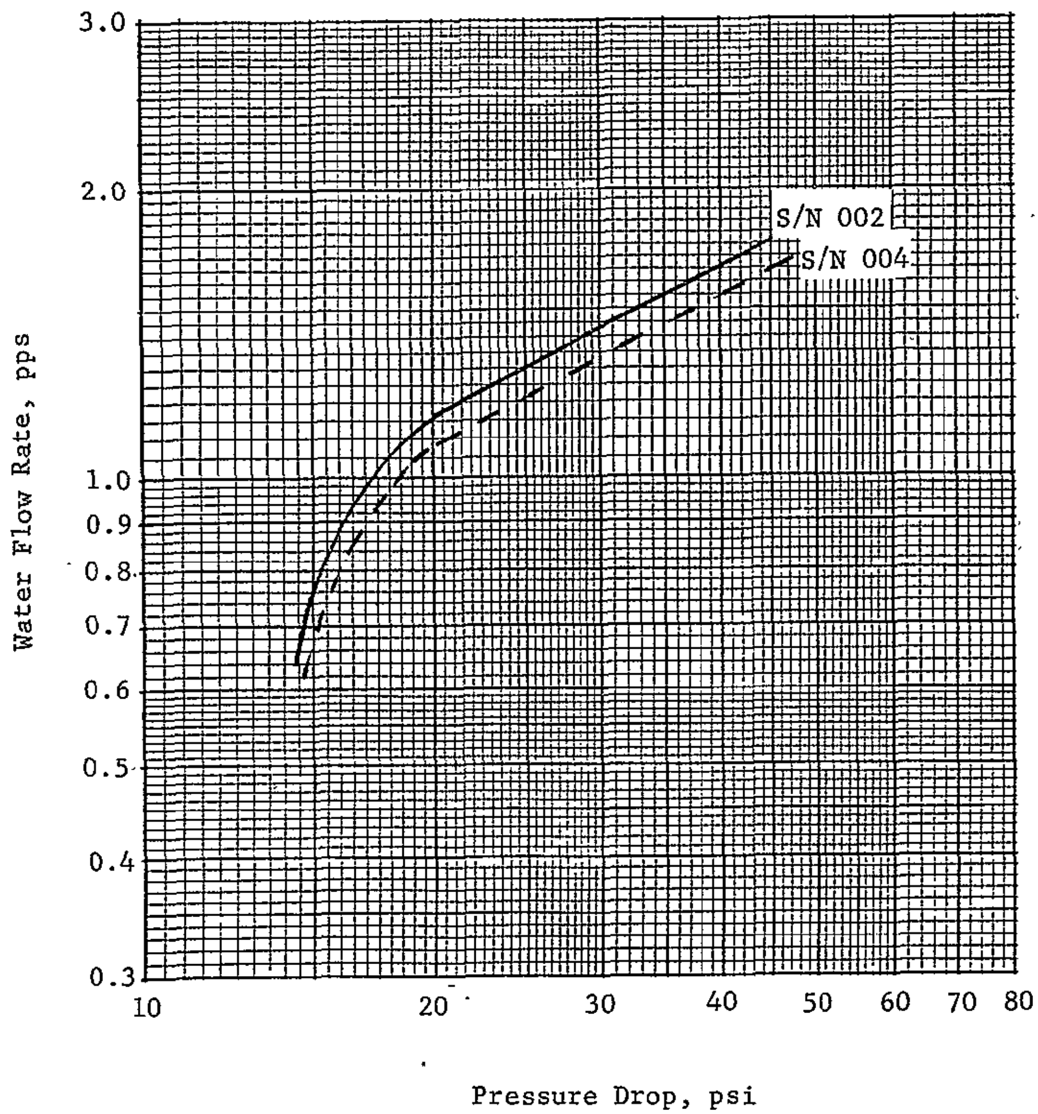

Figure 3-39

3.5.2.2 Performance Mapping

Performance mapping tests were performed to document the valves characteristics as a function of the operating variables of inlet pressure, coil voltage, and temperature. At each test condition, operating current and response times were recorded using water as the flow media. The valves were then nitrogen purged, the test temperature reestablished, and helium leakage rate measured at the test inlet pressures.

The operating current characteristics of the two test valves are plotted in Figure 3-40 and Figure 3-41. The pressure dependence of operating current (pull-in) is readily apparent and is attributable to the pressure unbalance of the pilot valve. The difference in operating current levels between the two test valves reflects the dimensional differences between the valves, in particular, the excessive parasitic magnetic gap of the S/N 002 valve results in the higher pull-in current values measured. Operating current variation with temperature was well within $\pm$ 10% at each test pressure. In addition to test error, which accounts for a majority of the variation, temperature has a slight impact on electromagnetic permeability and thermal growth or contraction will slightly alter pertinent dimensions that contribute to the force-stroke parameter of the solenoid circuit.

Figures 3-42 thru 3-47 summarize the response characteristics of the prototype valves over the range of pressure, temperature and voltage. Opening response characteristics of the pilot stage only, are plotted in Figures 3-41 and 3-42. The increase in opening response time with increasing pressure, increasing temperature and decreasing voltage is characteristic of the pressure unbalanced direct acting solenoid design. The difference in respective pilot valve response times, at similar conditions reflects the dimensional differences between the valves, particularly the parasitic "air" gaps (Table 3-III, Pilot Armature Gap-Valve Open). Response trends correlate with the measured pull-in current trends of Figures 3-40 and 3-41.

Total valve opening response (pilot + main) is plotted in Figures 3-44 and 3-45. When compared with Figures 3-42 and 3-43, it is readily apparent that main stage travel time was independent, within test error, of both voltage and temperature, and only slightly a function of inlet pressure. Main stage transit time differences between the two prototype valves are within 2.0 milliseconds which is attributable to the cumulative effects of differences in main stage stroke, pilot stroke and labyrinth seal clearance. Demonstrated opening transit times correspond closely with the predicted times of the analog computer model.

VALVE OPERATING CURRENT VS. TEMPERATURE AND PRESSURE

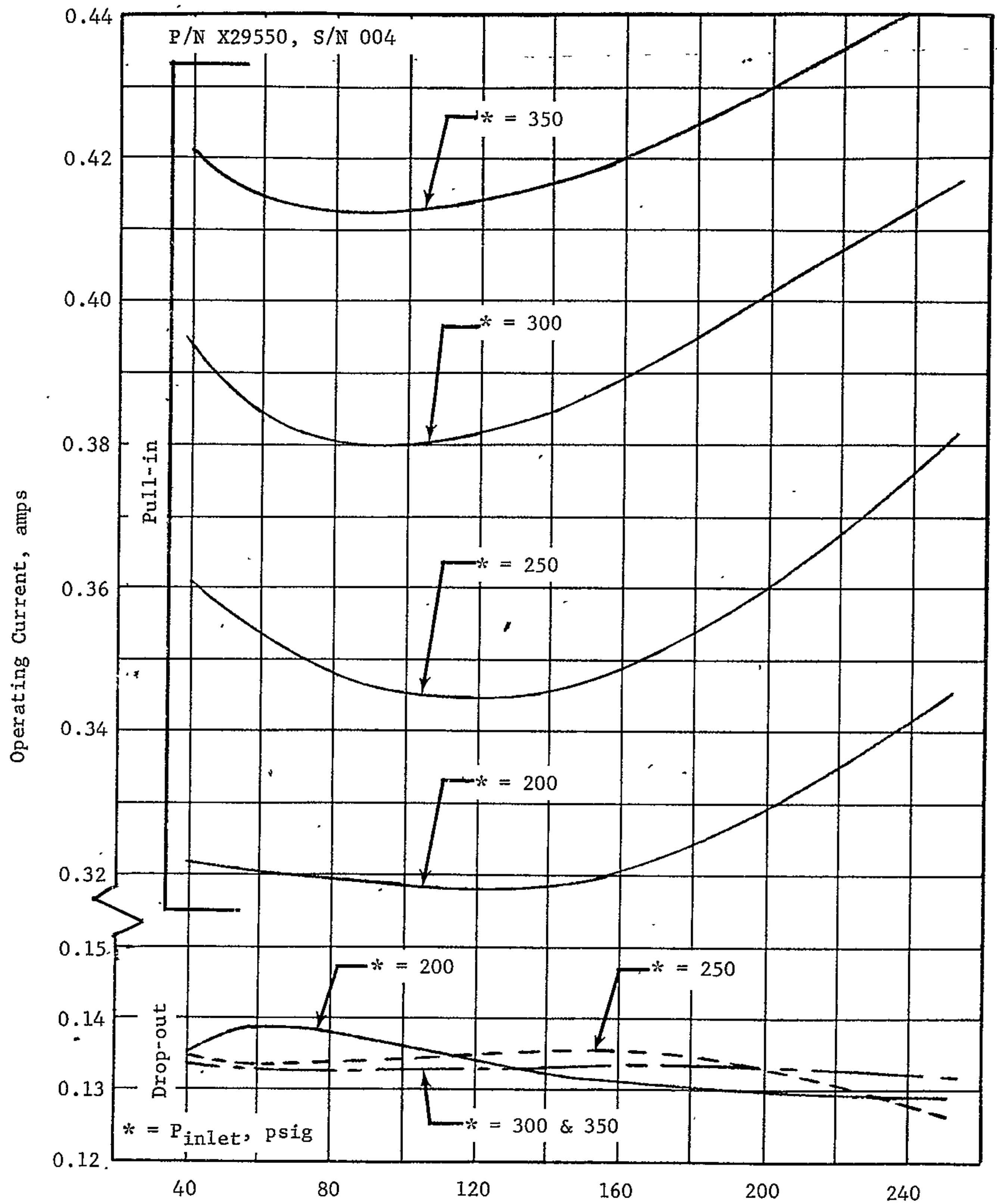

Figure 3-40

ORIGINAL PAGE IS OF POOR QUALITY

VALVE OPERATING CURRENT VS. TEMPERATURE AND PRESSURE

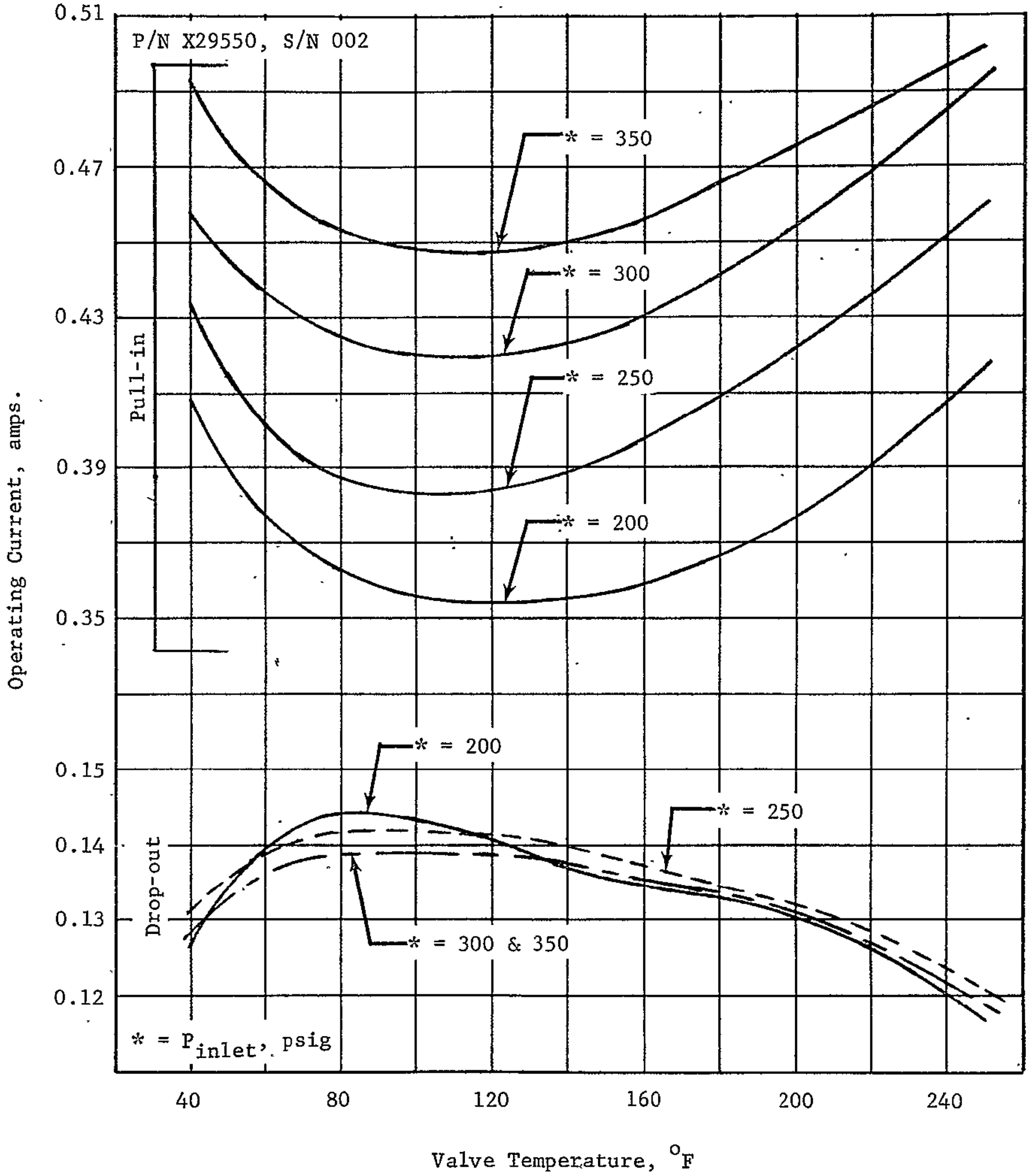

Figure 3-41

PILOT VALVE RESPONSE VS. TEMPERATURE, PRESSURE AND VOLTAGE

P/N X29550, S/N 004

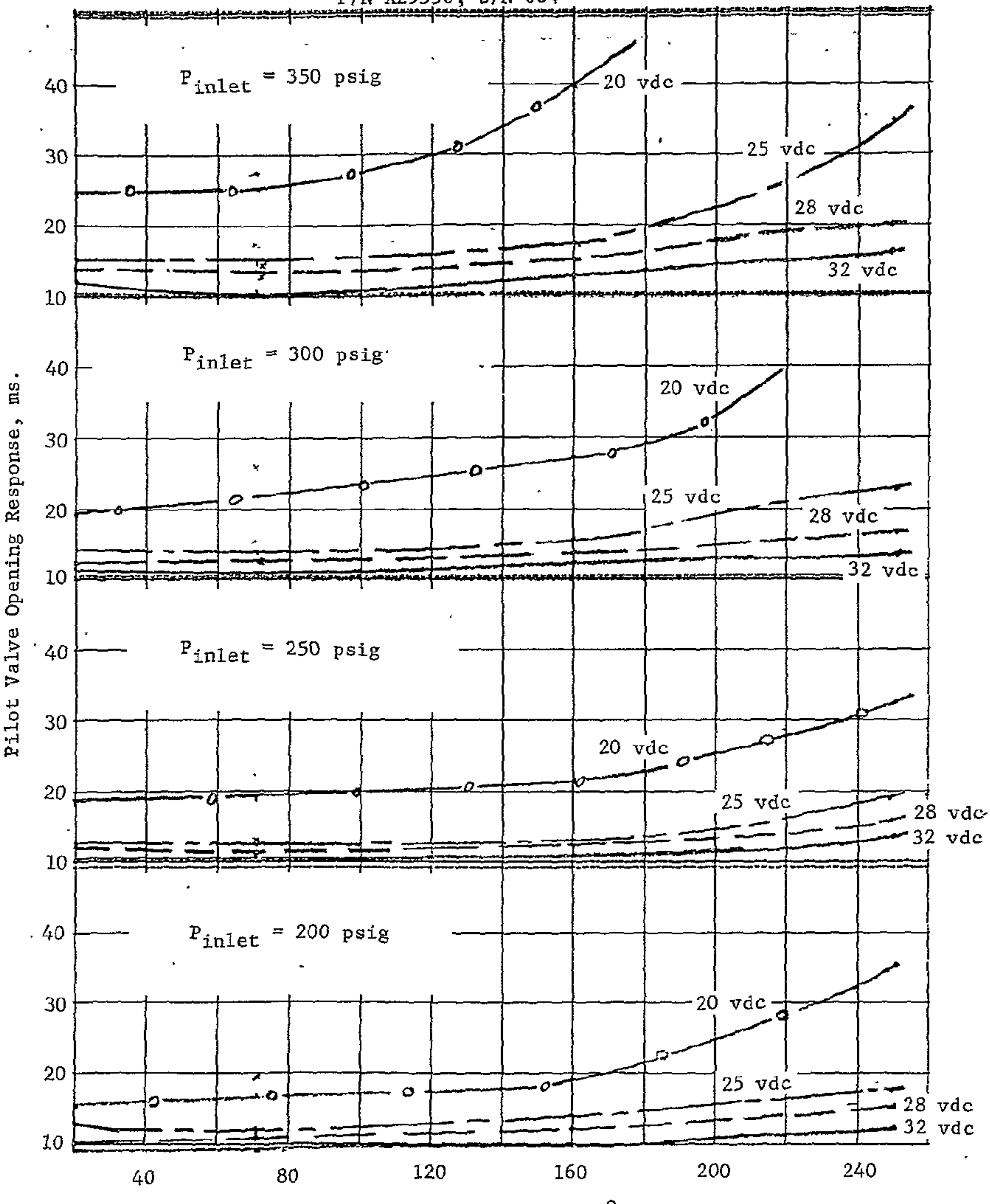

Figure 3-42

PILOT VALVE RESPONSE VS. TEMPERATURE, PRESSURE AND VOLTAGE

P/N X29550, S/N 002

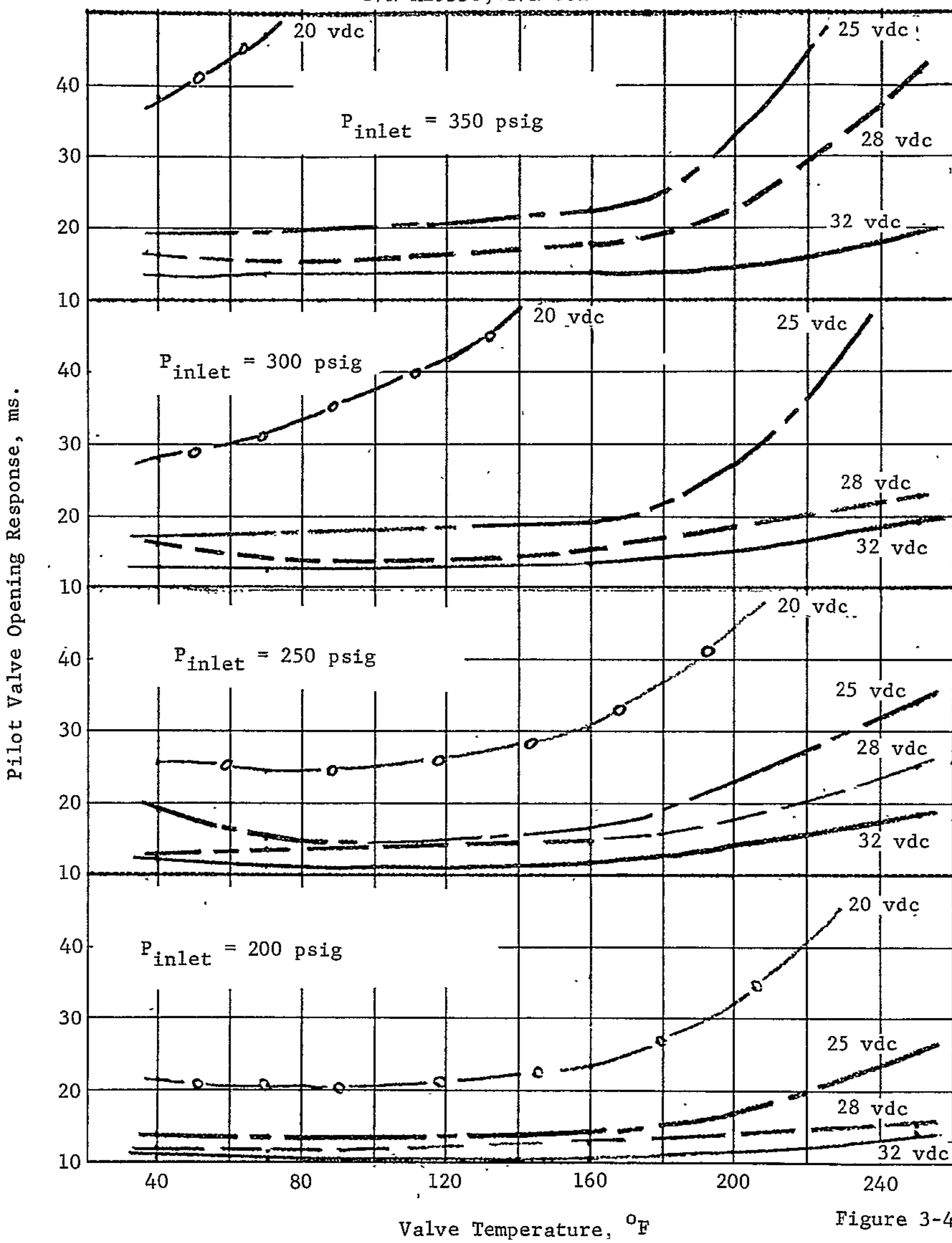

Figure 3-43

MAIN VALVE RESPONSE VS. TEMPERATURE, PRESSURE AND VOLTAGE

P/N X29550, S/N 004

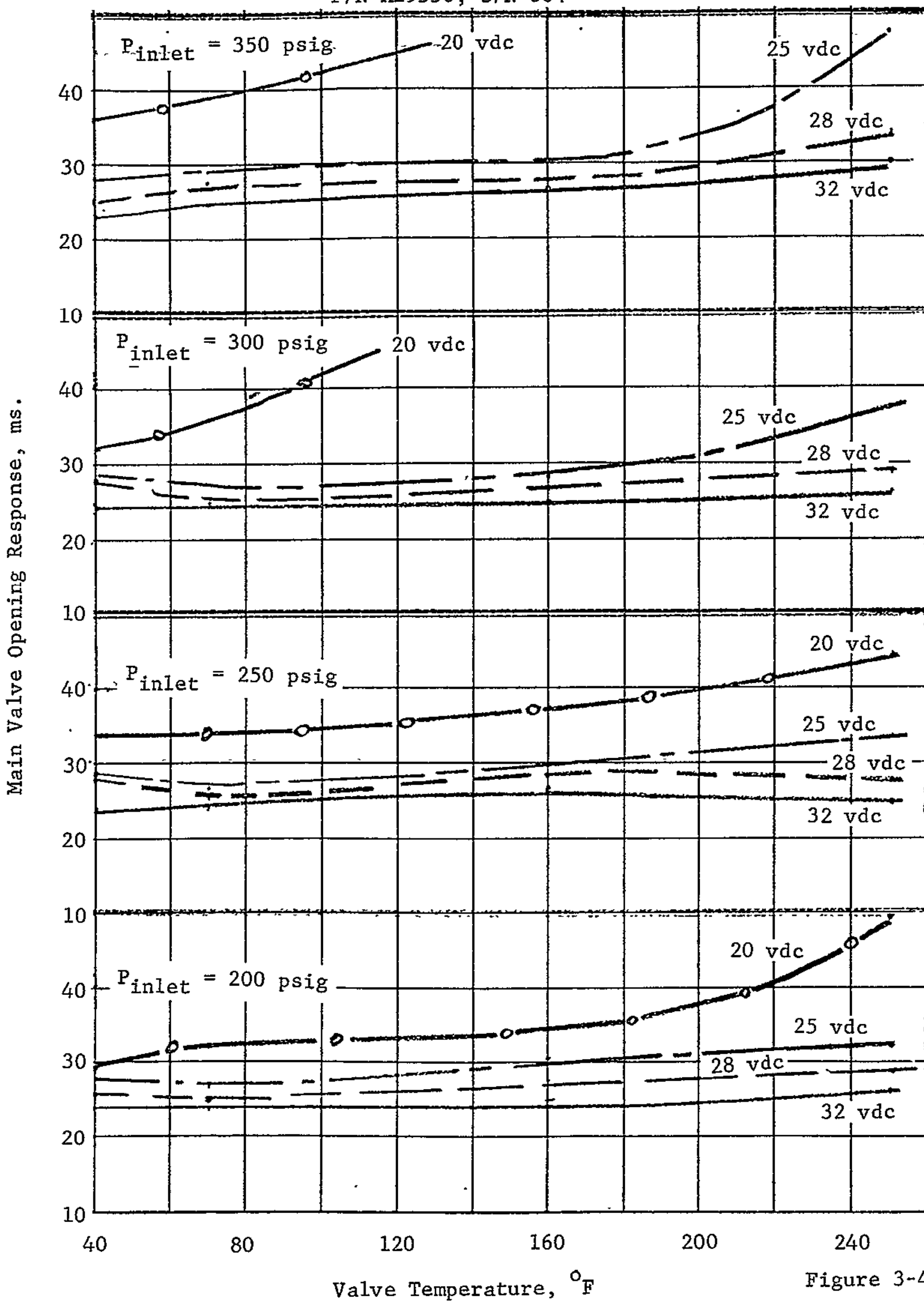

Figure 3-44

MAIN VALVE RESPONSE VS. TEMPERATURE, PRESSURE AND VOLTAGE

P/N X29550, S/N 002

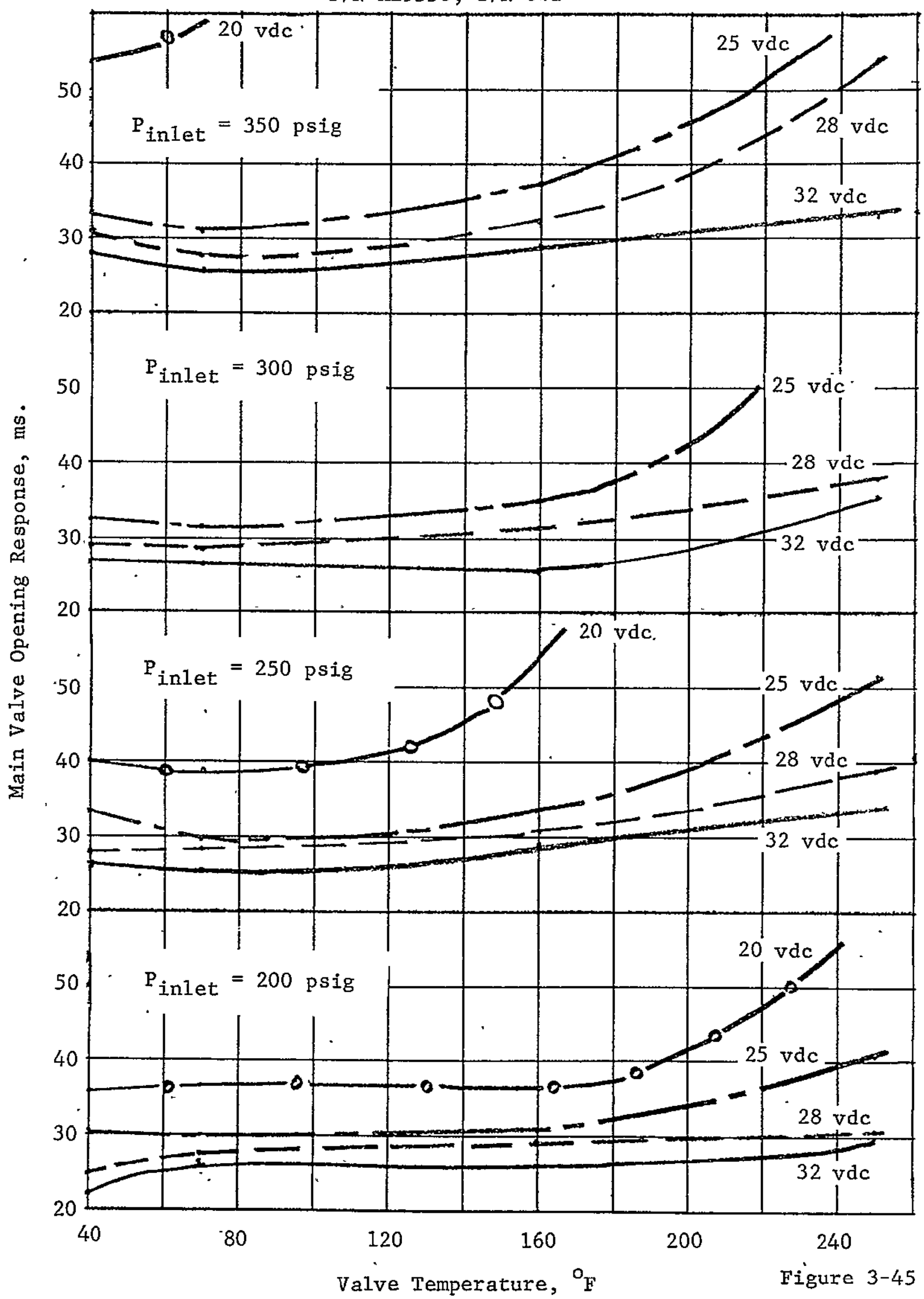

Figure 3-45

VALVE CLOSING RESPONSE VS. TEMPERATURE, PRESSURE AND VOLTAGE

P/N X29550, S/N 004

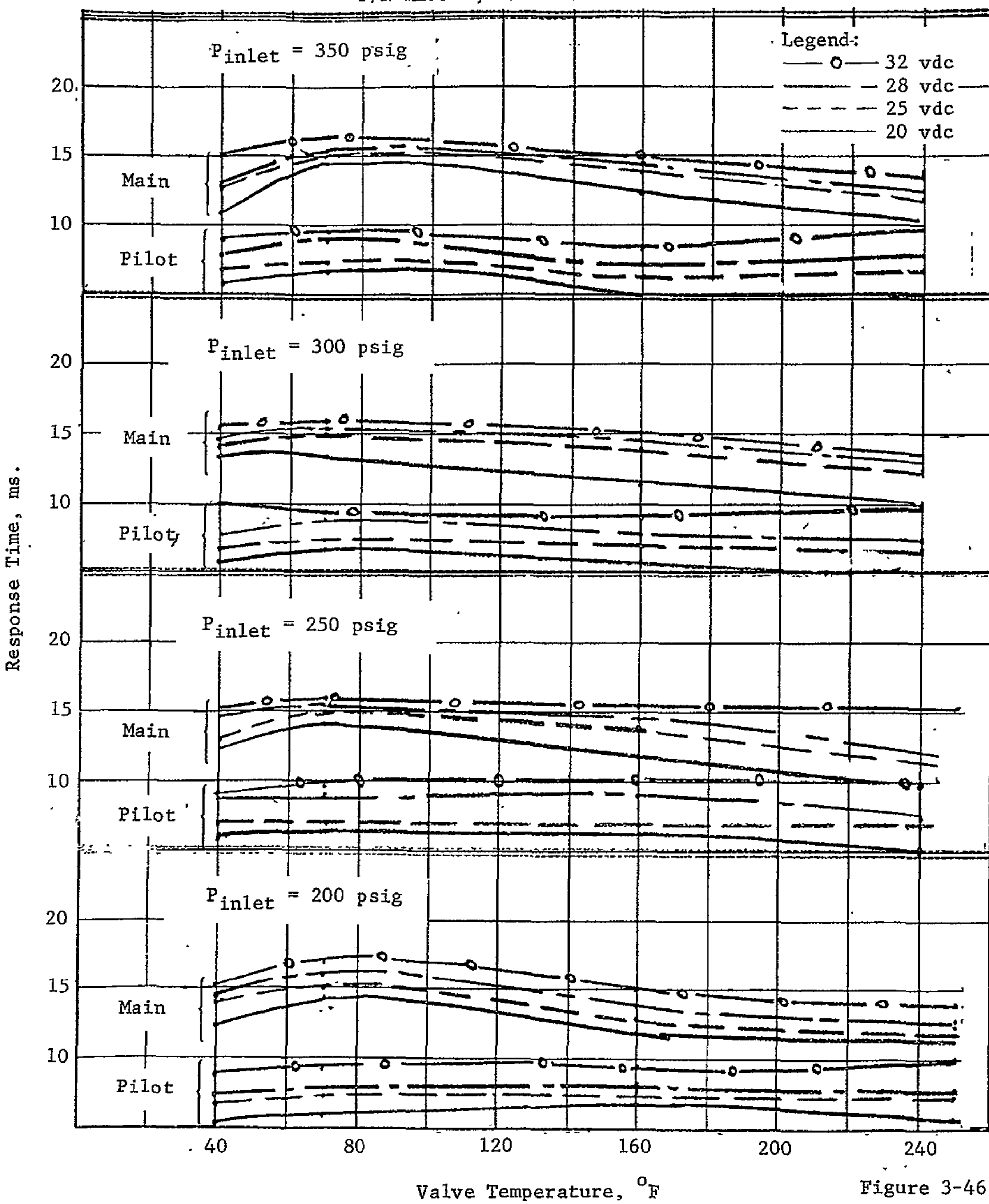

Figure 3-46

VALVE CLOSING RESPONSE VS. TEMPERATURE, PRESSURE AND VOLTAGE

P/N X29550, S/N 002

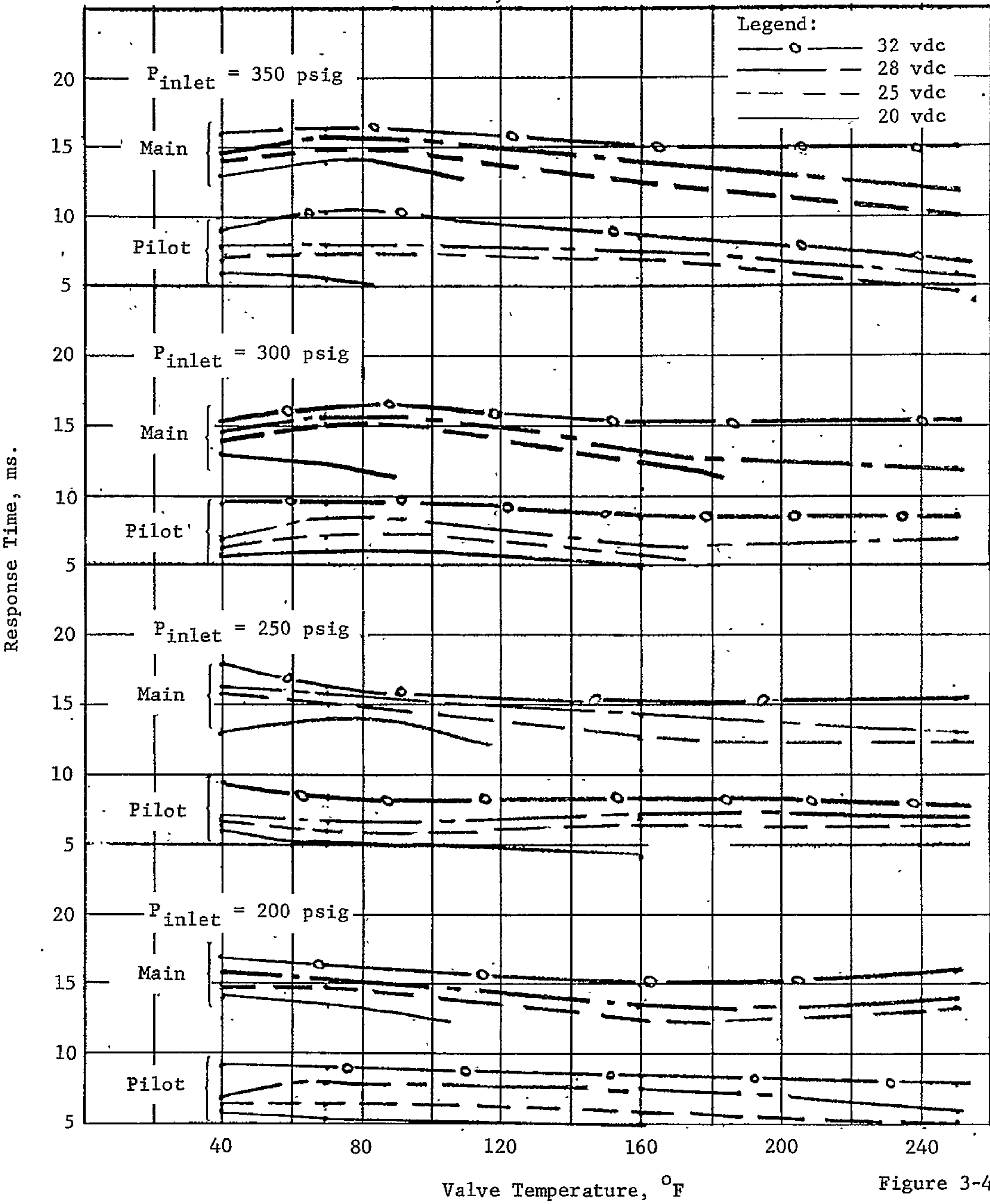

Figure 3-47

Valve closing times, both pilot and total, are summarized in Figures 3-46 and 3-47. Closing transit times of the main stage agree closely with the analog model predictions. Both the pilot and main closing times are relatively independent of temperature and inlet pressure level. Voltage dependence is readily apparent and holds with electromagnetic theory in that the higher levels of energy to which higher operating voltages drive the magnetic circuit require longer times to collapse to levels allowing drop-out, once the voltage signal is terminated.

The overall response mapping test results were most encouraging. Variability with pressure, voltage and temperature were well within analytically projected values. The slower pilot opening response than predicted resulted in no serious impact, particularly with respect to minimum impulse bit characteristics when employed on a thruster of the thrust range anticipated for the Space Shuttle Orbiter RCS.

Helium leakage characteristics at the various test temperatures and pressures are summarized in Table 3-V. With the exception of the initial S/N 002 valve leakage, subsequently found to be attributable to metallic contaminant, sealing was virtually "zero-leak" at all temperatures. The initial S/N 002 leakage was traced to a metallic sliver imbedded in the TFE seal at the sealing interface. It was removed by ultrasonic cleaning and nylon brush scrubbing. Reassembly and an ambient temperature leak check indicated full recovery of sealing integrity and testing resumed. Sealing over the total operating temperature was demonstrated.

3.5.2.3 Vibration

To substantiate structural integrity, determine critical resonance characteristics and demonstrate surviveability of the design, the two prototype units were subjected to a vibration test sequence. Two potential modes of launch were evaluated - dry, unpressurized, and wet at full system operating pressure.

Before subjecting the valves to the vibration, performance checkout tests were performed to document characteristics for assessment of the impact of the vibration exposure. These tests consisted of response and operating current measurements, water flow characteristics, and leakage measurement. It is also noted that the main stage upper and lower flexure assemblies were replaced in both valves. The original flexures which had been fabricated of in-house stock, (Inconel 718) were not traceable and certification was not available. The replacement flexures were identical in design, but were fabricated of certified material.

TABLE 3-V

PERFORMANCE MAPPING LEAKAGE SUMMARY

Temperature °F	Pressure PSIG	Helium Leakage Rate, scch S/N 002	Helium Leakage Rate, scch S/N 004	Remarks
70	200	305	1.0	
	250	168	0.5	
	300	125	1.0	
	350	54.5	0.0	
160	200	Excessive	2.0	Disassemble S/N 002, clean metal chips from pilot seal.
	250	"	3.0	
	300	"	3.5	
	350	"	3.0	
70	20	0.0		
	300	0.0		
40	200	0.0	2.0	
	250	0.5	0.0	
	300	0.0	0.8	
	350	0.5	0.5	
160	200	158		
	250	0.0		
	300	0.0		
	350	0.0		
250	200	0.0	4.0/0.5	
	250	0.0	2.5/0.5	
	300	0.5	0.0/0.5	
	350	0.0	0.0	
70	200	0.5	0.0	
	250	0.0	0.0	
	300	0.3	0.0	
	350	0.0	0.0	

Sine sweeps at approximately 3 g's input were performed in each of the three major axes, while employing a monitor accelerometer to indicate valve response to the excitation. The S/N 002 valve was pressurized with GN_2 at 10 psi to simulate a dry launch condition, yet provide a means of monitoring valve leakage by connecting the valve outlet to a water-filled burette. Wet launch simulation was achieved by pressurizing the S/N 004 valve with water, at 100 psi, through a sight tube to allow leakage monitoring during vibration exposure. No evidence of resonance was revealed by the sine sweeps of either valve in any of the axes of excitation. No significant evidence of leakage was observed.

Random vibration exposure under the two launch simulation conditions resulted in significant leakage of both valves while being vibrated. The spectrum and duration of exposure were equivalent to 50 missions of the launch boost intensity.

After vibration, both valves were performance-tested for correlation with the previbration performance characteristics. The total vibration test results are summarized in Table 3-VI. A tear-down and visual examination was performed to verify structural integrity and assess any other impacts on the valve, not reflected in valve performance. No abnormalities were observed in the inspection of the S/N 004 valve (wet launch simulation). The S/N 002 valve (dry launch simulation), evidenced two areas of unusual appearance. The main seat sealing surface texture evidenced scuff marks (Figure 3-48), apparently due to lateral movement of the main poppet and perhaps the origin of the leakage noted immediately after each random vibration exposure. This surface texture effect was apparently not a serious degradation of the seal since a zero leak seal resulted after the few valve cycles performed in the post vibration checkout test. The second observation was a large quantity of small, black flakes in several areas. The origin of this contaminant was traced to "stop-off", a titanium oxide material employed in flexure assembly brazing to limit braze alloy flow onto functional surfaces. The inert quality of the material makes its removal, after brazing, difficult and residues are invariably left on inaccessible surfaces. Its release from the surfaces was apparently stimulated by the vibration environment. No leakage is traceable to its presence within the valve, even that located on, or imbedded in the TFE seal surfaces.

3.5.2.4 Cycle Life

Cycle life testing consisted of accumulating 200,000 cycles of valve operation in ten equal increments. After each increment, performance and leakage characteristics were measured. Each increment of cycling was performed at a temperature, such that the total operating temperature would be experienced.

TABLE 3-VI

VIBRATION TEST SUMMARY

(1) Pre Vibration Checkout

TEST VALVE S/N	002	004
H_e LEAKAGE AT 20 PSIG	0.5 SCCH	6.0 SCCH
200 PSIG	0.0 SCCH	2.0 SCCH
FLOW	1.431 PPS AT 30 PSID	1.359 PPS AT 30 PSID
RESPONSE AT 250 PSI 28 VDC	29.5 MS OPEN, 14.5 MS CLOSE	27.0 MS OPEN, 14.0 MS CLOSE
OPERATING CURRENT	0.358 AMPS AT 250 PSI	0.336 AMPS AT 250 PSI

TABLE 3-VI (Continued)

VIBRATION TEST SUMMARY

(2) Vibration

a) SINE SWEEP AT 3 $^{OCT}/_{MIN}$ ~ 3 g INPUT (RESONANCE SEARCH)

b) RANDOM - 15 $^{MIN}/_{AXIS}$

+6 db/OCT	20 - 70 Hz	
1.2 g^2/Hz	70 - 500 Hz	
-3 db/OCT	500 - 2000 Hz	(38.2 g_{rms} overall)

RESULTS

TEST VALUE S/N	002			004		
TEST CONDITION	INLET GN_2 PRESSURIZED AT 10 PSIG			INLET H_2O PRESSURIZED AS NOTED		
SINE SWEEP	NO EVIDENCE OF RESONANCE			NO EVIDENCE OF RESONANCE		
AXIS OF VIBRATION	X	Y	Z	X	Y	Z
LEAK RATE DURING VIBRATION	.24 SCCH	0.0SCCH	0.0 SCCH	11.5 CCH	0.0CCH	0.0CCH
RANDOM VIBRATION						
AXIS OF VIBRATION	X	Y	Z	X	Y	Z
LEAK RATE DURING VIBRATION	OVER SCALE	~2880SCCH	~4500SCCH	11380 CCH at 100 PSIG 6125 CCH at 175 PSIG 3890 CCH at 230 PSIG	4.28 CCH at 230 PSIG	25.7 CCH at 230 PSIG
LEAK RATE IMMEDIATELY FOLLOWING VIB.	3.67 SCCH	17.2 SCCH	180SCCH	NOT PERFORMED AT VIB TEST SITE		

TABLE 3-VI (Continued)

VIBRATION TEST SUMMARY

(3) Post Vibration Checkout

TEST VALVE S/N	002	004
He LEAKAGE AT 20 PSIG AT 200 PSIG	OVER SCALE* OVER SCALE*	15.0 SCCH 5.0 SCCH
FLOW RESPONSE RESPONSE OPERATING CURRENT	WITHIN .004 PPS OF PRE VIB. AT 30 PSID WITHIN 1 MS of pre VIB. WITHIN .05a of PRE VIB.	WITHIN .01 PPS OF PRE VIB. AT 30 PSID WITHIN 1 MS OF PRE VIB. WITHIN .02A OF PRE VIB.
He LEAKAGE AT 20 PSIG AT 200 PSIG	15.5 SCCH 4.0 SCCH	0.0 SCCH 0.0 SCCH
DISASSEMBLY & INSPECTION	PULVERIZED "STOP-OFF" IN PILOT MAIN SEAT SCUFFED	NO EVIDENCE OF DAMAGE OR WEAR
REASSEMBLY FLOW RESPONSE OPERATING CURRENT	WITHIN .004 PRS OF PRE VIB. AT 30 PSID WITHIN 1 MS OF PRE VIB. WITHIN .02a OF PRE VIB.	WITHIN .001 PPS OF PRE VIB. AT 30 PSID WITHIN 1.5 MS OF PRE VIB. WITHIN .015a OF PRE VIB.

* NO LIQUID LEAKAGE NOTED DURING WATER FLOW TESTS

S/N 002 MAIN SEAT - AFTER VIBRATION TEST (50 MISSIONS)

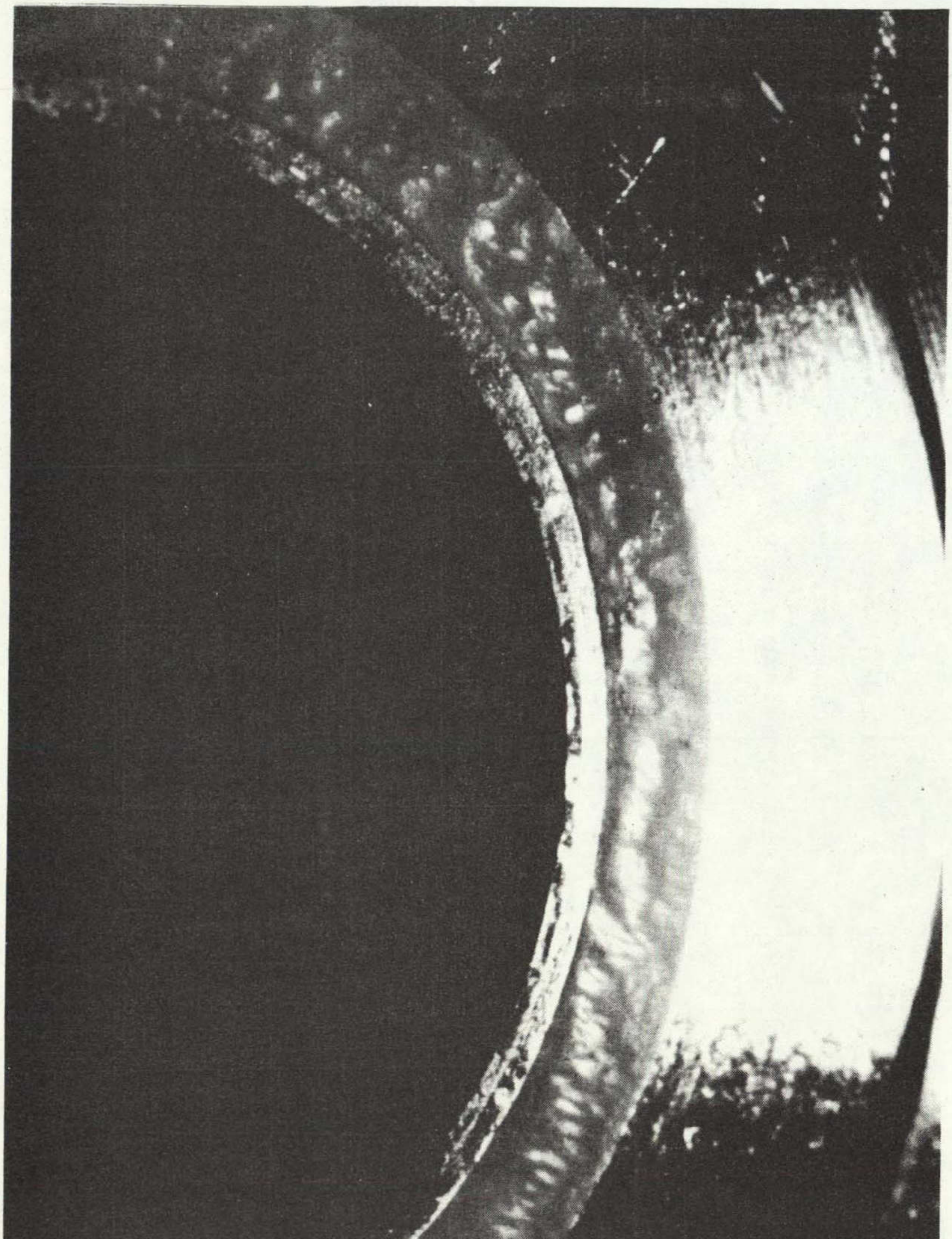

N74-352-44

Figure 3-48

cr

ORIGINAL PAGE IS
OF POOR QUALITY

During the cycle testing, evidence of out-of-specification leakage occurred as shown in Table 3-VII. A disassembly and inspection indicated premature failure of the pilot seal. The failure was erosion of the teflon immediately downstream of the sealing interface, which propagated upstream until a leak path was generated. The failures were similar to those experienced in the Initial Assembly Checkout (paragraph 3.5.1), in spite of the success of the 200,000 cycle demonstration of this design which lead to its committment for the Development Test Program. The photograph of the S/N 002 valve pilot seat after 60,000 cycles (Figure 3-49), is typical of all the experienced failures. In all instances, the site of the erosion is aligned with one of the vent slots in the metal cap which contains the seal and coil spring. The similarity of all failures, in that they all were similarly aligned with a potential flow turbulence generator, indicates that flow phenomenon was the origin of the failure and cavitation the most probable phenomenon. The leakage versus cycle history indicates the progression of failure in that first indications are evidenced during low pressure leak tests, then diminish as increased inlet pressure compresses seal material sufficiently to close off the leak path. When erosion has progressed, ultimately leakage becomes proportional to inlet pressure, indicating that a finite path exists through the seal interface.

Performance characteristics, including leakage, as a function of cycles is plotted in Figures 3-50 through 3-53. Operating current and response times were repeatable considering normal test variables. Concurrent with pilot seal replacement, some changes in performance might be anticipated, due to its effect on pilot stroke, resulting from dimensional variations and preload variations.

After the initial 20,000 cycles of operation of the S/N 004 valve, a coil short to the case was evidenced. The cover was removed and the cause of the short was identified as a small void in the potting at the outer surface near the upper flange (Figure 3-54). Since no failure or breakage of the coil wire was evidenced, potting in the failure point area was scrapped to allow a mylar tape layer patching of the wire insulation. A new coil cover, relieved at the I.D. in the area of the coil window, was installed and potting introduced under vacuum. Coil to case insulation resistance recovered to 10^6 megohms.

Considering the total cycle life of the valve, from the initial valve assembly and checkout through the conclusion of the cycle life test, the valves cyclic durability is well substantiated. The cycle logs of the respective valves are presented in Tables 3-VIII and 3-IX. Main seat life characteristics greatly exceeded the design goal.

TABLE 3-VII

LIFE CYCLE TEST LEAKAGE SUMMARY

Valve S/N	Cumulative Cycles On Valve	SCCH He Leakage @ 20 psi	200 psi	300 psi	Cumulative Cycles On Pilot Seal
002	20,000	300	7.4	20	20,000
	40,000	102	1,030	1,090	40,000
	60,000	Immeasurable			60,000
Pilot Shaft Assembly Replaced					
	60,000	0	2	4.5	0
	120,000	Excessive	42.5	12	60,000
	140,000	18,947	1,714	1,565	80,000
Cycle Test Terminated					
004	100,000	765	5	0	100,000
	120,000	2,120	1,440	400	120,000
	140,000	7,420	18,000	20,000	140,000
Pilot Shaft Assembly Replaced					
	140,000	30.5	6.5	2	0
	180,000	300	0	0	40,000
	200,000	2,999	5,760	7,826	60,000

Note: All leakages other than those shown were less than 5.0 SCCH.

S/N 002 VALVE PILOT POPPET AFTER 60,000 CYCLES

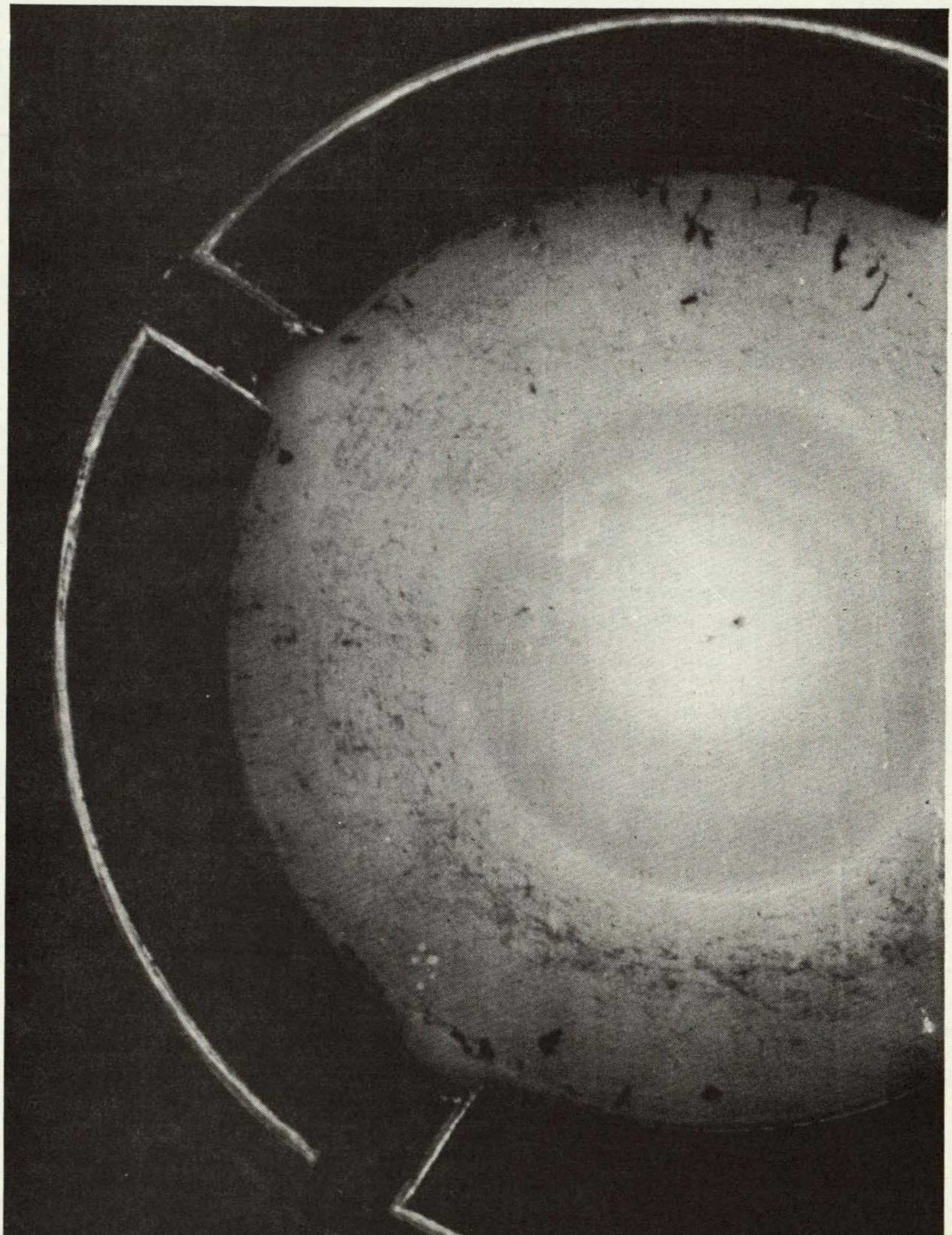

N74-352-62

Figure 3-49

LIFE CYCLE TEST PERFORMANCE

P/N X29550, S/N 002

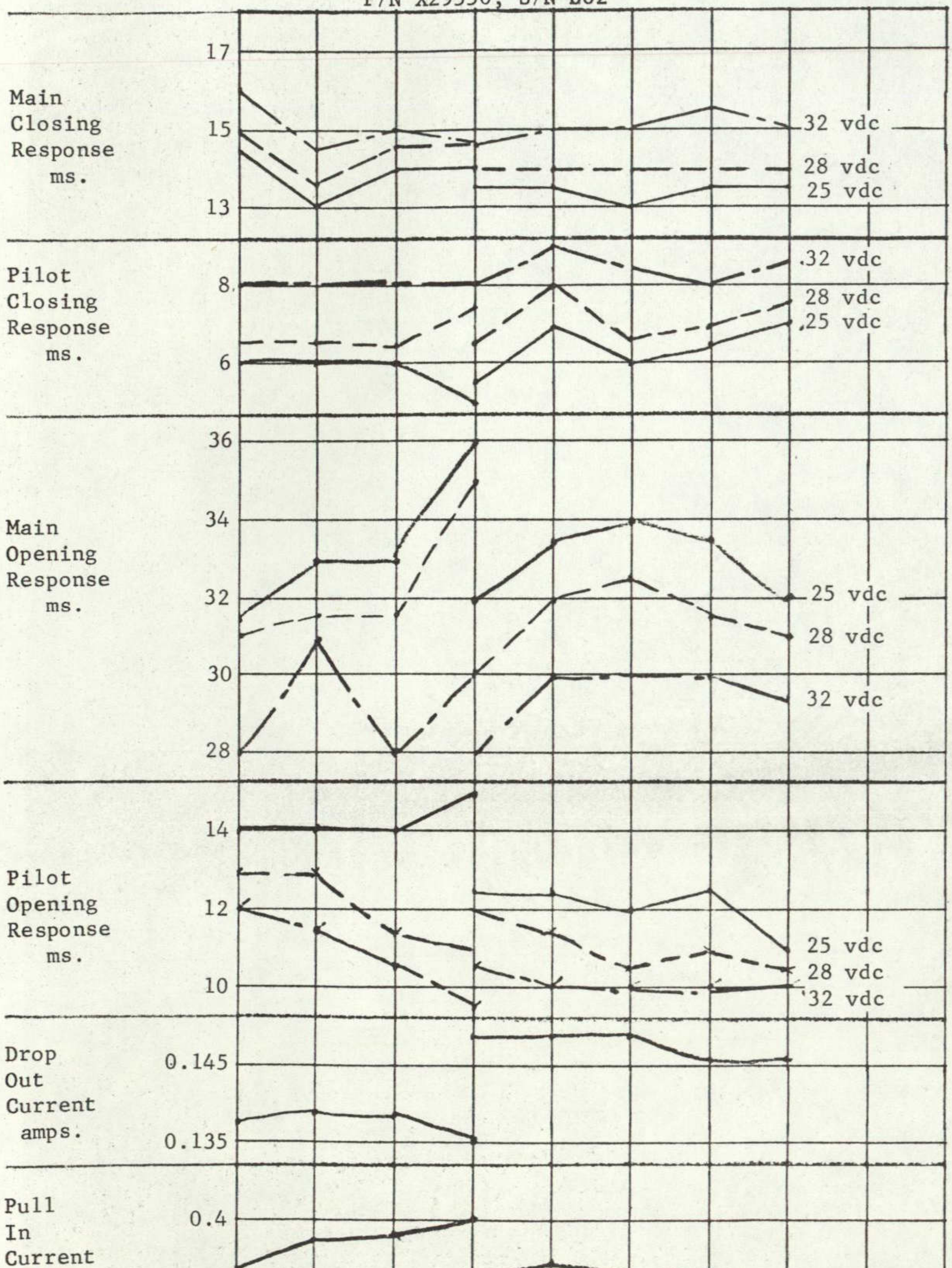

Figure 3-50

ORIGINAL PAGE IS OF POOR QUALITY

LIFE CYCLE TEST LEAKAGE

P/N X29550, S/N 002

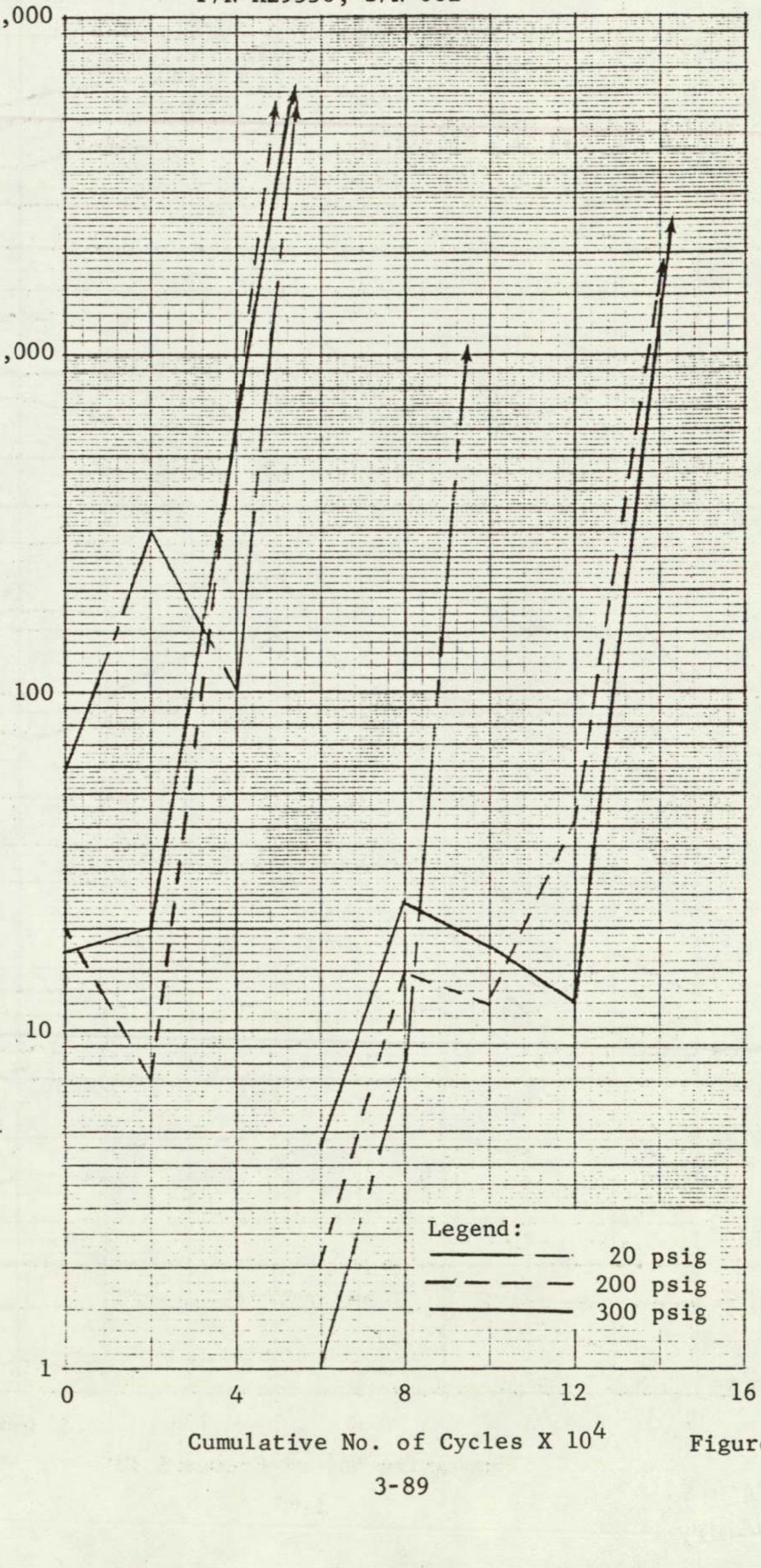

Figure 3-51

LIFE CYCLE TEST PERFORMANCE

P/N X29550, S/N 004

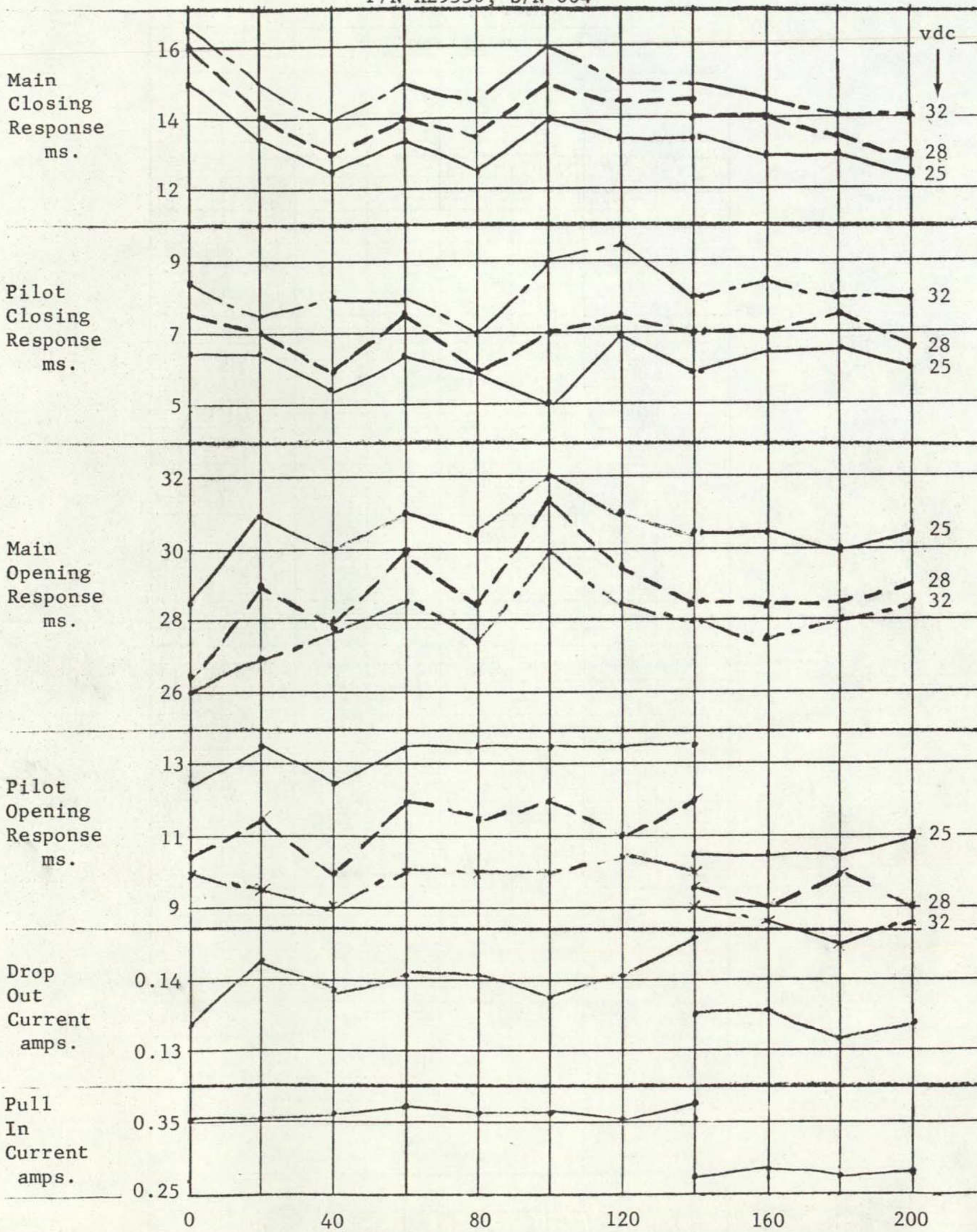

Figure 3-52

ORIGINAL PAGE IS OF POOR QUALITY

LIFE CYCLE TEST LEAKAGE VS. CYCLES

P/N X29550, S/N 004

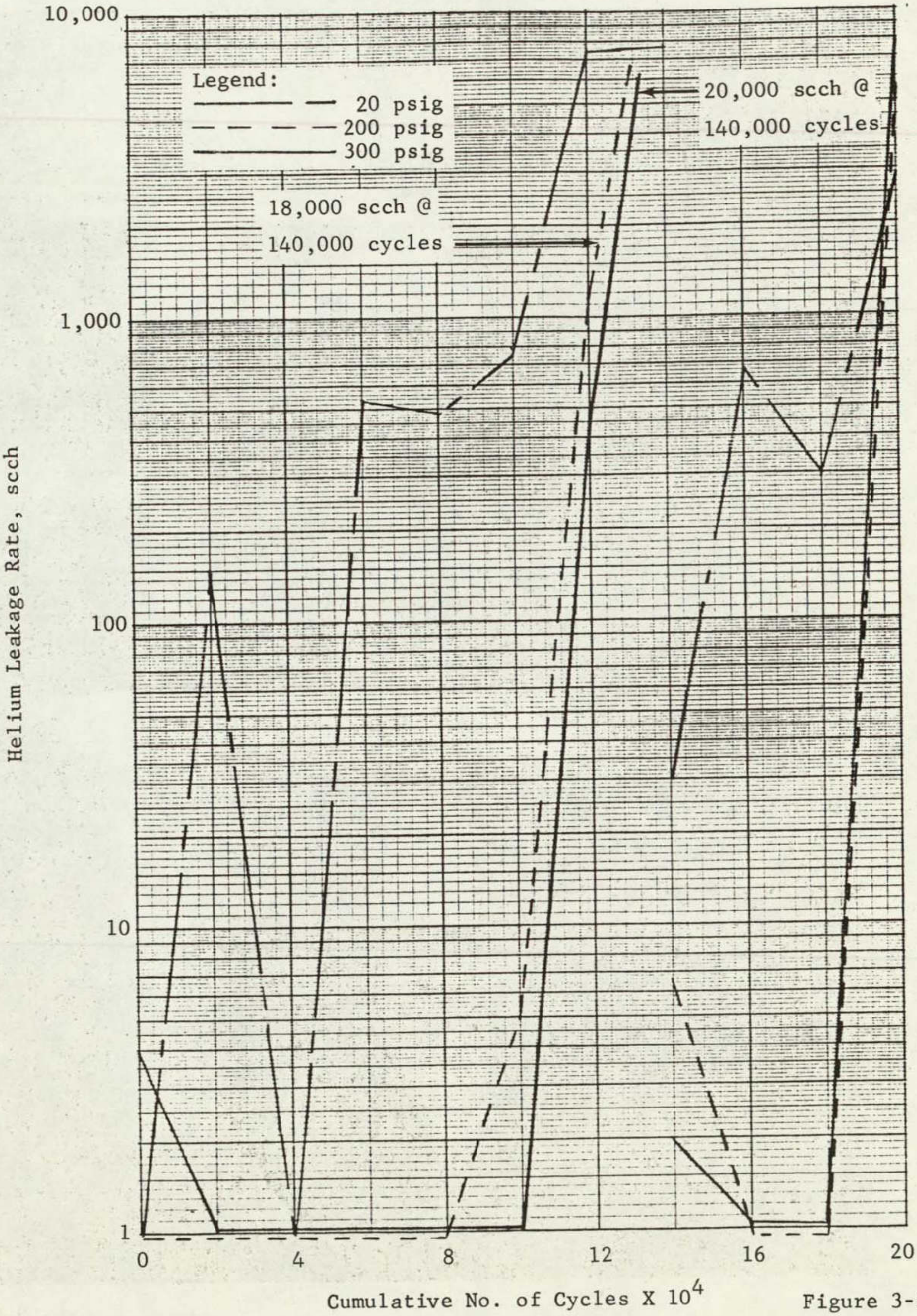

Figure 3-53

S/N 002 COIL FAILURE

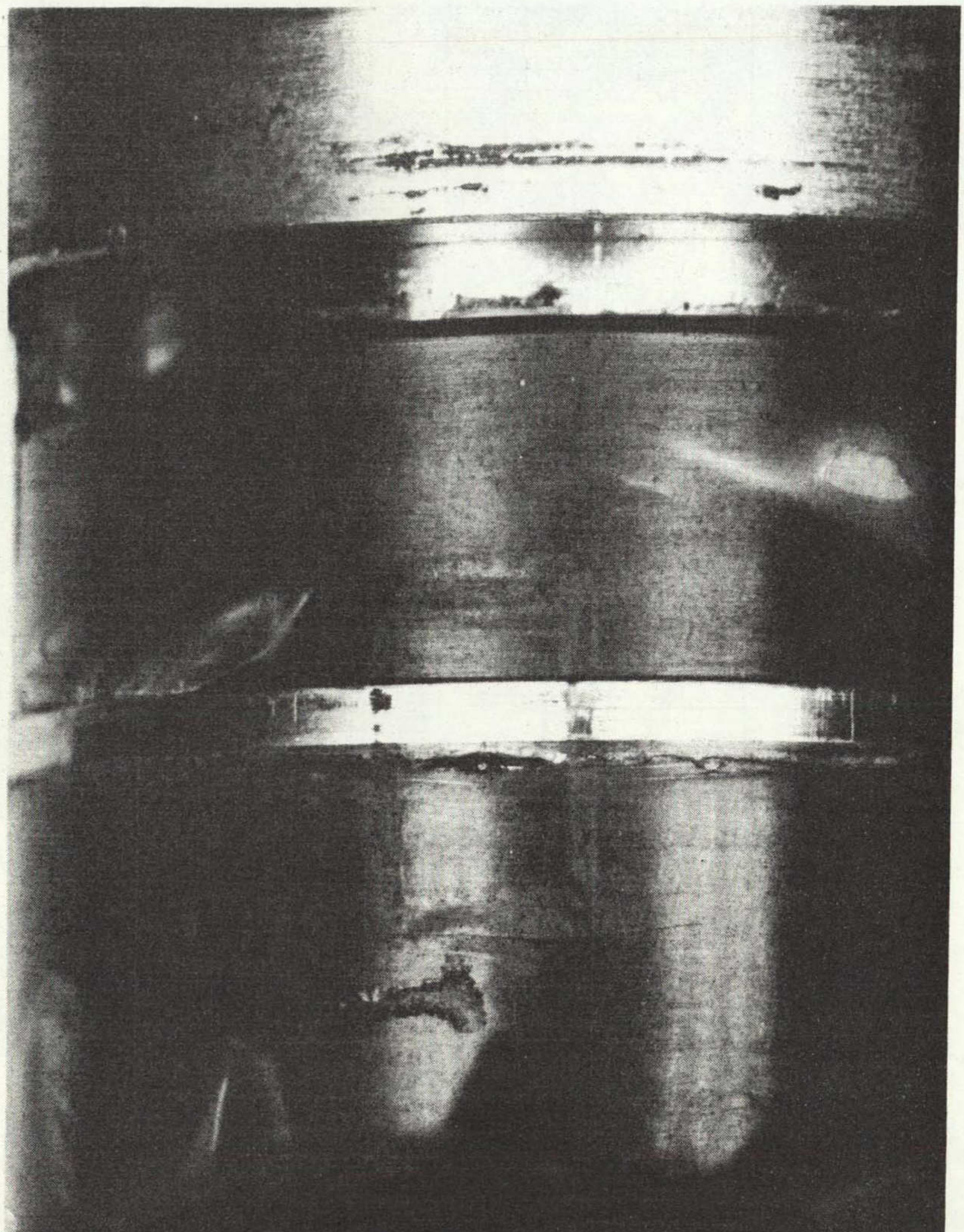

Figure 3-54

TABLE 3-VIII

Cycle Log S/N 002

Date	Pilot Valve		Main Valve	
	Cycles per Test	Total Cycles	Cycles per Test	Total Cycles
12-20-73	18	18	18	18
12-24-73	10	28	10	28
12-26-73	19	47	19	47
12-29-73			Replaced Seat (New Angle)	
12-29-73	16	63	16	16
1-4-74	12	75	12	28
3-7-74	New Design			
3-7-74	20,000	20,000	20,000	20,028
3-10-74	New Design			
3-10-74	20,016	20,016	20,016	40,044
3-14-74	80,000	100,016	80,000	120,044
3-25-74	New Design			
3-25-74	19	19	19	120,063
3-26-74	28	47	28	120,091
3-27-74	115,000	115,047	115,000	235,091
4-24-74	New Design			
4-29-74	7	7	7	235,098
4-30-74	21	28	21	235,119
5-3-74	26	54	26	235,145
5-3-74	Clean Pilot Seat			
5-10-74	29	83	29	235,174
5-13-74	27	110	27	235,201
5-16-74	28	138	28	235,229
8-6-74		Main Flexures Replaced		
9-10-74	35	173	35	235,264
9-13-74		Vibration Test		
9-16-74	29	202	29	235,293
9-23-74	19	221	19	235,312
9-26-74	20,018	20,239	20,018	255,330
10-10-74	20,000	40,239	20,000	275,330
10-11-74	38	40,277	38	275,368
	20,000	60,277	20,000	295,368
	33	60,310	33	295,401
10-16-74	Replace Pilot Shaft Assy.			
	28	28	28	295,429
10-17-74	20,000	20,028	20,000	315,429
	31	20,059	31	315,460
	20,000	40,059	20,000	335,460

TABLE 3-VIII (Continued)

Cycle Log S/N 002

Date	Pilot Valve		Main Valve	
	Cycles per Test	Total Cycles	Cycles per Test	Total Cycles
10-18-74	33	40,082	33	335,493
10-25-74	20,000	60,082	20,000	355,493
	29	60,111	29	355,522
10-28-74	20,000	80,111	20,000	375,522
	31	80,142	31	375,553

TABLE 3-IX

Cycle Log S/N 004

Date	Pilot Valve		Main Valve	
	Cycles per Test	Total Cycles	Cycles per Test	Total Cycles
1-12-74	33	33	33	33
1-13-74	52	85	52	85
1-15-74	23	108	23	108
1-16-74	38	146	38	146
1-17-74	17	163	17	163
2-21-74	New Design			
2-21-74	10,000	10,000	10,000	10,163
2-21-74	New Design			
2-21-74	13,000	13,000	13,000	23,163
2-22-74	12,000	25,000	12,000	35,163
2-26-74	New Design			
2-26-74	50,023	50,023	50,023	85,186
2-27-74	33,250	83,273	33,250	118,436
3-6-74	New Design			
3-6-74	18	18	18	118,454
3-7-74	50,182	50,200	50,182	168,636
3-7-74	New Design			
3-7-74	20,000	20,000	20,000	188,636
4-2-74	New Design			
4-2-74	50,018	50,018	50,018	188,654
4-2-74	100,000	150,018	100,000	288,654
4-3-74	50,000	200,018	50,000	338,654
4-8-74	Replace Pilot Poppet			
4-8-74	50	50	50	338,704
4-29-74	8	58	8	338,712
5-1-74	23	81	23	338,735
	22	103	22	338,757
5-10-74	26	129	26	338,783
5-15-74	20	149	20	338,803
5-16-74	23	172	23	338,826
9-6-74			Replace Main Flexures	
9-10-74	17	189	17	338,843
9-13-74		Vibration Tests		
9-16-74	18	207	18	338,861
9-23-74	17	224	17	338,878
9-24-74	20,019	20,243	20,019	358,897
10-1-74	38	20,281	38	358,935

TABLE 3-IX (Continued)

Cycle Log S/N 004

Date	Pilot Valve		Main Valve	
	Cycles per Test	Total Cycles	Cycles per Test	Total Cycles
10-11-74	20,000	40,281	20,000	378,935
	43	40,324	43	378,978
10-14-74	20,000	60,324	20,000	398,978
	36	60,360	36	399,014
	20,000	80,360	20,000	419,014
	34	80,394	34	419,048
10-16-74	20,000	100,394	20,000	439,048
	31	100,425	31	439,079
10-18-74	20,000	120,425	20,000	459,079
	33	120,458	33	459,112
10-25-74	20,000	140,458	20,000	479,112
	38	140,496	38	479,150
10-28-74	Replace Pilot			
	35	35	35	479,185
10-29-74	20,000	20,035	20,000	499,185
	37	20,072	37	499,222
	20,000	40,072	20,000	519,222
	32	40,104	32	519,254
10-30-74	20,000	60,104	20,000	539,254
	31	60,135	31	539,285

3.6 Post Test Inspection Analysis and Design Modifications

On completion of the testing (paragraph 3.5.2), both valves were disassembled and inspected for evaluation of the condition of their respective components. Photographs of critical sealing elements are shown in Figures 3-55 thru 3-60. No other abnormalities, such as erosion or structural failures, were observed. With the exception of the pilot seals and the S/N 002 main seat, all elements of the valves appeared unaffected by the test exposure accumulated. Traces of "stop-off" used in brazing of flexures were found in varying quantities on the respective seals, but did not appear to affect sealing capabilities.

Design modifications appear warranted to correct the deficiencies of pilot seat seal life and leakage during vibration. In view of the continuing development of this valve for application on the SSRCT, and with the concurrence of the technical monitor, proposed modifications to correct these deficiencies will be verified as an integral part of the SSRCT program which TMC is currently performing under contract to Rockwell/SD. Testing to substantiate the design modifications will be performed using the prototype valves (S/N's 002 and 004).

The proposed design modifications and the rationale for these changes are as follows:

- In view of the successful life and sealing characteristics of the main seat, a redesign of the pilot seat and poppet employing similar design criteria and configuration is proposed. Analysis has confirmed that identical criteria, relative to thermal characteristics, volumetric compression and elasticity are practical for a seat scaled to the pilot valve size. The proposed configuration is shown in Figure 5-1.

- Before a leakage-during-vibration design modification can be proposed, more insight into the origin of response to vibrational excitation, through testing, is required. Specifically, it must be determined which seat leaks or if both seats leak when exposed to the required vibration intensity. This testing should include sine sweeps at higher input intensities, and random exposure to establish overall intensities of excitation, in the respective axes, that create various leak rates at various inlet pressures. Random vibration should then be performed with the main poppet blocked closed. If a marked change in the leak rate versus input intensity results, repeat the random vibration with the pilot poppet blocked closed. Appropriate changes to the respective preloads can then be made.

Further discussion of the design modifications and some design refinements are presented in Section 5.0 of this document.

S/N 004 VALVE PILOT POPPET AFTER 140,000 CYCLES

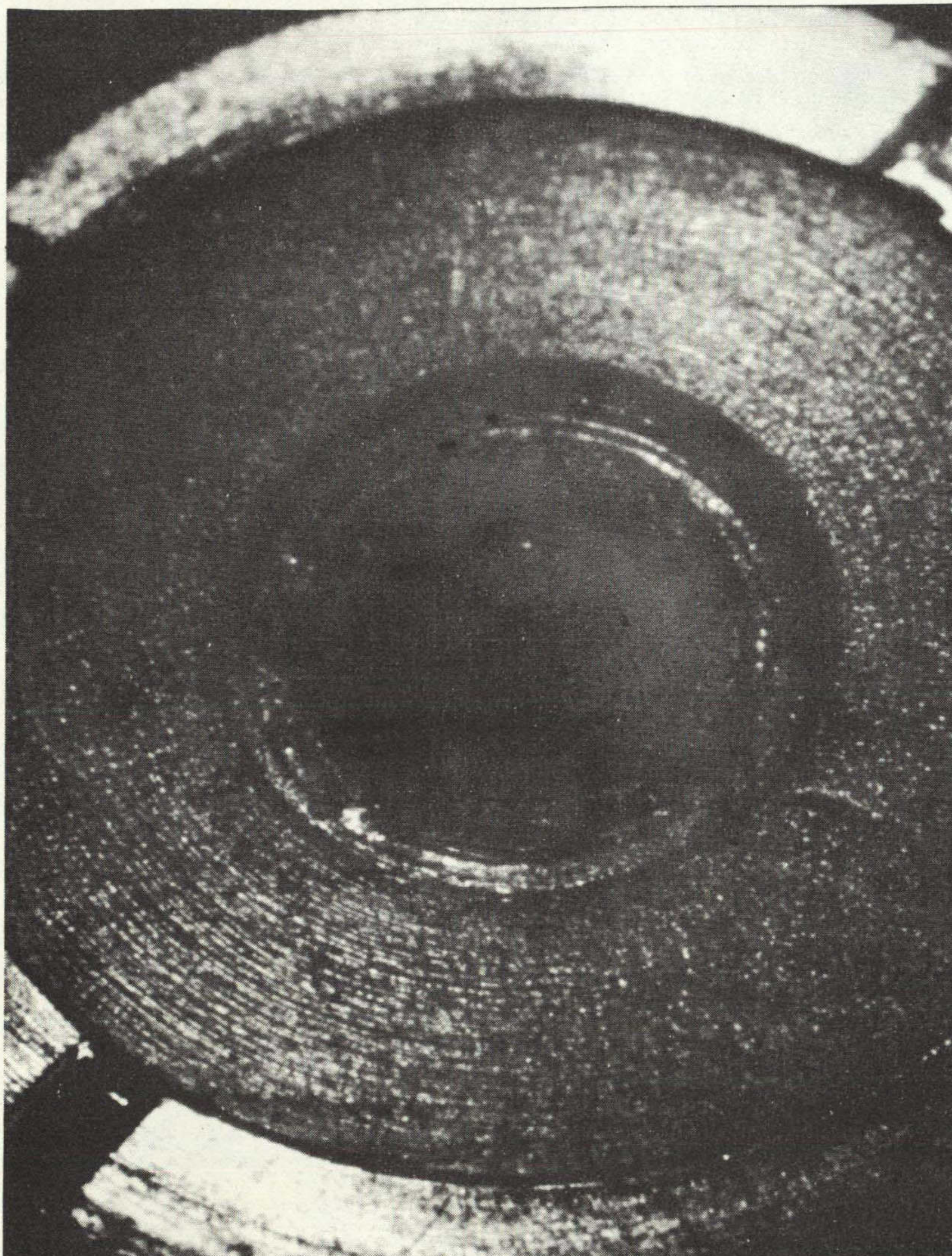

N74-352-81

Figure 3-55

S/N 004 VALVE PILOT SEAT AFTER LIFE CYCLE TEST

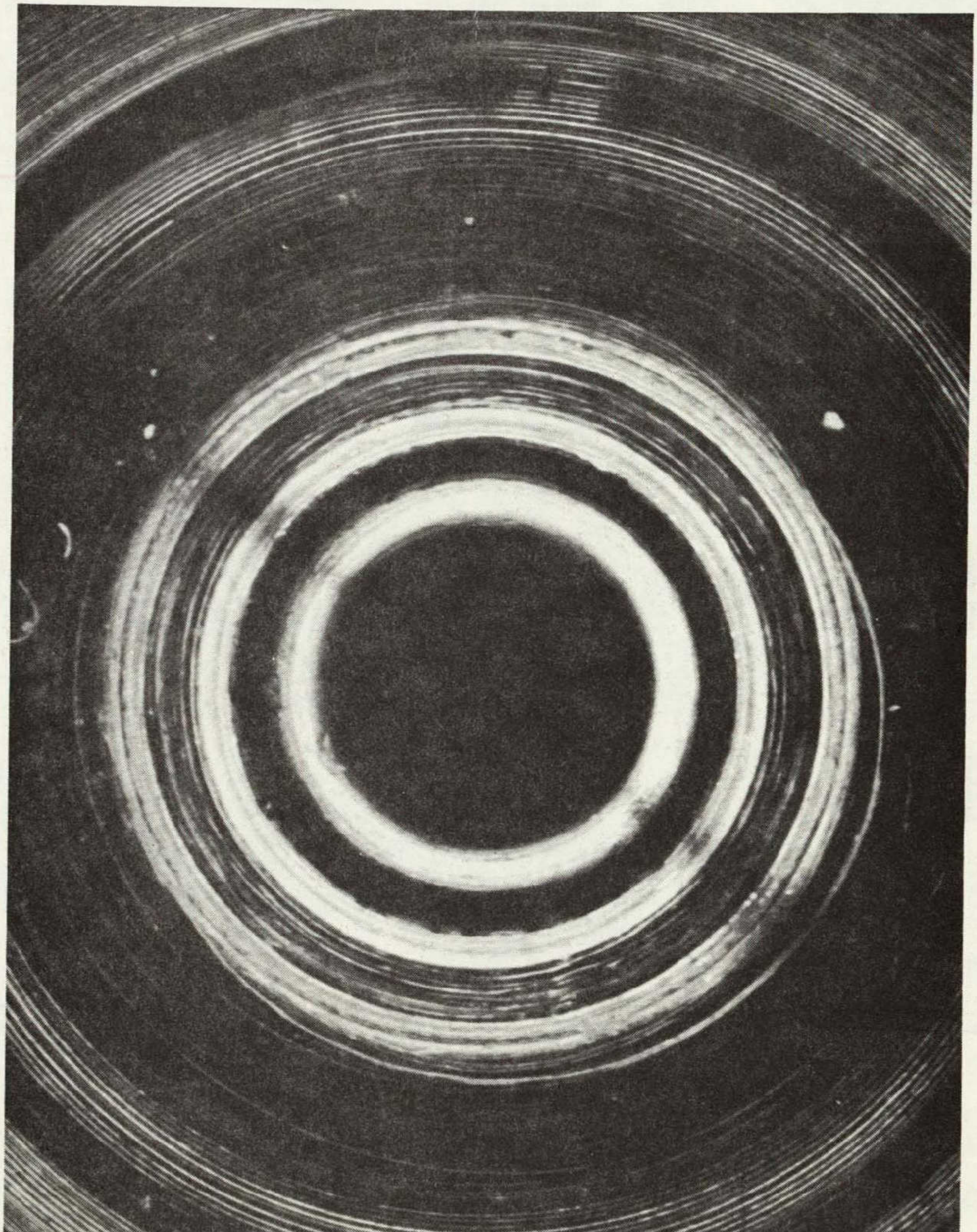

N74-352-132

Figure 3-56

S/N 004 VALVE MAIN POPPET AFTER LIFE CYCLE TEST

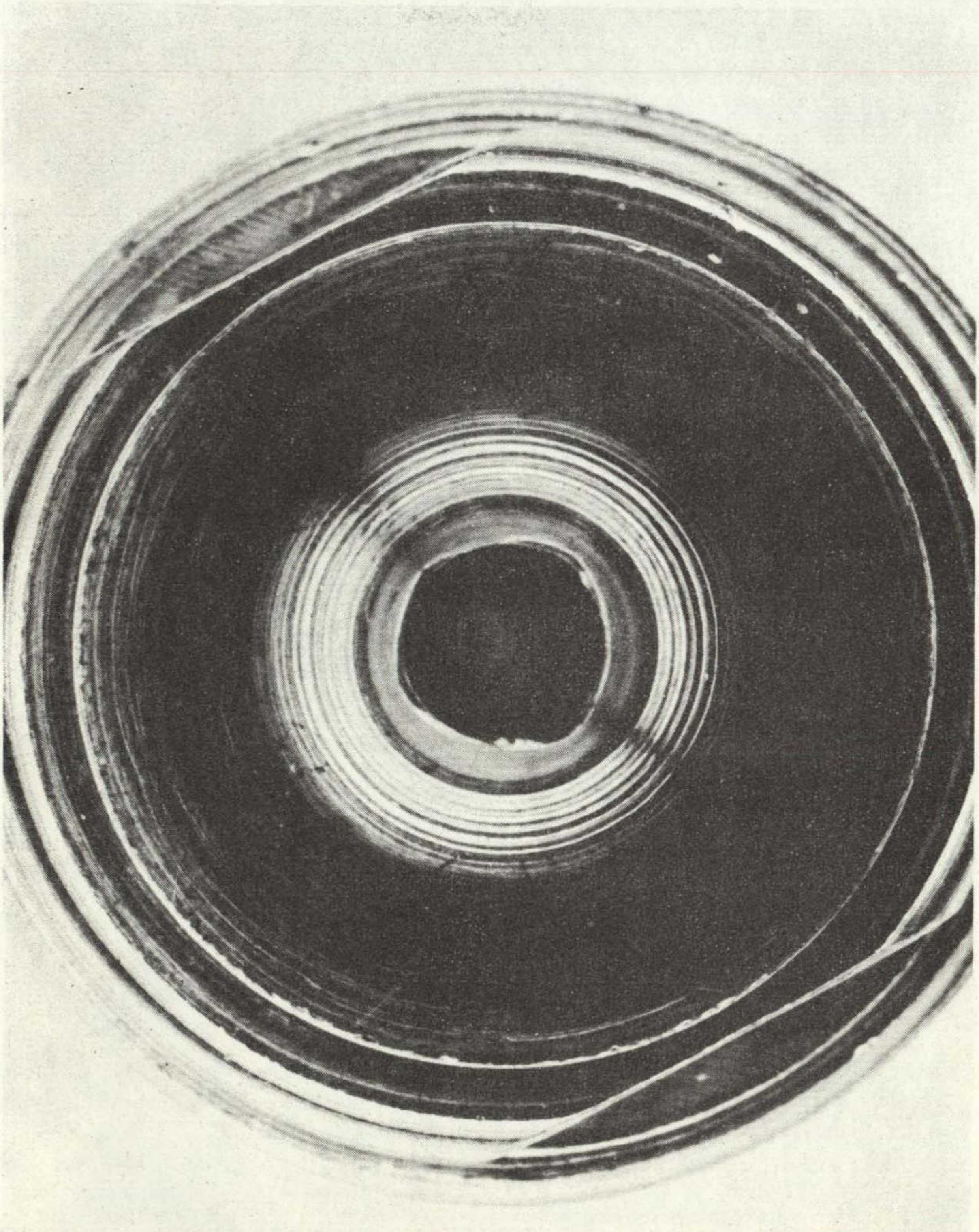

N74-352-131

ORIGINAL PAGE IS OF POOR QUALITY

Figure 3-57

S/N 002 VALVE PILOT POPPET AFTER 60,000 CYCLES

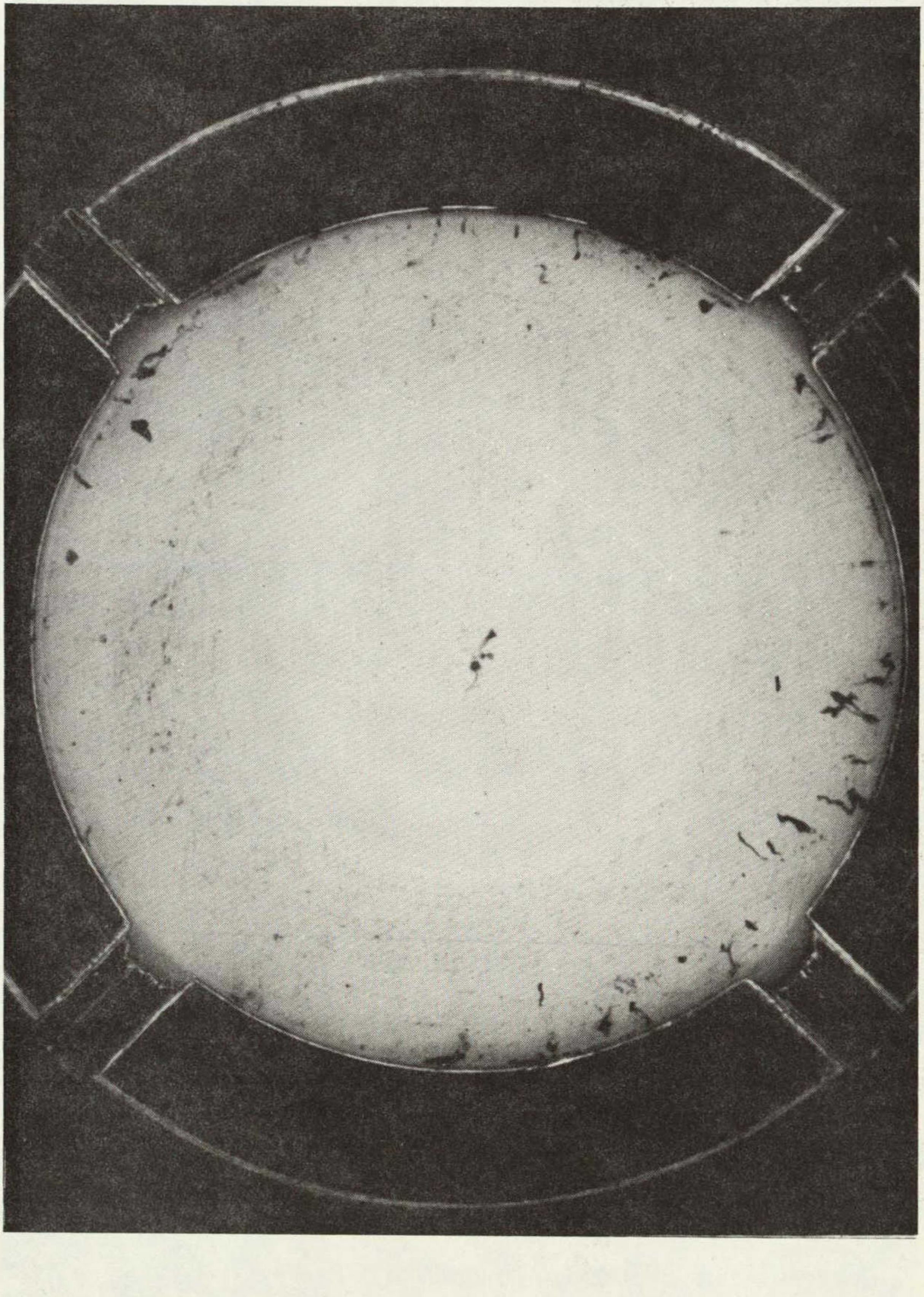

Figure 3-58

S/N 002 VALVE PILOT SEAT AFTER LIFE CYCLE TEST

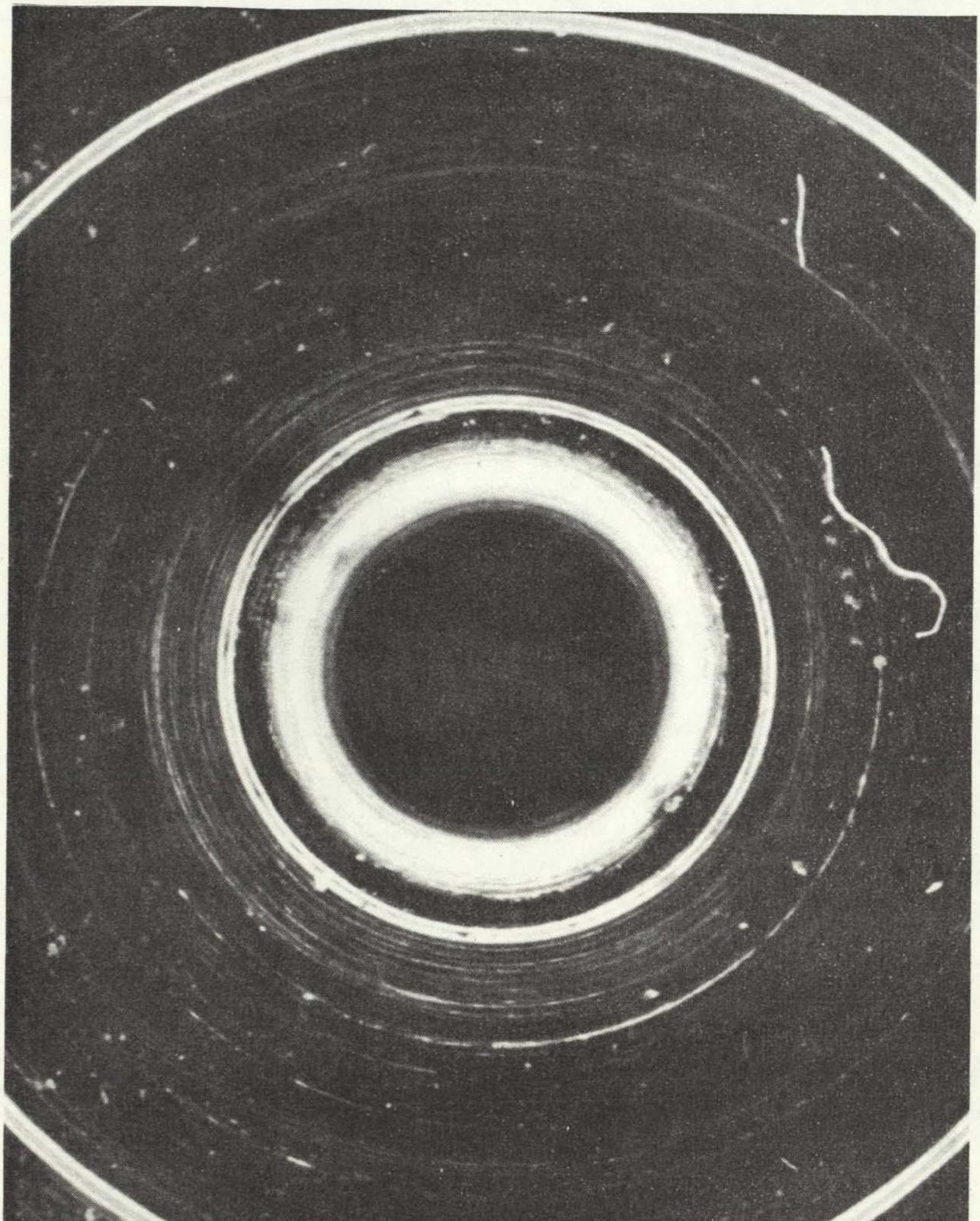

N74-352-133

Figure 3-59

S/N 002 VALVE MAIN POPPET AFTER LIFE CYCLE TEST

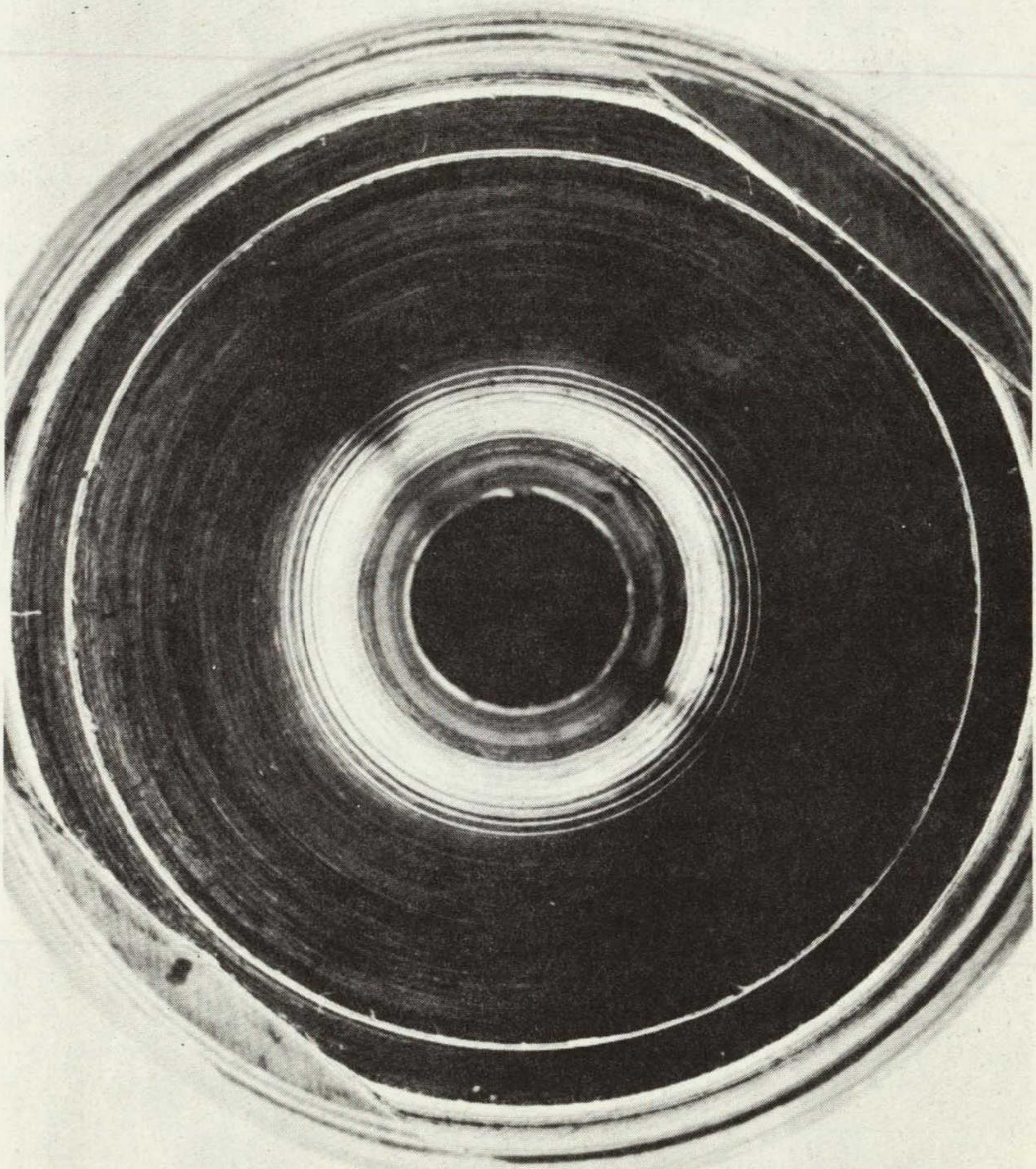

N74-352-130

ORIGINAL PAGE IS
OF POOR QUALITY

Figure 3-60

3.7 Hardware Fabrication, Acceptance Test and Delivery

In view of the continuing development of the valve, planned as an integral part of the SSRCT program, the incorporation of the design modifications, acceptance testing and delivery of the valves to NASA-JSC will be delayed. This delay will allow test verification of the design modifications in valves which are well documented and thus permit a more reliable assessment of the effects of the modifications on all valve characteristics. The nature of these tests is projected to be relatively short term, therefore, the prototype valves will, at all times, be maintained in a condition that will allow acceptance testing and delivery in a matter of days, should the need arise.

THIS PAGE LEFT INTENTIONALLY BLANK

5.0 RECOMMENDATIONS

The program reported herein has demonstrated the feasibility of the design of a line fluid actuated valve and has disclosed several areas wherein design modifications or refinements are required to achieve the design goals. The following recommendations include courses of action to resolve identified design deficiencies, investigate operational regimes wherein potential impacts on operational characteristics may occur, and address areas wherein performance, though short of design goals, was deemed acceptable for the SSRCT application.

- Leakage During Launch-Boost Vibration

  To determine if leakage originates with excitation of the pilot stage or main stage and determine responses of the respective components of the assembly, a more extensive sine sweep at increased input intensities is required. In addition, leakage isolation (pilot or main) can be determined by blocking the main closed with spacers and conducting investigatory sine sweeps, then repeating the sweeps with only the pilot blocked closed. A random test to determine the input intensity tolerance of the assembly in the normal mode of assembly and with the respective stages blocked will allow assessment of the magnitude of correction required to overcome the leakage problem. Corrective action will then be appropriately applied to preloads, spring rates (both axial and radial), and mass distribution with confirmation by a vibration demonstration test.

- Pilot Seal Cycle Life Prolongation

  Degradation of the pilot seal appears to be traceable to cavitation phenomenon. In view of the total success of the main seat, a redesign of the pilot seat and poppet, reflecting commonality of configuration and design criteria, is proposed as shown in Figure 5-1. The tested valves should be modified to this configuration and cycle tested with periodic performance and leakage checks to assure seal integrity and evaluate the impact of the change on performance characteristics.

- Coil Short to Case

  The use of a mylar tape insulation layer on the valve coil window was elected as a convenience for development valves. Replacing this layer with an alkyd dielectric sprayed on coating and also applying this coating to selected areas of the cover will preclude failure of the type experienced, since a secondary

PROPOSED PILOT REDESIGN

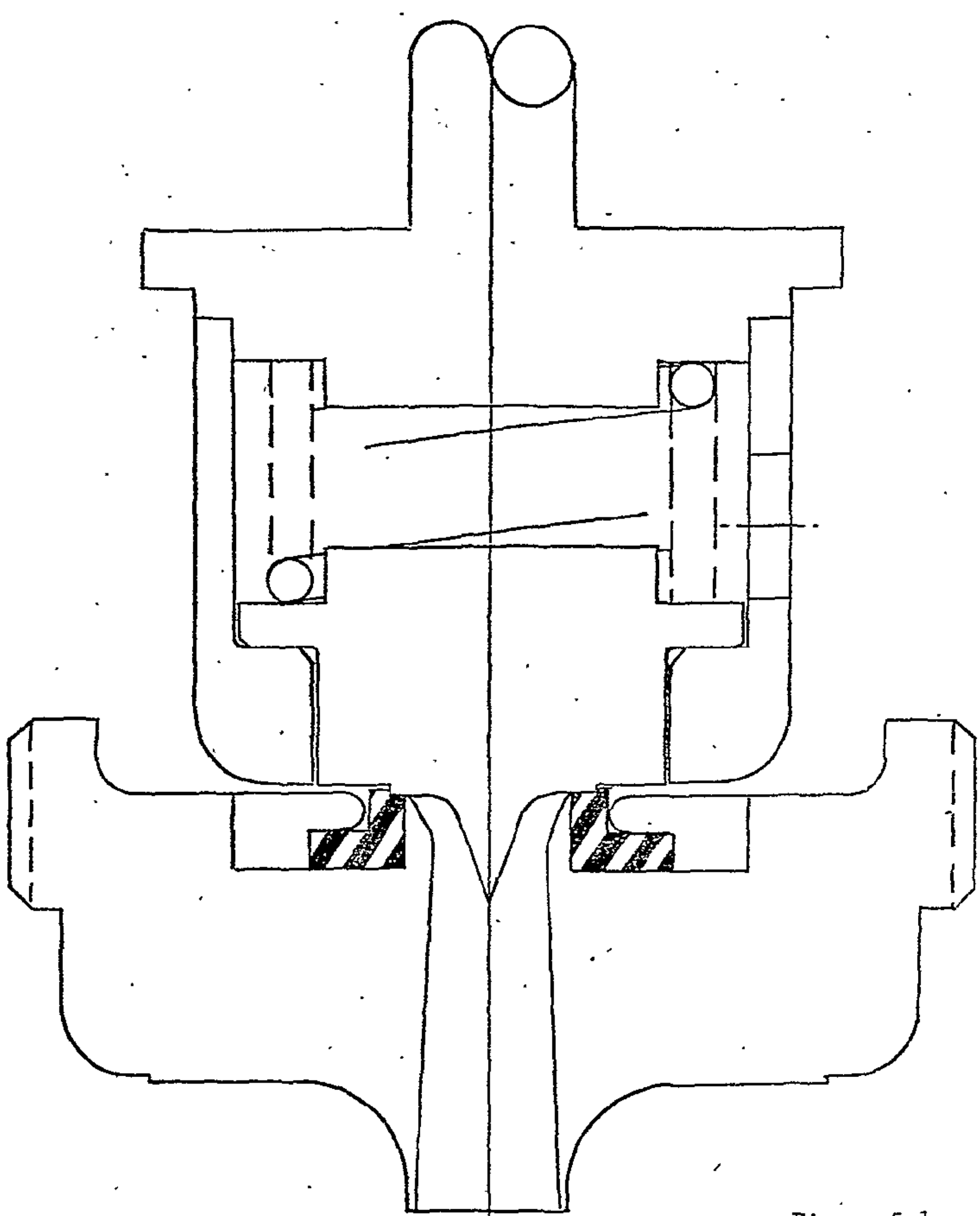

Figure 5-1

dielectric barrier will exist to compensate for potting voids. Additional controls to the potting procedure and improving flow paths for ingress of potting and egress of entrained air will greatly reduce the probability of potential shorting paths. Figure 5-2 summarizes the history of the coil window design and presents the configuration proposed for all future valves.

- Mixed Phase Flow Phenomenon

During design analysis and testing, incompressible fluid flow was assumed. It has been demonstrated by this valve, as well as other pilot operated valves, that priming may cause spontaneous valve operation. In a pressurized propellant system, gases will be entrained in the fluids in varying quantities and the feed system dynamic may create distinct bubbles in the influent to the valve. The passage of these bubbles may cause spontaneous reactions of the valve, since the principle of operation of the valve depends upon utilizing fluid properties and dynamics. A test effort is therefore warranted to evaluate the valve's response to various bubble sizes. Concurrent with this testing, inlet fluid dynamics and the effects of downstream flow phenomenon should be evaluated, since these phenomenon may create momentary mixed phase flow through the valve.

- Pilot Valve Opening Delay

As indicated in Table 2-I, valve opening response exceeded the design goal. Demonstrated pilot valve opening response times (Figures 3-42, 3-43, 3-50, and 3-52) were considerably longer than had been originally anticipated for the selected electrical power level. (Electrical power design goal was not defined.) The deviation from analytically projected pilot valve response times appears attributable to an overly optimistic assessment of parasitic air gap effects on the valve inductance. If improvement in pilot valve opening response is desired, a higher powered coil or a slightly higher valve weight to allow a larger coil to be wound of larger wire but of the same total coil resistance as the tested valves is required.

- Valve Pressure Drop

As shown in Figures 3-34 and 3-39, valve pressure drop at rated flow (2.0 pps N_2O_4) exceeded the design goal (30 psid) by 7 to 16 psi. As shown in Figure 3-39, a 6 psi pressure drop difference existed between the two test valves at the design flow rate. This difference is attributable to the difference in main poppet strokes of the two valves of .007 inch. Therefore, further pressure drop reduction can be achieved by increasing main poppet stroke. Pressure drop reduction can be realized by improving the valve

VALVE COIL/COVER MODIFICATION

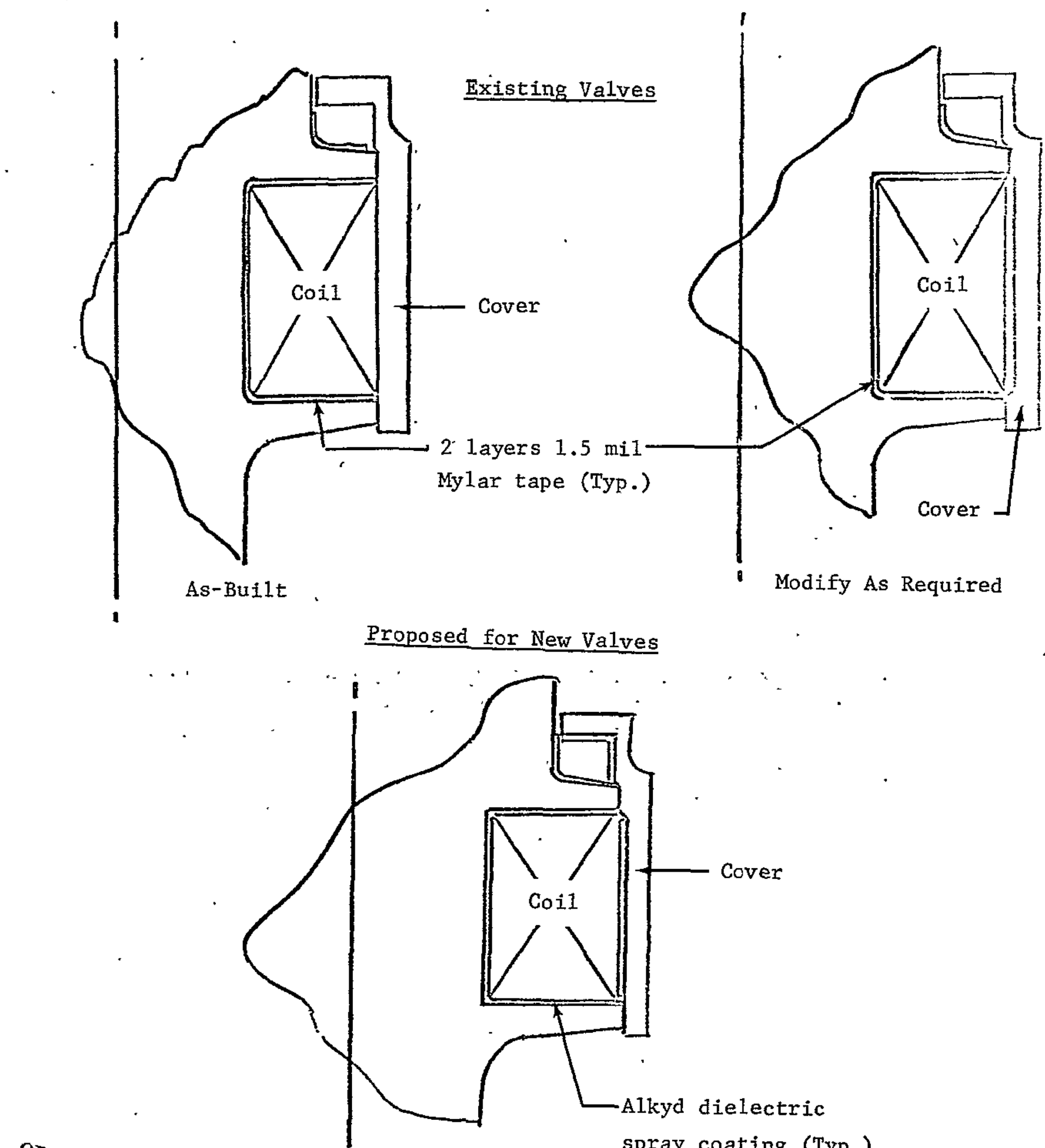

Figure 5-2

inlet flow contours, since it was demonstrated that the valve body pressure drop, without any valve internals, is 32 psi.

- Minimum Operating Voltage

Converting the measured operating current values of Figures 3-40 and 3-41 at 225°F to voltage indicates a 3 to 5 v deviation from the minimum operating voltage design goal (18 vdc @ 225°F). The higher than predicted pull-in current values resulted from an optimistic appraisal of the impact of parasitic gaps on the magnetic circuit. Improving the operating voltage can be accomplished by a higher powered coil or a larger coil (more turns) of the same resistance as the tested valves but at some weight penalty.

- "Stop-Off" Contaminant

Total removal of the "stop-off" used during flexure brazing to prevent braze alloy flow onto functional surfaces of the flexures was unsuccessful prior to valve assembly. Subsequent test environments resulted in residual quantities flaking off and depositing on other surfaces or flushing from the valve. Flexure producibility studies include methods of brazing that do not require the use of "stop-off" and its elimination is anticipated.

THIS PAGE LEFT INTENTIONALLY BLANK

6.0 REFERENCES

1. "Analysis Report, Space Shuttle OMS Helium Regulator Design and Development," by R. Lynch, Contract NAS 9-12992, October 1972, TMC Report 5103-7-1.

2. "Elastomeric Valve Seat Materials for Hydrazine Propulsion Systems," by J. E. Martin and J. F. Jones, TRW Systems Group, AFML-TR-7-200, December 1970.

3. Final Report - "Seal Material Development Program - Phase I," by H. W. Wright, TRW Systems Group, NASA-MSC Report No. CR114822, December 1970.

4. "The Design and Development of a Miniature Bi-Stable Latching Solenoid Valve for Low Thrust Resistojets," by R. Lynch, The Marquardt Company, NASA CR-112161, June 1972.

5. Electromagnetic Devices, H. C. Roters, John Wiley & Sons, Inc., 1941.

6. "Analysis of the Visco Seal," W. K. Stair, NASA CR-285, August 1965.

7. "Through Flow in Concentric and Eccentric Annuli of Fine Clearance With and Without Relative Motion of the Boundaries," L. W. Tao and W. F. Donovan, ASME Paper No. 54-A-175.

8. "The Labyrinth Seal - Theory and Design," F. Arnold and W. K. Stair, University of Tennessee Engineering Experimental Station, Report No. ME-5-62-1, March 1962.

9. "Pressure Drop and Flow Characteristics of Short Capillary Tubes at Low Reynolds Number," F. Keith and R. Cisenstadt, ASME Paper No. 56-SA-15.

10. "Close Clearance Orifices," A. Lenkei, Product Engineering, April 26, 1965.

11. "Compressive and Thermal Expansion Property Determination - Marquardt Pressed and Sintered TFE Teflon," J. D. Grunert, Marquardt Report S-915, January 1969.

12. "Space Shuttle Line Fluid Actuated Valve Design and Analysis Report," MIR No. 432, The Marquardt Company, December 1973.

13. "Development Test Plan, X29550, Line Fluid Actuated Valve," MTP 0218, The Marquardt Company, December 1973.

14. NASA - Johnson Space Center Contract NAS 9-13684, , Dated 1 September 1973.

15. Marquardt Proposal P4-105, "Line Fluid Actuated Shut-Off Valve in Response to NASA-JSC RFP No. 9-BC72-7-3-133P, Dated 2 July 1973.

16. Test Report, TMC No. 3293-6-5, "P/N X29550 Line Fluid Actuated Valve," January 1975.